

Ministry of Energy & Mines
Energy & Minerals Division
Geological Survey Branch

**ASSESSMENT REPORT
TITLE PAGE AND SUMMARY**

TITLE OF REPORT [type of survey(s)]	TOTAL COST
-------------------------------------	------------

AUTHOR(S) _____ SIGNATURE(S) _____

NOTICE OF WORK PERMIT NUMBER(S)/DATE(S) _____ YEAR OF WORK _____

STATEMENT OF WORK - CASH PAYMENT EVENT NUMBER(S)/DATE(S) _____

PROPERTY NAME _____

CLAIM NAME(S) (on which work was done) _____

COMMODITIES SOUGHT _____

MINERAL INVENTORY MINFILE NUMBER(S), IF KNOWN _____

MINING DIVISION _____ NTS _____

LATITUDE _____° _____' _____" LONGITUDE _____° _____' _____" (at centre of work)

OWNER(S)

1) _____ 2) _____

MAILING ADDRESS

OPERATOR(S) [who paid for the work]

1) _____ 2) _____

MAILING ADDRESS

PROPERTY GEOLOGY KEYWORDS (lithology, age, stratigraphy, structure, alteration, mineralization, size and attitude):

REFERENCES TO PREVIOUS ASSESSMENT WORK AND ASSESSMENT REPORT NUMBERS _____

TYPE OF WORK IN THIS REPORT	EXTENT OF WORK (IN METRIC UNITS)	ON WHICH CLAIMS	PROJECT COSTS APPORTIONED (incl. support)
GEOLOGICAL (scale, area)			
Ground, mapping _____			
Photo interpretation _____			
GEOPHYSICAL (line-kilometres)			
Ground			
Magnetic _____			
Electromagnetic _____			
Induced Polarization _____			
Radiometric _____			
Seismic _____			
Other _____			
Airborne _____			
GEOCHEMICAL			
(number of samples analysed for ...)			
Soil _____			
Silt _____			
Rock _____			
Other _____			
DRILLING			
(total metres; number of holes, size)			
Core _____			
Non-core _____			
RELATED TECHNICAL			
Sampling/assaying _____			
Petrographic _____			
Mineralographic _____			
Metallurgic _____			
PROSPECTING (scale, area) _____			
PREPARATORY/PHYSICAL			
Line/grid (kilometres) _____			
Topographic/Photogrammetric (scale, area) _____			
Legal surveys (scale, area) _____			
Road, local access (kilometres)/trail _____			
Trench (metres) _____			
Underground dev. (metres) _____			
Other _____			
		TOTAL COST	

**2007-2008 DIGHEM AIRBORNE SURVEY
ASSESSMENT REPORT
ON THE
SWIFT KATIE PROJECT**

**NELSON MINING DIVISION
BRITISH COLUMBIA
49°09'N 117°20'W
NTS 1:50,000 MAP SHEET - 82F/03
NAD 83, ZONE 11
474700E 5442700N**

**PREPARED FOR:
VALTERRA RESOURCE CORP.
OF
MANEX RESOURCE GROUP
1100-1199 WEST HASTINGS ST.
VANCOUVER, B.C. V6E 3T5**

**PREPARED BY:
BRIAN MCGRATH, B.SC., P.GEO., SENIOR GEOLOGIST**

SUBMITTED: JANUARY 2009



TABLE OF CONTENTS

<u>1.0</u>	<u>SUMMARY</u>	<u>1</u>
<u>2.0</u>	<u>INTRODUCTION</u>	<u>3</u>
<u>3.0</u>	<u>LOCATION, ACCESS AND INFRASTRUCTURE.....</u>	<u>4</u>
<u>4.0</u>	<u>PHYSIOGRAPHY, CLIMATE AND VEGETATION</u>	<u>5</u>
<u>5.0</u>	<u>MINERAL CLAIMS.....</u>	<u>6</u>
<u>6.0</u>	<u>EXPLORATION HISTORY.....</u>	<u>8</u>
<u>7.0</u>	<u>REGIONAL GEOLOGY</u>	<u>10</u>
<u>8.0</u>	<u>PROPERTY GEOLOGY.....</u>	<u>12</u>
<u>9.0</u>	<u>AIRBORNE GEOPHYSICAL EXPLORATION PROGRAM</u>	<u>15</u>
<u>10.0</u>	<u>CONCLUSIONS AND RECOMMENDATIONS</u>	<u>18</u>
<u>11.0</u>	<u>STATEMENT OF EXPENDITURES.....</u>	<u>20</u>
<u>12.0</u>	<u>STATEMENT OF QUALIFICATIONS.....</u>	<u>21</u>
<u>13.0</u>	<u>REFERENCES</u>	<u>22</u>

TABLE OF CONTENTS

LIST OF TABLES

TABLE 1: CLAIM TENURE STATUS	6
TABLE 2: PROPERTY GEOLOGY LEGEND	14

LIST OF FIGURES

FIGURE 1: SWIFT KATIE PROJECT LOCATION MAP	3
FIGURE 2: CLAIM TENURE MAP	7
FIGURE 3: REGIONAL TERRANE MAP	11
FIGURE 4: PROPERTY GEOLOGY MAP	13
FIGURE 5: AIRBORNE FLIGHT LINES MAP	16

APPENDICES

APPENDIX A: DIGHEM SURVEY REPORT, SWIFT KATIE BLOCK BC, NTS: 82F/3

APPENDIX B: DIGHEM GEOPHYSICAL BASE MAPS (*IN POCKET*)

MAP 1: ELECTROMAGNETIC ANOMALIES.....	SCALE 1:20,000
MAP 2: APPARENT RESISTIVITY 7,200Hz COPLANAR	SCALE 1:20,000
MAP 3: APPARENT RESISTIVITY 56,000Hz COPLANAR	SCALE 1:20,000
MAP 4: TOTAL MAGNETIC FIELD	SCALE 1:20,000
MAP 5: CALCULATED VERTICAL MAGNETIC GRADIENT	SCALE 1:20,000

1.0 Summary

This report describes the results obtained from 505 line-kilometres of heli-borne DIGHEM electromagnetic-resistivity-magnetic geophysical surveying over the Swift Katie claims during late 2007 and early 2008. The Swift Katie Cu-Au property is located in the Nelson Mining Division near the village of Salmo, in south-eastern British Columbia, Canada. The deposits are the south-eastern-most significant example of Late Triassic-Early Jurassic alkaline intrusion-associated copper-gold deposits in the Quesnel arc.

Fugro Airborne Surveys Corp. was contracted by Valtterra Resource Corp. from December 5th, 2007 to January 16th, 2008 to complete the survey over approximately 95% of the 7,064 hectare claim group. The purpose of the survey was to detect zones of conductive mineralization, to locate any plug-like structures that might represent porphyritic intrusions, and to provide specifics on an array of geological and structural features.

The principal flight lines were flown in an azimuthal direction of 20°-200° with a line separation of 200 metres. Tie lines were flown orthogonal to the traverse lines at 110°-290° at a spacing of 400 metres. The survey employed the DIGHEM V multi-coil, multi-frequency electromagnetic system outfitted with a magnetometer, radar and barometric altimeters, a video camera and a digital recorder. The instrumentation was installed in an AS350B3 turbine helicopter flown by Questral Helicopters Ltd. The helicopter flew at an average speed of 72 km/h with a sensor height of approximately 30 metres.

From the resulting data, Fugro personnel concluded that the surveyed region contains many anomalous features, several of which are considered to be of moderate to high priority as exploration targets.

Glacially-derived overburden dominates the project area that is underlain primarily by volcanic, volcanoclastic and sedimentary rocks assigned to the Archibald, Elise and Hall formations of the Lower Jurassic Rossland Group. The Elise Formation hosts the mineralization on the property and has been subdivided into four informal lithofacies: a dacite-rhyolite sequence, an augite-phyric andesite flow and breccia package, and a sequence of fine grained to feldspar- and hornblende-phyric andesite tuffs and breccias. Minor clastic sedimentary rocks of uncertain Formation assignment are spatially associated with the three volcanogenic packages.

The stratigraphic sequence is interpreted as a subaqueous vent-distal volcanic environment related to dominantly andesitic marine arc volcanism with local dacite to rhyolite magmatic centres that may be flows, lava domes or shallow intrusions. These packages have been intruded by dyke-like to stock-like, northwest-trending hornblende diorites, pyroxene diorites, feldspar porphyritic intrusions, and monzonites to quartz monzodiorites as well as biotite gabbros.

The layered rocks are largely homoclinally-east-dipping, locally overturned and isoclinally folded with steeply-dipping axial surfaces and fold hinges that are shallowly north-northeast-plunging. The structural architecture of the area suggests that the shallowly plunging, northwest-trending Cu-Au deposits may have originally been pipe-shaped vertical bodies that were subsequently deformed during periods of shortening.

The region has undergone a prolonged and often highly productive mining history that dates to the early 1900s. Key advantages associated with this area include the favourable geology and metallogeny, a well established transportation network, proximity to power generating infrastructure, and a well educated and skilled regional workforce.

The property is within a metallogenic belt that historically has hosted several important gold and base-metal mining camps. The property includes three mineral showings called the Katie (or Jim), Swift (Gus) and Ace in the Hole that were for many years explored separately in claims with different ownership.

Recently, the Swift Katie property has been amalgamated into a contiguous land package covering 7,064 hectares. Valtterra Resource Corp. has optioned the property from a group of vendors and can earn up to 100% interest (subject to a 3% NSR) by completing a series of cash payments, issuing shares and completing various work commitments on the property.

There have been numerous geological, geochemical and geophysical surveys completed on the Swift Katie property in the past. These programs have identified several exploration targets resulting in 60 drill holes intersecting portions of the Katie deposit (15,100 metres) and eight drill holes (892 metres) intersecting portions of the Swift prospect.

Due to the success of the 2007-2008 airborne geophysical program in defining known deposit areas and highlighting several new anomalous features, it is recommended that an expanded, multi-faceted exploration program be conducted in 2009. Exploration techniques that should be implemented include mapping-prospecting and sampling, ground-based geophysics (Mag-VLF and IP), and a minimum of 2,000 metres of diamond drilling.

All known deposits within the property remain open along strike and downdip. Activity should target the Katie Main Zone, 17 Zone, West and Swift areas and focus on the augite-phyric lithofacies of the Elise Formation that often is associated with elevated Cu-Au mineralization.

The estimated cost of the exploration campaign outlined above is CDN\$ 1.0 million dollars.

2.0 Introduction

The Swift Katie Cu-Au project is located in the Nelson Mining Division approximately seven kilometres southwest of the village of Salmo in south-eastern British Columbia. The property is centred at 49° 09' N latitude and 117° 20' W longitude and is located within NTS 1:50,000 map sheet 82F/03. The project location and related infrastructure are provided in Figure 1 below.

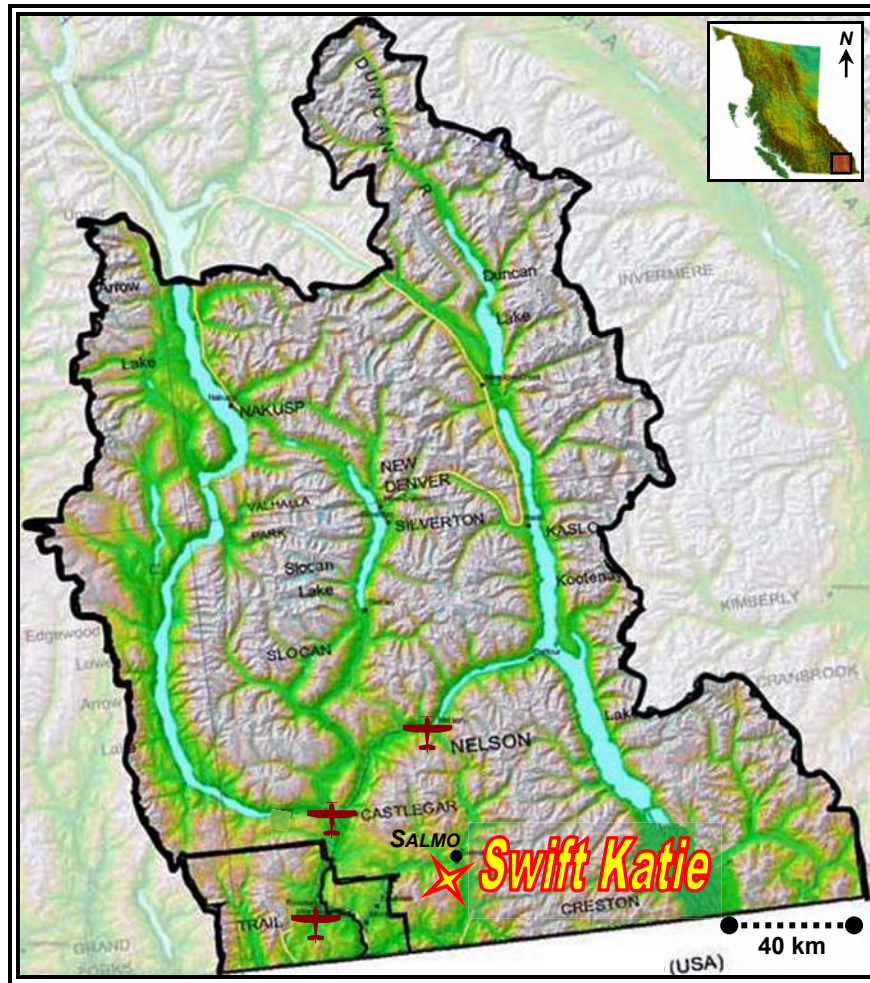


Figure 1: Swift Katie Project Location Map

The deposit is hosted in the Lower Jurassic Elise Formation of the Rossland Group that forms the easternmost part of the Quesnel Terrane. This geological setting is similar to that of the alkaline suite of porphyry copper deposits defined by Barr *et al.* (1976) and includes Copper Mountain, Afton, Mount Milligan and Mount Polley. The Katie deposit includes drill-defined, Cu-Au mineralized zones in the north-central part of the property and is considered the most south-easterly significant example of this deposit class found to date in the Canadian Cordillera (Naciuk and Hawkins, 1995).

Previous exploration programs have divided the Katie Cu-Au deposits into three main zones: the Main Zone, the 17 Zone and the West Zone. The Main Zone strikes northwest, has a true thickness ranging from 70 to 135 metres, and is a minimum of 500 metres in length. The 17 Zone strikes west-northwest, has a true thickness of 90 metres, and is a minimum of 300 metres in length. The zones are defined by grades that typically exceed 0.2% copper and 0.25 g/t gold (Naciuk and Hawkins, 1995).

The Swift Zone, located three kilometres southwest of the Katie deposits is under explored, although encouraging gold-silver mineralization was intersected during a 1987 drilling campaign (Clemmer, 1988). Recently, the Katie claim area and the adjoining Swift property have been combined into a single coherent 7,064 hectare exploration property.

Previous geologic work focused on the Main Zone and addressed the style of mineralization and deposit-specific geology (Cathro *et al.*, 1993; Naciuk and Hawkins, 1995).

This report compiles the results of the airborne geophysics survey conducted in 2007-2008 by Fugro Airborne Surveys Corp. (Farquhar *et al.*, 2008). Overall, the airborne geophysical survey program was encouraging and warrants future exploration endeavours. The recommendations for 2009 includes an expanded mapping-prospecting and sampling program; localized ground-based geophysical surveys on broad targets detected via airborne; and an expanded diamond drill program targeting the Katie Main Zone, 17 Zone, West and Swift areas.

The cost of the proposed exploration program is estimated at CDN\$ 1.0 million dollars.

3.0 Location, Access and Infrastructure

The Swift Katie project is located in the Nelson Mining Division approximately seven kilometres southwest of Salmo in south-eastern British Columbia. The property is centred at 49° 09' N latitude and 117° 20' W longitude and is located within NTS 1:50,000 map sheet 82F/03.

Access to the property via the Crowsnest Pass, Provincial Highway Number 3 is excellent. A brief two kilometre highway drive south of Salmo leads to the main access road on Hellroaring Creek. Overall, the forestry logging roads provide for a well established network of gravel-surfaced roads to much of the property. The main showing is easily accessed by following the main artery for approximately 6.5 kilometres paralleling Hellroaring Creek and its northern tributary. During winter months, vehicular travel to some areas may be limited by snow, unless roads are ploughed. Beaumont Timber Company Ltd. has locked gates on some roads, but ongoing access agreements are in place.

The village of Salmo (population 1,007) provides adequate accommodation, catering and general supply outlets. The town is strategically located near larger service-oriented

centres such as the City of Nelson (population 9,258) a 20 minute drive to the north, the City of Castlegar (population 7,259) 40 kilometres drive to the northwest, and the City of Trail (population 7,237) to the west (2006 Census). Socio-economically, the area is suitably positioned to provide a population base that is well educated, skilled and knowledgeable.

In addition to the well established highways, forest service road system and population centres outlined above, the property also has the added advantage of existing rail and power capacity. The Canadian Pacific Railways branch line runs from Trail through Nelson and Creston before connecting with its main lines in Cranbrook. Three-phase power is available along the Crowsnest Pass corridor and a main power transmission line is located three kilometres south of the claims. Moreover, a natural gas pipeline runs through the southern portion of the property.

Daily flights connecting with either Vancouver or Calgary can be arranged from the Castlegar and Trail airports. There is also a paved airstrip that can accommodate small plane traffic located within the City of Nelson.

4.0 *Physiography, Climate and Vegetation*

The properties physiography is dominated by a transitional, rounded mountain area with wide, glacially-sculpted valleys that are marked by incised creeks that have cut steep valleys into the ridges and highlands. The elevation ranges from 950 metres above sea level at the northernmost property area to 1,770 metres on the highest peaks in the centre of the claims. The relief is moderate on the flanks of Swift Katie ridge and flat to moderate along the ridge itself.

Soil development ranges from moderately well-developed podzols below 1,500 metres to regosol in the higher elevations (Clemmer, 1988). Organic-rich soils are confined to low-lying areas and around creeks. There is extensive glacial overburden that limits the amount of outcrop on the property.

Ecosystem classification by the provincial Ministry of Environment positions the claims within the Selkirk-Bitterroot Foothills Ecoregion of the Southern Interior Mountains Ecoprovince (Demarchi, 1996). The conditions are dominated by moist, cool to cold, temperate climates in a mountainous setting, where the majority are higher than 1,000 metres. Significant total annual snow accumulation of one to three metres depth is common in the area between December and March with the drainage basins receiving the majority of the snow. Exploration can be conducted year round; however conditions that are most favourable usually persist from May to October.

The Swift Katie property is in the Arrow Boundary Forest District where forest cover consists of spruce, balsam and alder. Approximately 50% of the claim group has been clear-cut logged and replaced by second growth timber that is currently in various stages

of maturation. The western portion of the Katie deposit has been recently burned resulting in rapid second growth vegetation.

Surface forest rights coincident with the mineral claims are shared by two forest companies. Beaumont Timber Company Ltd. owns the surface rights to more than half of the southern portion of the property and utilizes it as a forest plantation. Atco Lumber Ltd. has a timber license on the Crown Land in the northern portion of the claims.

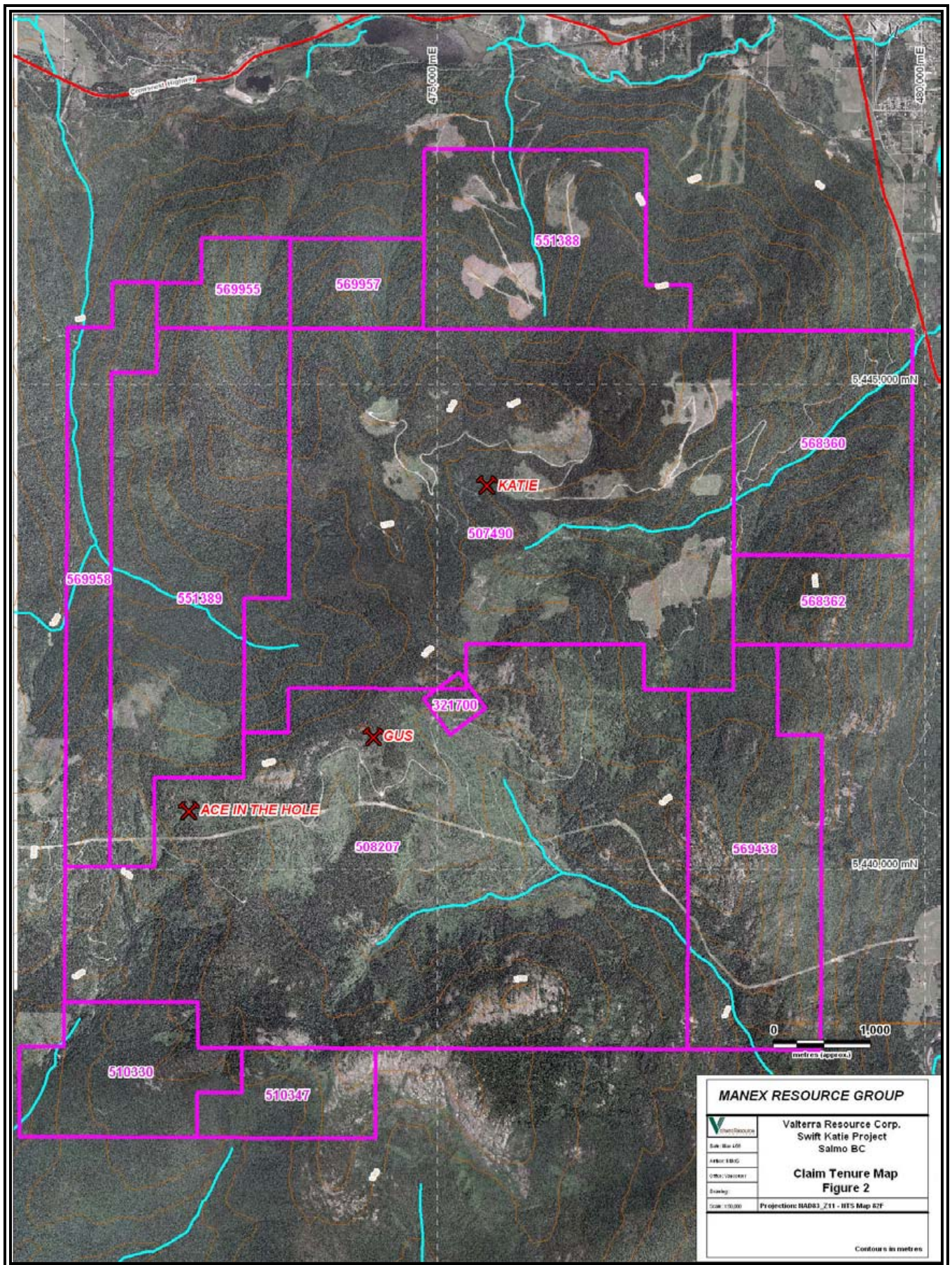
5.0 Mineral Claims

The Swift Katie property is comprised of 13 mineral tenure claim blocks that total 7,063.575 hectares. On March 30, 2006 the owners optioned the Swift Katie claim group to Valterra Resource Corporation of Vancouver, B.C. The claims are owned by Mr. Gerald Carlson (33.75% - held on behalf of KGE Management Ltd.), Mr. John Chapman (33.75%), Doublestar Resources Ltd. (22.50%) and Mr. Ken Murray (10.00%).

Valterra Resource Corp. can earn up to 100% interest (subject to a 3% NSR) by completing a series of cash payments, issuing company shares and completing various work commitments on the property. The claim statistics are listed below in Table 1 and their layout is illustrated in Figure 2.

Table 1: Claim Tenure Status

Tenure Number	Type	Claim Name	Good Until (yyyy/mm/dd)	Area (ha)
321700	Mineral	MIKE 1	2017/01/31	25.0
507490	Mineral	-	2017/01/31	1669.332
508207	Mineral	SWIFT GROUP	2017/01/31	2114.524
510330	Mineral	NEW SWIFT	2017/01/31	253.843
510347	Mineral	NEW SWIFT 2	2017/01/31	148.08
551388	Mineral	ROARING ONE	2017/01/31	443.531
551389	Mineral	ROARING TWO	2017/01/31	781.944
568360	Mineral	ROARING NORTH	2010/01/31	422.55
568362	Mineral	ROARING SOUTH	2010/01/31	169.071
569438	Mineral	SWIFT CREEK	2010/01/31	507.473
569955	Mineral	KATIE LATE ONE	2010/01/31	105.616
569957	Mineral	KATIE LATE TWO	2010/01/31	126.738
569958	Mineral	KATIE LATE THREE	2010/01/31	295.873
Total Area (ha)				7,063.575



6.0 Exploration History

The early mining history of this area of the province started ca. 1865 with placer operations that were active until the 1890s when lode gold operations became dominant in the Sheep Creek camp. Over the next half century, numerous hardrock mine developments at Rossland (Le Roi), Ymir-Nelson area (Yankee Girl), Slocan (Mammoth), Sheep Creek (Reno, Nugget, Queen) and Salmo (Jersey, HB mine, Reeves MacDonald and Emerald Tungsten) began producing ores of gold, lead, zinc, molybdenite and tungsten (Fyles and Hewlett, 1959).

With regard to the beginning of exploration on the current Swift Katie claim group, there are several collapsed trenches and pits on the Ace in the Hole occurrence that apparently date back to the early 1900s and likely record the earliest exploration history on the property.

During the 1950s, active placer gold mining operations are reported for Tillicum Creek on the southwest corner of the Swift claim block (Naciuk and Hawkins, 1995).

In 1969 and 1970, the first extensive exploration program was conducted over the property and included an airborne magnetic survey (MEMPR-GSC Map 8479G, 1973). This survey produced a kidney-shaped magnetic high anomaly in the north survey area that was coincident with the Katie deposit.

In 1977, The National Geochemical Reconnaissance Survey produced copper, zinc, nickel and cobalt anomalies from silt collected in the creeks draining the claim block (Ballantyne *et al.*, 1978).

In 1980, the earliest recorded assessment work on the Katie property was a soil sampling program conducted by Amoco Canada Petroleum Company Ltd. while exploring for molybdenum, lead and zinc. The company collected 390 samples but failed to locate any anomalies for Mo, Pb or Zn and hence the claims were dropped. However, a centrally located zone, now referred to as Katie, was highlighted. Values of >100 ppm Cu were delineated over an area of approximately 1,200 metres length x 300 to 400 metres width. Within this broad zone there is also a higher grade area of >200 ppm Cu that covers approximately seven hectares and includes an individual sample of 1,220 ppm Cu (MacIsaac, 1980).

From 1984 to 1986, Kidd Creek Mines Ltd. and Falconbridge Ltd. conducted 1:10,000 scale mapping, soil sampling and geophysical surveys over the Swift and Gus claims to the south of Katie. Exploration at the time was focused primarily upon VMS associated Cu-Zn mineralization.

In 1986, local prospector Ken Murray, conducted a Cu-Au-Ag geochemical soil sampling survey on the Katie claims in order to evaluate the copper anomaly outlined previously by Amoco. A broad 400 x 500 metre zone was outlined that assayed between 200 ppm and 1,200 ppm Cu, and contained up to 34 ppb Au (Murray, 1987).

In 1987, 40 backhoe trenches totalling 1,946 metres in length were excavated, sampled and mapped at 1:200 scale on the Swift-Gus and Ace in the Hole claims by Falconbridge Ltd. (von Fersen, 1987 and Bakker 1987). A combined total of 463 channel and grab samples were collected for Au-Ag +/- 17 element ICP and select whole rock analysis. The trenching successfully defined five bedrock areas at Swift-Gus with >1,000 ppb Au that each measured at least two metres in width. The trenching was followed by a diamond drill program on the Swift-Gus claim group consisting of eight, inclined NQ core holes totalling 891.80 metres. The best drill results were obtained from holes drilled directly under Trench 19. Drill hole 87-6 intersected 1.45 g/t Au over 5.40 metres and 1.83 g/t Au over 10.0 metres (Clemmer, 1988).

In 1988, Corona Corporation staked 1,131 units in 62 new claims covering a contiguous claim block area of 17 square kilometres. Concurrent with the staking, Corona completed a 114 sample heavy mineral and/or silt sampling program. Additionally, Aerodat Ltd. was contracted to conduct an extensive airborne Mag-EM geophysical survey covering 2,260 line-kilometres. The survey was successful in outlining 84 conductors with 12 of them being ranked as highest priority (Gaunt, 1989). This work was followed by a ground geochemical reconnaissance survey in the southern portion of the present mineral block in 1988. The results of these surveys outlined some weak Cu-Au soil anomalies on the Katie property.

In 1988 Stetson Resources Ltd. carried out ground-based VLF-EM and total field magnetic geophysical surveys on the Katie claims that identified four significant conductors and a "high magnetic structure" (McIntyre, 1990). Also in 1988, Baloil Lassiter Petroleum Ltd. undertook a geological and ground geophysical survey on the Katie claims.

During 1989, anomalous streams that were identified previously in 1988 were sampled at regular intervals upstream from the original sample locations. In addition, a 50.1 line-kilometre grid was established for mapping and soil sampling. A total of 1,443 "B" horizon soil samples were collected from the grid returning individual values up to 110 ppb Au (Gaunt, 1990). Baloil Lassiter Petroleum Ltd. also undertook exploration in 1989. Baloil completed a limited diamond drill program on the Katie deposit consisting of four holes totalling 305 metres. Three of the holes intersected mineralization, the best result was near surface in hole KT-89-4 that returned 0.24% Cu and 0.20 g/t Au over 6.0 metres (McIntyre, 1990).

In 1990, Yellowjack Resources Ltd. acquired the Katie portion of the claims. A new joint venture was then formed between Brenda Mines Ltd. and Hemlo Gold Mines Inc. whereby they agreed to allow the operator of the joint venture to be Noranda Exploration Co. Ltd.

During 1990, Noranda conducted geological, geochemical and ground geophysical surveys on the Katie property. Subsequently, in 1990 and 1991 they completed 34 diamond drill holes totalling over 8,652 metres at the Main, West and 17 zones. The best

results in 1990 came from hole NKT-90-9 (West) that averaged 0.16% Cu, 0.18 g/t Au and 0.4 g/t Ag over 169 metres and included 16.71 metres of 0.538% Cu, 1.04 g/t Au and 1.30 g/t Ag. One of the best intercepts in 1991 was in hole NKT-91-13 (Main) with 0.277% Cu, 0.331 g/t Au and 4.44 g/t Ag over 83.05 metres (McIntyre, 1991).

Yellowjack Resources Ltd. became the operator of the property in 1992 and implemented a two phased exploration approach that focused on previously drilled anomalies. Overall, the company drilled 18 holes totalling 4,477 metres that resulted in several encouraging results, especially in the Main Zone area. Holes YKT-92-40 to 43 produced several wide zones between 50 to 150 metres wide that averaged 0.12 - 0.36% Cu and 0.435 g/t Au (Wells, 1994).

Over the winter months of 1994 and 1995, Yellowjack completed two diamond drill holes totalling 606 metres on the Main Zone testing the north-easterly plunge potential of the deposit. The drilling intercepted two well mineralized sections highlighted by hole YKT-95-58 that returned 0.168% Cu and 0.20 g/t Au over 35.50 metres.

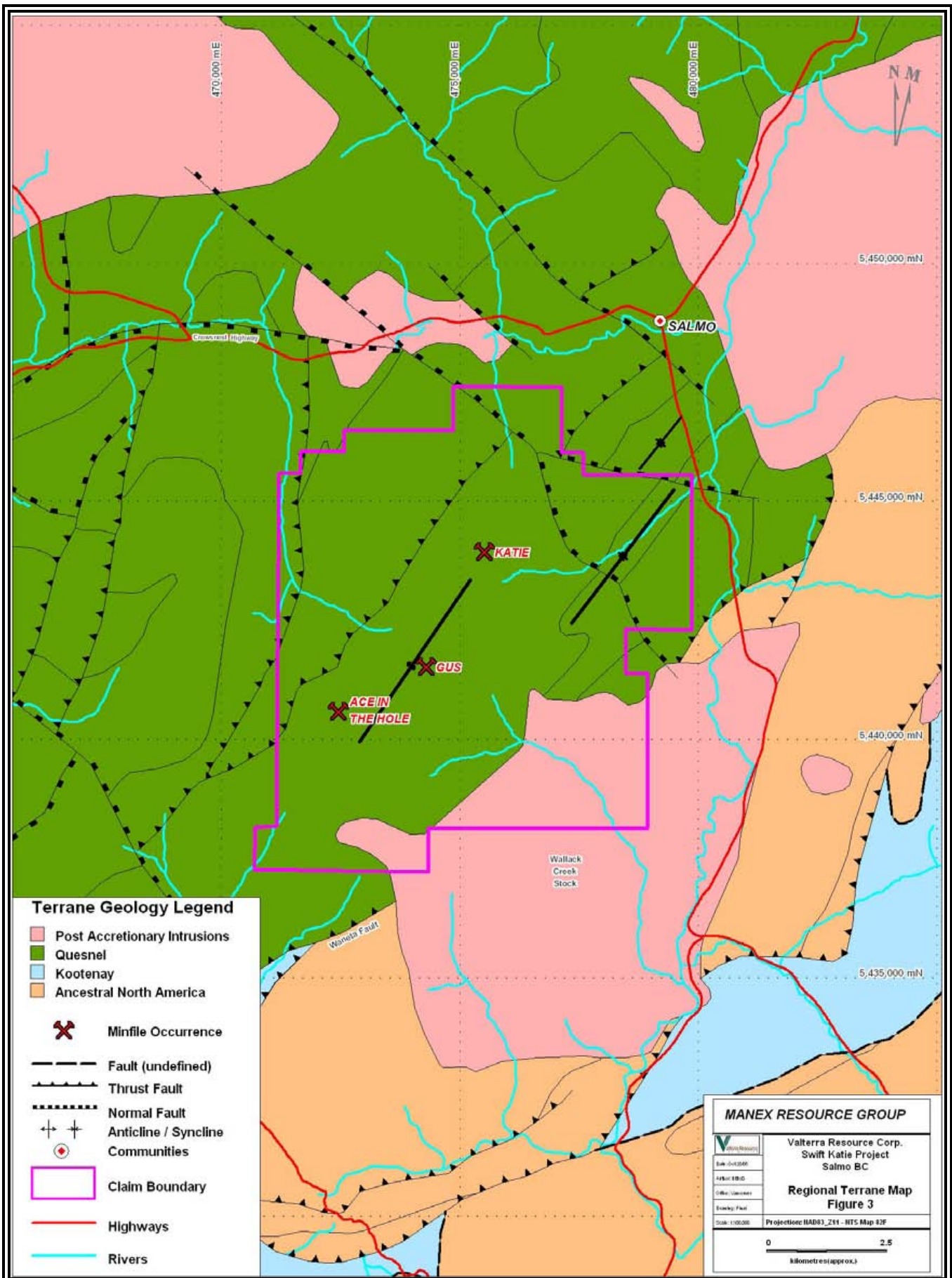
In 2001, John Chapman and Gerald Carlson staked the Katie claim block. They commenced a limited program in 2005 whereby the entire Swift core library was re-boxed and moved to Salmo and selected portions of core were re-logged and re-sampled. Several of the historical Katie drill collars were re-located by GPS and the survey data aided the transformation of the collar data to UTM NAD83 co-ordinates. This was followed in 2006 by creating a digital drill hole database of the Katie deposit and generating an in-house, preliminary mineral resource to assist in defining the mineral potential of the deposits (Chapman, 2006).

In 2006, the Swift Katie property was finally amalgamated into one package when the Chapman-Carlson team joined with Ken Murray and Doublestar Resources Ltd. Also, three additional claims were added to the existing claim group immediately to the north and northwest of the Swift Katie claim block. In March 2006, Valtterra Resource Corp. optioned the entire amalgamated property and commenced to lay the ground work for future project exploration.

In 2007, Valtterra compiled the historical data and added six mineral claims to the property holdings. Furthermore, the Company conducted a month-long 1:5,000 scale reconnaissance property mapping program followed by a diamond drilling campaign on the Katie Main and 17 zones that totalled 1,126 metres in three holes. Hole VKT07-060 contained one of the best intercepts that graded 0.23% Cu and 0.27 g/t Au over 45.41 metres from 209.90 metres. This interval also included a higher grade zone of 0.39% Cu and 0.60 g/t Au over 14.98 metres (McGrath *et al.*, 2008).

7.0 Regional Geology

The Rossland Group volcanic succession is the most easterly exposed stratigraphic sequence of the Triassic-Jurassic Quesnel arc terrane (Figure 3). A few kilometres south



of the property, the Lower Jurassic Rossland Group is juxtaposed against Paleozoic rocks of the Kootenay Terrane by the west-dipping Waneta thrust fault. In the Salmo area, the group comprises a basal succession of fine and coarse grained clastic sedimentary rocks assigned to the Archibald Formation; volcanic, volcanoclastic and epiclastic rocks assigned to the Elise Formation; and overlying fine grained clastic sedimentary rocks of the Hall Formation (Höy and Andrew, 1990; Cathro *et al.*, 1993).

The earliest structures in the Katie area (ca. 180 Ma) are tight folds locally associated with penetrative mineral foliation and intense shearing and thrusting (Höy and Andrew, 1990). These structures are more pronounced near the Waneta fault, where the overturned and east-dipping Hellroaring Creek syncline exposes Hall Formation in its core and sheared Elise Formation rocks in its limbs (Höy and Andrew, 1990). The compressional structures are sealed by Late Jurassic to Cretaceous intrusions such as the Wallack Creek stock (Höy and Andrew, 1990), exposed in the south-eastern corner of the property (Burge, 1986), suggesting a minimum age for the shortening.

8.0 Property Geology

The Swift Katie project is underlain by a sequence of volcanic, volcanoclastic and sedimentary rocks that have been intruded by fine grained to porphyritic and equigranular stocks and dykes (Figure 4 and Table 2). These rocks have been deformed by north-northeast-striking folds and shear zones as well as east-west to northwest-striking faults.

The northern part of the property is underlain by predominantly volcanoclastic breccias and clastic sedimentary rocks. The Main Zone area is underlain mainly by andesite breccias. The Swift area is underlain by a sequence of augite-phyric andesites and andesitic lapilli tuffs and the southern part of the mapped area is underlain by rhyolite and andesite. The layered rocks have been intruded by hornblende diorites, pyroxene diorites, monzonites to quartz monzodiorites, and by biotite gabbros.

These successions are assigned to the Archibald, Elise and the Hall formations (Cathro *et al.*, 1993), consistent with the regional stratigraphic framework defined in the area by Höy and Andrew (1990). The Archibald and Hall formations are dominantly fine grained clastic sedimentary sequences and the Elise Formation consists largely of volcanic, volcanoclastic and epiclastic rocks (Höy and Andrew, 1990). Broadly-similar sequences in both outcrop and drill core have been observed. However, there remains uncertainty as to the relationship between the lithofacies and the thickness of individual units due to the structural complexity of the property geology.

Sediments located in the most westerly parts of the property are tentatively assigned to the Archibald Formation. Volcanic units of the Elise Formation dominate the central part of the property, while the northeast portion of the mapped area contains distinctive black shales that are assigned to the Hall Formation.

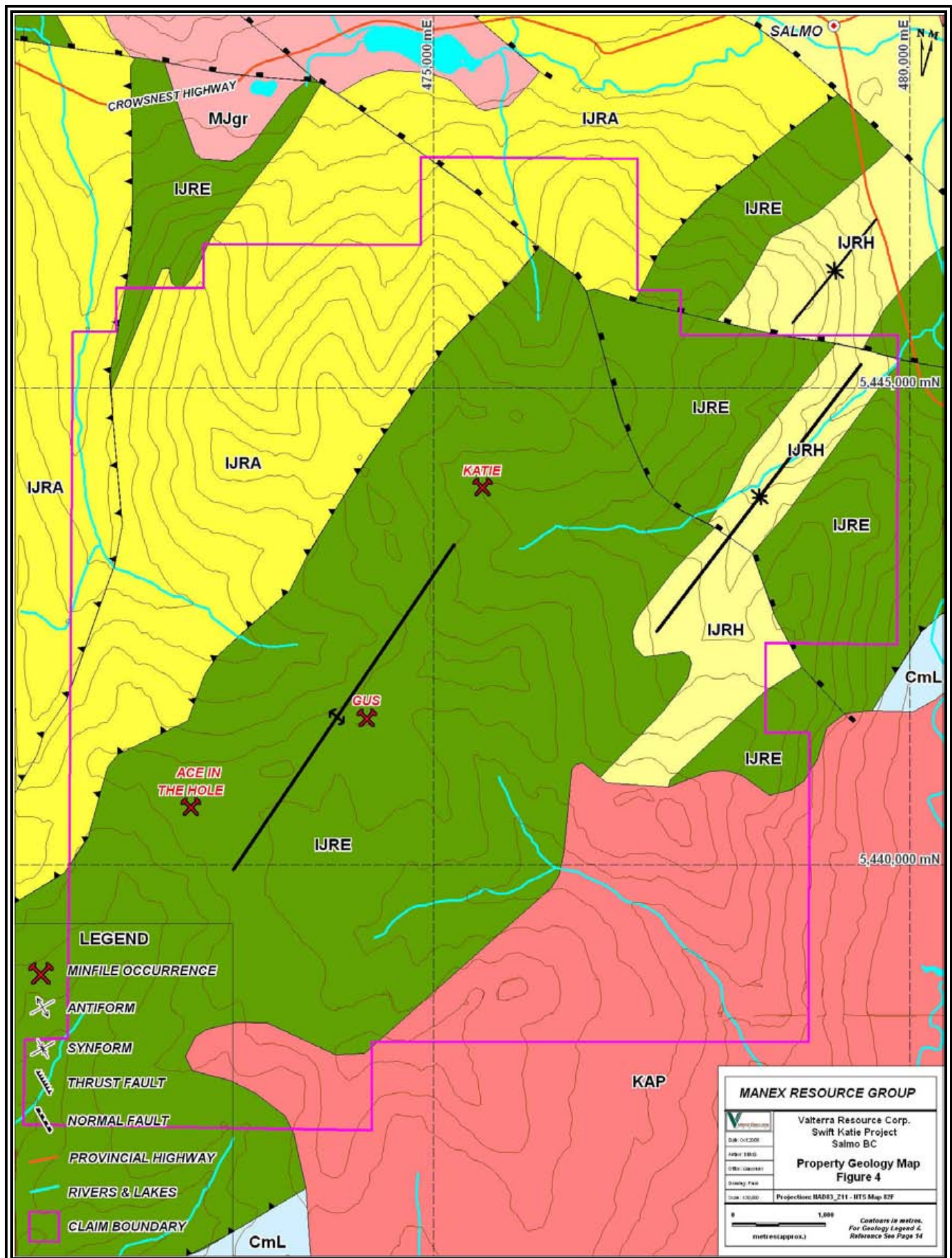


Table 2: Property Geology Legend

(Modified from Digital Geology Map of British Columbia, Massey et al., 2005)

<i>Era</i>	<i>Period</i>	<i>Age</i>	<i>Terrane</i>	<i>Belt</i>	<i>Map Unit</i>	<i>Lithology</i>
					<i>Intrusive Rocks</i>	
Mesozoic	Cretaceous	Early to Late Cretaceous (65-145.6 Ma)	Post Accretionary	Omenica	KAP	Wallack Creek Stock Granodioritic intrusive rocks
	Jurassic	Middle Jurassic (157.1–178 Ma)			MJgr	Granite, alkali feldspar granite intrusive rocks (porphyritic granite, granodiorite, monzonite)
					<i>Sedimentary & Volcanic Rocks</i>	
	Jurassic	Lower Jurassic (178–208 Ma)	Quesnellia	Omenica	IJRH	Rossland Group Hall Formation Sedimentary rocks: argillite, carbonaceous siltstone; minor pebble conglomerate and carbonate
					IJRE	Rossland Group Elise Formation Volcanic rocks: mafic flows, pyroclastic breccia; mafic to intermediate tuffs, tuffites
					IJRA	Rossland Group Archibald Formation Sedimentary rocks: argillite, turbiditic siltstone, conglomerate and minor maroon siltstone
Paleozoic	Cambrian	Lower Cambrian (510–570 Ma)	Kootenay		CmL	Laib Formation Undivided sedimentary rocks: phyllite, argillite, schist, micaceous quartzite; Reeves (Badshot) limestone member

Intercalated crystal-lithic sandstones and banded shale-sandstone sequences that resemble Archibald Formation units occur throughout the central portion of the property in close contact with rocks of the Elise Formation. The variable distribution of these sediments leaves some doubt as to their actual stratigraphic position within the Rossland Group.

9.0 Airborne Geophysical Exploration Program

Fugro Airborne Surveys Corp. was contracted by Valtterra Resource Corp. from December 5th, 2007 to January 16th, 2008 to complete an airborne geophysical survey over the Swift Katie claim group. The survey consisted of a DIGHEM V electromagnetic-resistivity-magnetic system that was flown for a total of 505 line-kilometres over approximately 95% of the 7,064 hectare Swift Katie claim group (Farquhar *et al.*, 2008).

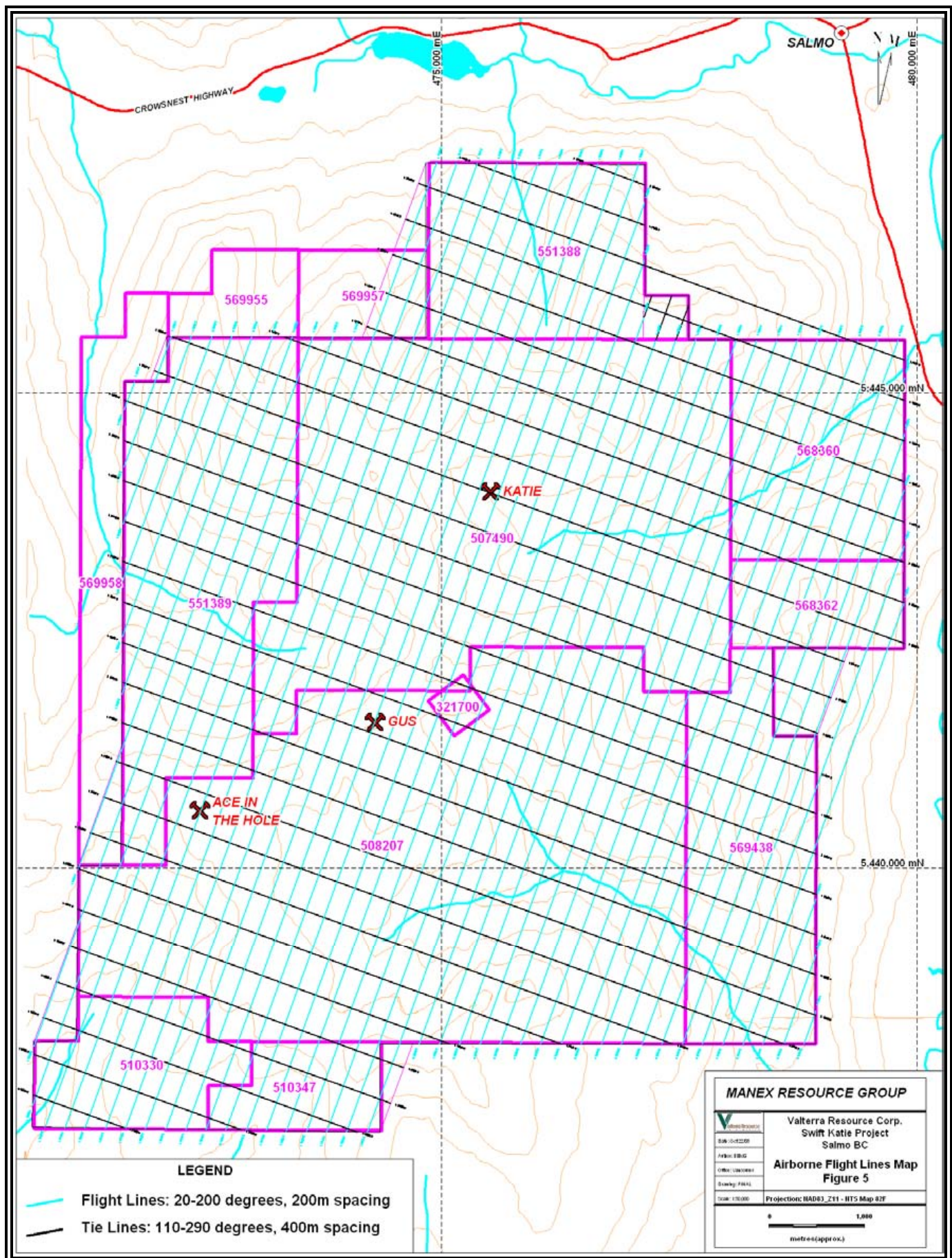
The primary focus of the survey was to detect conductive mineralized zones, aid in definition of any plug-like structures that might represent porphyritic intrusions, and to provide specifics on a variety of geological and structural features on the property that are often masked by overburden. Overall, the survey should assist with deposit definition, future targeting and prioritization.

The principal flight lines were flown in an azimuthal direction of 20°-200° with a line separation of 200 metres. Tie lines were flown orthogonal to the traverse lines at 110°-290° with a line separation of 400 metres (Figure 5). The survey employed the DIGHEM V electromagnetic system outfitted with a magnetometer, radar and barometric altimeters, a video camera and a digital recorder. The instrumentation was installed in an AS350B3 turbine helicopter flown by Quesstral Helicopters Ltd. The helicopter flew at an average speed of 72 km/h with a sensor height of approximately 30 metres (Farquhar *et al.*, 2008).

From the resulting data, Fugro personnel concluded that the surveyed region contains many anomalous features, several of which are considered to be of moderate to high priority as exploration targets.

The total magnetic field and calculated vertical magnetic gradient maps potentially delineated numerous zones of either magnetite enrichment or magnetite destruction as high nanoteslas (nT) and low nT anomalies, respectively. These anomalies might lead to future increases in mineral tenor by focusing the exploration efforts toward zones of potential economic mineral concentrations and/or zones of increased hydrothermal alteration or fluid flow.

With respect to electromagnetics, Farquhar *et al.* (2008) categorize four different airborne EM anomalies as being either discrete (conductive sulphides or graphite associated with bedrock sources), broad (conductive rocks, deep weathering profiles, weathered tops of plugs or pipes, or wide alteration zones), magnetite-related or cultural (gas pipelines etc.). Statistically, Fugro has identified 438 EM anomalies where roughly



20% fall within the moderate to high range and consequently warrant further investigation. Most of the conductors are non-magnetic, suggesting graphite or argillaceous shales (Farquhar *et al.*, 2008).

The foremost conductor detected is labelled “D1” on the EM base map and represents a lengthy northeast-southwest trending anomaly measuring approximately 10 kilometres long by up to 600 metres in width. The northeast sector of this conductor correlates well with a sequence of synclinal Hall Formation sediments shown on many regional government geology maps. However, no current geological correlation or interpretation is known to exist for the remaining five kilometre-long southwest portion of the conductor (approximately 50%). If this lower conductive region is related to the sediments then the Formation may persist much further to the southwest than is currently mapped.

Conversely, this conductive source may be related to other sedimentary units such as Lithofacies 4 - Unassigned Units (possibly Archibald and/or Elise formations) mapped on the property in 2007, or the conductor might result from graphitic shears/faults or conductive sulphides.

Base maps for apparent resistivity were presented in frequencies of 7,200Hz and 56,000 Hz. These maps offer a large dynamic range by utilizing multiple frequencies and hence are considered excellent mapping tools (Farquhar *et al.*, 2008). Empirical results related to porphyritic intrusions have indicated that these features can be more resistive, less resistive or indistinguishable from the host rocks. Therefore, any subtle resistivity anomalies may be of interest especially those that are circular or plug-like (Farquhar *et al.*, 2008).

Summarizing the resistivity data briefly, it appears to have outlined many important features worthy of further ground-truthing. Several circular and broadly elliptical resistivity highs have been defined on the property, especially within the highly prospective Elise Formation volcanogenic package. These anomalies may be related to igneous emplacement or more specifically, buried porphyritic intrusions. Likewise, several resistivity lows were identified and many appear coincident with some of the conductors described earlier.

For a more detailed account of the airborne geophysical program conducted at Swift Katie the reader is referred to Appendix A where the entire Fugro written report and accompanying 1:20,000 scale geophysical base maps are located; including the following:

- Electromagnetic Anomalies map
- Apparent Resistivity 7,200Hz Coplanar map
- Apparent Resistivity 56,000Hz Coplanar map
- Total Magnetic Field map
- Calculated Vertical Magnetic Gradient map

10.0 Conclusions and Recommendations

The results of the 2007-2008 airborne geophysics program, flown over almost the entire Swift Katie project area, was very encouraging. Detailed maps produced from the survey were of a very good quality and the project area contains many anomalies that are considered to be of moderate to high priority as exploration targets. The program highlighted the complex geology associated with the claims thereby reinforcing the need for future multi-disciplinary exploration endeavours.

The total magnetic field and calculated vertical magnetic gradient maps illustrate numerous zones that might represent either magnetite enrichment or magnetite destruction. These areas should be prioritized and investigated during future exploration programs as they are often key parameters identified in metallogenic enriched areas.

Fugro categorize the airborne electromagnetic anomalies as being either “discrete”, “broad”, “magnetite-related” or “cultural”. The DIGHEM survey identified 438 EM anomalies, approximately 20% are within the moderate to high range and should be further explored. The majority of the conductors were concluded as being non-magnetic, suggesting graphite or argillaceous shale sources.

A prominent northeast-southwest trending EM anomaly (D1) was delineated by the survey. The northeast sector of this conductor correlates with Hall Formation sediments, however an estimated 50% of the southwest section remains enigmatic. If this lower conductive area is related to the sediments then the Formation potentially continues south-westward, well beyond the current map interpretation.

Conversely, this conductive source may be related to other undifferentiated sedimentary units or the conductor might be caused by graphitic shears/faults or conductive sulphides. A surface exploration program is recommended for this prospective area attempting to resolve the apparent map discrepancies and potentially generating new targets for exploration.

The resistivity data outlined many important features that should be considered for follow-up. Several circular and broadly elliptical resistivity highs were detected, especially within the highly prospective Elise Formation volcanogenic package. These anomalies may be igneous-related or more importantly, porphyries. Likewise, several resistivity lows were identified and many appear coincident with some of the conductors described earlier.

Due to the success of the airborne geophysical program in defining known deposit areas and highlighting several new anomalous features, it is recommended that an expanded, multi-faceted exploration program be conducted in 2009. Exploration techniques that should be implemented include mapping-prospecting and sampling, ground-based geophysics (Mag-VLF and IP), and a minimum of 2,000 metres of diamond drilling.

All known deposits within the property remain open along strike and downdip. Activity should target the Katie Main Zone, 17 Zone, West and Swift areas and focus on the

augite-phyric lithofacies of the Elise Formation that often is associated with elevated Cu-Au mineralization.

The estimated cost of the exploration program outlined above is CDN\$ 1.0 million dollars.

11.0 Statement of Expenditures

During 2007-2008, the following Assessment-related airborne geophysical exploration expenditures were made by Valtterra Resource Corp. on the Swift Katie Project in southeast BC.

STATEMENT OF EXPENDITURES				
Cost Centres	Details of Expensed Items		Individual Costs	Cost Totals (CDN\$)
PERSONNEL (3.2%)	ARIS Report (Writing-Drafting)	Brian McGrath (7 days @ \$680/day)	\$4,760.00	\$4,760.00
CONTRACTOR (96.8%)	Fugro Airborne Surveys Corp.	505 Line Kilometres of Airborne	\$143,474.69	\$143,474.69
TOTAL EXPLORATION EXPENDITURES			\$148,234.69	\$148,234.69

12.0 Statement of Qualifications

I, Brian T. McGrath, P.Geo., of Langley, British Columbia hereby certify as follows:

1. I graduated from Memorial University of Newfoundland with a Bachelor of Science degree in Earth Sciences, Geology, in 1992.
2. I am a registered Professional Geoscientist with the Association of Professional Engineers and Geoscientists of British Columbia, Registration Number 23643, since March 1998.
3. I have practiced my profession continuously since graduation.
4. I was involved in the planning of the program herein described and the writing of this report.
5. This report is an accurate account of the 2007-2008 DIGHEM airborne geophysical program conducted by Fugro Airborne Surveys Corp. for Valtterra Resource Corp. on the Swift Katie Project, south-eastern BC.

Dated at Vancouver, British Columbia, this 15th day of January, 2009.

Brian T. McGrath, B.Sc., P.Geo.

13.0 References

- Andrew, K.P.E., Höy, T. and Simon P. (1991): Geology of the Trail Map Area, B.C. Ministry of Energy, Mines and Petroleum Resources, Open File 1991-16, scale 1:100,000.
- Andrew, K.P.E. and Höy, T. (1989): Geology and Exploration of the Rossland Group in the Swift Creek Area. Exploration in B.C. 1989, B.C. Ministry of Energy, Mines and Petroleum Resources pages 73-80.
- Andrew, K.P.E. and Höy, T. (1988): Preliminary Geology and Mineral Deposits of the Rossland Group between Nelson and Ymir, Southeastern British Columbia; B.C. Ministry of Energy, Mines and Petroleum Resources, Open File 1988-1.
- Bakker, E. (1987): Report on Trenching, Mapping and Sampling on the Swift and Gus Claims, B.C. Assessment Report 16901.
- Ballantyne, S. B.; Kalnins, T. E.; Lynch, J. J. (1978): National Geochemical Reconnaissance Release NGR 25-1977, Regional Stream Sediment and Water Geochemical Reconnaissance Data, South-eastern British Columbia, GSC Open File Map 514, scale 1:250,000.
- Barr, D.A., Fox, P.E., Northcote, K.E. and Preto, V.A. (1976): The Alkaline Suite Porphyry Deposits - A Summary. Porphyry Deposits of the Canadian Cordillera, Sutherland-Brown, A. Editor, CIMM. Special Volume 15, pages 359–367.
- Brown, D.A. and Logan, J.M. (1989): Geology and Mineral Evaluation of Kokanee Glacier Provincial Park, Southeastern British Columbia; B.C. Ministry of Energy, Mines and Petroleum Resources, Paper 1989-5, 47 pages.
- Burge, C.M. (1986): Geology, Lithogeochemistry and Economic Potential of the Swift Group Area, B.C. Assessment Report 14933.
- Burge, C. M. (1986): Geology, Lithogeochemistry and Economic Potential of the Ace-in-the-Hole Group Area, B.C. Assessment Report 14934.
- Carr, S.D. (1995): The Southern Omineca Belt, British Columbia: New Perspectives from the Lithoprobe Geoscience Program; Canadian Journal of Earth Sciences, Volume 32, pages 1720-1739.
- Cathro, M.S., Dunne, K.P.E. and Naciuk, T.M. (1993): Katie - An Alkaline Porphyry Copper-Gold Deposit in the Rossland Group, Southeastern B. C., Geological Fieldwork 1992, B.C. Ministry of Energy, Mines and Petroleum Resources, Paper 1993-1.
- Chapman, J.A. (2006): Report on Core Sampling, Core Examination, Drill Collar Locating (GPS) and Block Modeling, Swift Katie Mineral Property, B.C. Assessment Report.

Clemmer, S.G. (1988): Diamond Drilling Report on the Swift and Gus Claims. B.C., Falconbridge Ltd., Assessment Report 17296.

Cooke, D.L. (1991): Exploration Report Katie Property (82F/3, 4) for Yellowjack Resources Ltd.

Delta Geoscience Ltd. (1986): Geophysical Report on Gus Claims, Salmo Area, B.C., NTS Map Sheet 82F3.

Demarchi, D. A. (1996): An Introduction to the Ecoregions of British Columbia, Wildlife Branch, Ministry of Environment, Lands and Parks, Victoria, British Columbia.

Draut, A. E. and Clift, P. D. (2006): Sedimentary Processes in Modern and Ancient Oceanic Arc Settings; Evidence from the Jurassic Talkeetna Formation of Alaska and the Mariana and Tonga Arcs, Western Pacific Journal of Sedimentary Research, Volume 76, No. 3-4, pages 493-514.

Drysdale, C.W. (1915): Geology and Ore Deposits of Rossland, British Columbia; Geological Survey of Canada, Memoir 77, 317 pages.

Dunne, K.P.E. and Höy, T. (1992): Petrology of Pre to Syntectonic Early and Middle Jurassic Intrusions in the Rossland Group, Southeastern British Columbia (82F/SW), Geological Fieldwork 1991, B.C. Ministry of Energy, Mines and Petroleum Resources, Paper 1992-1.

Epp, W. (1991): Executive Summary Report – Katie Project, Noranda Exploration Company Ltd.

Farquhar, E. (2008): DIGHEM Survey for Valtterra Resource Corporation, Swift Katie Block, British Columbia, NTS: 82F/3, Fugro Airborne Surveys Corp., Report # 07114, 109 pages.

Fyles, J.T. (1984): Geological Setting of the Rossland Mining Camp; B.C. Ministry of Energy, Mines and Petroleum Resources, Bulletin 74, 61 pages.

Fyles, J.T. and Hewlett, C.G. (1959): Stratigraphy and Structure of the Salmo Lead-Zinc Area; British Columbia Department of Mines, Bulletin 41, 162 pages.

Gaunt, D. (1990): Geological and Geochemical Report on the Salmo Project, International Corona Corp., B.C. Assessment Report 20193.

Gaunt, D. (1989): Geochemical and Geophysical Report on the Salmo Claims, Corona Corp., B.C. Assessment Report 18990.

Höy, T. and Dunne, K.P.E. (1997): Early Jurassic Rossland Group, Southern British Columbia Part I - Stratigraphy and Tectonics; B.C. Ministry of Employment and Investment, Energy and Minerals Division, Geological Survey Branch, Bulletin 102.

Höy, T., Church, B.N., Legun, A., Glover, J.K., Grant, B., Wheeler, J.O. and Dunn, K.P.E. (1994): The Geology of the Kootenay Mineral Assessment Region, B.C. Ministry of Energy and Mines, Open File 1994-8.

Höy, T. and Andrew, K.P.E., (1991): Geology of the Rossland -Trail Area, Southeastern British Columbia (82F/4); B.C. Ministry of Energy, Mines and Petroleum Resources, Open File 1991-2.

Höy, T. and Andrew, K.P.E., (1990): Structure and Tectonic Setting of the Rossland Group, Mount Kelly-Hellroaring Creek Area, Southeastern British Columbia (82F/3W). In Geological Fieldwork 1989, BC Ministry of Energy Mines and Petroleum, Paper 1990-1, pages 11-17.

Höy, T. and Andrew, K.P.E. (1990): Geology of the Rossland Group, Mount Kelly - Hellroaring Creek Area, Southeastern British Columbia (NTS 82F/3W) B.C. Ministry of Energy, Mines and Petroleum Resources, Open File 1990-08.

Höy, T. and Andrew, K.P.E. (1989): Geology of the Rossland Group, Nelson Map-area, Southeastern British Columbia; B.C. Ministry of Energy, Mines and Petroleum Resources, Open File 1989-1.

Höy, T. (1980): Geology of the Riondel Area, Central Kootenay Arc, Southeastern British Columbia; B.C. Ministry of Energy, Mines and Petroleum Resources; Bulletin 80, 89 pages.

Kemp, R. (1992): Report on the Drilling Activities Carried Out on the Katie Group of Claims by Yellowjack Resources Ltd. for Noranda Mining and Exploration Inc., B.C. Assessment Report 22200.

Little, H.W. (1985): Geological Notes, Nelson West-half (82F,W1/2) Map-area; Geological Survey of Canada, Open File 1199.

Little, H.W. (1982): Geology, Rossland-Trail Map-area, British Columbia; Geological Survey of Canada, Paper 79-26, 38 pages.

Little, H.W. (1982): Geology, Bonnington Map Area, British Columbia; Geological Survey of Canada, Map 1571A.

Little, H.W. (1965): Geology, Salmo Map Area, British Columbia; Geological Survey of Canada, Map 1145A.

Little, H.W. (1960): Nelson Map-area, West-half, British Columbia; Geological Survey of Canada, Memoir 308, 205 pages.

Little, H.W. (1950): Salmo Map-area, British Columbia; Geological Survey of Canada, Paper 50-19, 43 pages.

Logan, J. and Vilkos, V. (2002): Geoscience Map 2002-1: Intrusion - Related Mineral Occurrences of the Cretaceous Bayonne Magmatic Melt, Southeast British Columbia NTS (82 E,F,G,J,K,L,M,N).

MacIlsac, B. (1980): Soil Geochemistry Report, Jim Group, Nelson Mining Division 82F 3W., Amoco Canada Petroleum Company Ltd., B. C. Assessment Report 8258.

- Massey, N.W.D., MacIntyre, Desjardins, P.J. and Cooney, R.T. (2005): Digital Geology Map of British Columbia: Tile NM11 Southeast B.C. Ministry of Energy and Mines, Geofile 2005-4, scale 1:250,000.
- McGrath, B., Wainwright, A. and Gofton, E. (2008): 2007 Geological Mapping & Diamond Drilling Assessment Report on the Swift Katie Project, NTS 82F/03, Valterra Resource Corp., 203 pages.
- McIntyre, T.J. (1991): Report on the Drilling Activities Carried Out on the Katie Group of Claims, Noranda Exploration Company Ltd, B. C. Assessment Report 21704.
- McIntyre, T.J. (1990): Report on the Geological and Geochemical Survey of the Katie Group of Claims, Noranda Exploration Company Ltd., B. C. Assessment Report 20331.
- Ministry of Energy, Mines and Petroleum Resources (1973): Salmo, Aeromagnetic Map 8479G. Aeromagnetic Survey / Salmo 082F/03.
- Mulligan, R. (1952): Bonnington Map Area, British Columbia; Geological Survey of Canada, Paper 52-13, 37 pages.
- Murray, K. (1987): Soil Geochemistry of the Katie Group Area, B.C. Assessment Report 15781.
- Murray, T.J. and Bradish, L. (1990): Geological and Geochemical Survey on the Katie Group of Claims for Noranda Exploration Company Limited.
- Naciuk, T.M. and Hawkins, T.G. (1995): The Katie copper-gold porphyry deposit, Southeastern British Columbia, Porphyry Deposits of the Northwestern Cordillera of North America, Schroeter, T. Editor, CIM Special Volume 46, pages 666-673.
- Okulitch, A.V. and Woodsworth, G.J. (1977): Kootenay map-area, British Columbia, Alberta, and the United States Geological Survey of Canada, Open File 481.
- Parrish, R.R., Carr, S.D. and Parkinson, D.L. (1988): Eocene Extensional Tectonics and Geochronology of the Southern Omineca Belt, British Columbia and Washington; Tectonics, Volume 7, pages 181-212.
- Pollard, P.J. (2006): An Intrusion-related Origin for Cu–Au Oxide–Copper–Gold (IOCG) Provinces, Mineralium Deposita, v.41, pages 179–187.
- Price, B.J. and Makepeace, D.M. (2007): Technical Report for Swift Katie Copper-Gold Property, Valterra Resource Corp.
- Rice, H.M.A. (1941): Nelson Map-area, East Half, British Columbia; Geological Survey of Canada, Memoir 228, 86 pages.
- Sillitoe, R.H. (2003): Iron Oxide-Copper-Gold Deposits: An Andean View, Mineralium Deposita v. 38, pages 787–812.
- Simony, P.S. (1979): Pre-Carboniferous Basement near Trail, British Columbia; Canadian Journal of Earth Sciences, Volume 16, Number 1, pages 1-11.

Skupinski, A. (1989): Report on Katie Claims - Drilling, Trenching, Mapping and Petrography of Rock Alteration, NTS 82F/3W, Baloil Lassiter Petroleum Ltd.

Uher, L. (1985): Rossland Regional Program, PN095 - 1984, Nelson Mining Division, NTS 82F/3,4, Falconbridge Ltd., 132 pages.

von Fersen, N (2002): Summary Review of the Swift Claims NTS 82F/03W, memo to A. Savage, January, 30.

von Fersen, N (1987): Report on Backhoe Trenching Program, Ace in the Hole Claim, Falconbridge Ltd., B. C. Assessment Report 16567.

von Fersen, N (1986): Geochemical and Geophysical Reports on the Swift and Gus Claims (Volumes I & II); Falconbridge Ltd. - Kidd Creek Mines Ltd, B. C. Assessment Report 15561.

Walker, J.F. (1934): Geology and Mineral Deposits of the Salmo Map Area, British Columbia; Geological Survey of Canada, Memoir 172, 102 pages.

Wells, R.C. (1996): Geological Assessment Report on the Sar Gold Mineral Exploration Project, Kamloops Geological Services, B. C. Assessment Report 24647.

Wells, R.C. (1994): Report on the Katie Property, Nelson Mining Division (82F/3), for Yellowjack Resources Ltd.

Wheeler, J.O., Brookfield, A.J., Gabrielse, H., Monger, J.W.H., Tipper, H.W. and Woodsworth, G.J. (1991): Terrane Map of the Canadian Cordillera; Geological Survey of Canada, Map 1713A, scale 1:2,000,000.

Wheeler, J.O. and McFeely, P. (1991): Tectonic Assemblage Map of the Canadian Cordillera and Adjacent Parts of the United States of America; Geological Survey of Canada, Map 1712A, scale 1:2,000,000.



APPENDICES



APPENDIX A

Fugro Airborne Surveys Corp.

DIGHEM Survey Report

for Valterra Resource Corp.

Swift Katie Block,

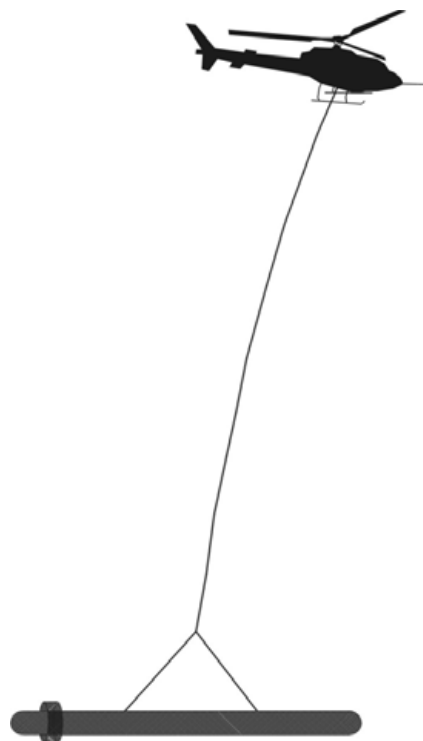
British Columbia

NTS: 82F/3

Report # 07114

**DIGHEM SURVEY
FOR
VALTERRA RESOURCE CORPORATION
SWIFT KATIE BLOCK,
BRITISH COLUMBIA**

NTS: 82F/3



Fugro Airborne Surveys Corp.
Mississauga, Ontario

March 14, 2008

SUMMARY

This report describes the logistics, data acquisition, processing and presentation of results of a DIGHEM airborne geophysical survey carried out for Valterra Resource Corporation, over the Swift Katie Block, in the province of British Columbia. Total coverage for the area amounted to 505 km. The survey was flown from December 5th, 2007, to January 16th, 2008.

The purpose of the survey was to detect zones of conductive mineralization, to locate any plug-like structures that might be due to porphyritic intrusions, and to provide information that could be used to map the geology and structure of the survey area. This was accomplished by using a DIGHEM multi-coil, multi-frequency electromagnetic system. The information from these sensors was processed to produce maps that display the magnetic and conductive properties of the survey area. A GPS electronic navigation system ensured accurate positioning of the geophysical data with respect to the base maps.

The survey data were processed and compiled in the Fugro Airborne Surveys Toronto office. Map products and digital data were provided in accordance with the scales and formats specified in the Survey Agreement.

The survey property contains many anomalous features, several of which are considered to be of moderate to high priority as exploration targets. Many of the inferred bedrock conductors appear to warrant further investigation using appropriate surface exploration

techniques, unless their causative sources have already been determined. Areas of interest may be assigned priorities on the basis of supporting geophysical, geochemical and/or geological information. After initial investigations have been carried out, it may be necessary to re-evaluate the remaining anomalies based on information acquired from the follow-up program.

CONTENTS

1.	INTRODUCTION	1.1
2.	SURVEY OPERATIONS.....	2.1
3.	SURVEY EQUIPMENT	3.1
	Electromagnetic System	3.1
	In-Flight EM System Calibration	3.2
	Airborne Magnetometer	3.3
	Magnetic Base Station.....	3.4
	Navigation (Global Positioning System)	3.6
	Radar Altimeter.....	3.8
	Barometric Pressure and Temperature Sensors	3.9
	Digital Data Acquisition System.....	3.9
	Video Flight Path Recording System	3.10
4.	QUALITY CONTROL AND IN-FIELD PROCESSING.....	4.1
5.	DATA PROCESSING	5.1
	Flight Path Recovery	5.1
	Electromagnetic Data	5.1
	Apparent Resistivity	5.2
	Dielectric Permittivity and Magnetic Permeability Corrections.....	5.4
	Resistivity-depth Sections (optional)	5.5
	Total Magnetic Field.....	5.6
	Calculated Vertical Magnetic Gradient	5.7
	EM Magnetite (optional)	5.7
	Magnetic Derivatives (optional)	5.7
	Digital Elevation (optional).....	5.8
	Contour, Colour and Shadow Map Displays.....	5.9
	Multi-channel Stacked Profiles	5.10
6.	PRODUCTS	6.1
	Base Maps.....	6.1
	Final Products.....	6.2
7.	SURVEY RESULTS	7.1
	General Discussion	7.1

Magnetic Data	7.4
Apparent Resistivity	7.5
Electromagnetic Anomalies.....	7.5
Potential Targets in the Survey Area.....	7.8
 8. CONCLUSIONS AND RECOMMENDATIONS.....	 8.1

APPENDICES

- A. List of Personnel
- B. Data Processing Flowcharts
- C. Background Information
- D. Data Archive Description
- E. EM Anomaly List
- F. Glossary

1. INTRODUCTION

A DIGHEM electromagnetic/ resistivity/ magnetic survey was flown for Valterra Resource Corporation, from December 5th, 2007 to January 16th, 2008, over the Swift Katie Block, British Columbia. The survey area can be located on NTS map sheet 82F/3 (Figure 2).

Survey coverage consisted of approximately 505 line-km, including 168 line-km of tie lines. Flight lines were flown in an azimuthal direction of 20°/200° with a line separation of 200 metres. Tie lines were flown orthogonal to the traverse lines with a line separation of 400 meters.

The survey employed the DIGHEM V electromagnetic system. Ancillary equipment consisted of a magnetometer, radar and barometric altimeters, a video camera, and a digital recorder. The instrumentation was installed in an AS350B3 turbine helicopter (Registration C-GECL) that was provided by Questral Helicopters Ltd. The helicopter flew at an average airspeed of 72 km/h with an EM sensor height of approximately 30 metres.



Figure 1: Fugro Airborne Surveys DIGHEM EM bird with AS350-B3

2. SURVEY OPERATIONS

The base of operations for the survey was established at Castlegar, British Columbia, in 2007, and then re-located to Nelson, British Columbia, in 2008. The survey area can be located on NTS map sheet 82F/3.

Table 2-1 lists the corner coordinates of the survey area in NAD83, UTM Zone 11 North, central meridian 117° West.

Table 2-1

Nad83 Utm zone 11N			
Block	Corners	X-UTM (E)	Y-UTM (N)
07114-1	1	471660	5445115
Swift	2	471929	5445115
Katie	3	472105	5445599
	4	474167	5445584
	5	474835	5447419
	6	477139	5447399
	7	477125	5446023
	8	477595	5446021
	9	477593	5445558
	10	479871	5445549
	11	479860	5442307
	12	479284	5442315
	13	478945	5441384
	14	478933	5438141
	15	474689	5438145
	16	474351	5437216
	17	470691	5437275
	18	470711	5438165
	19	471169	5439425
	20	471176	5440024

	21	471631	5441273
--	----	--------	---------

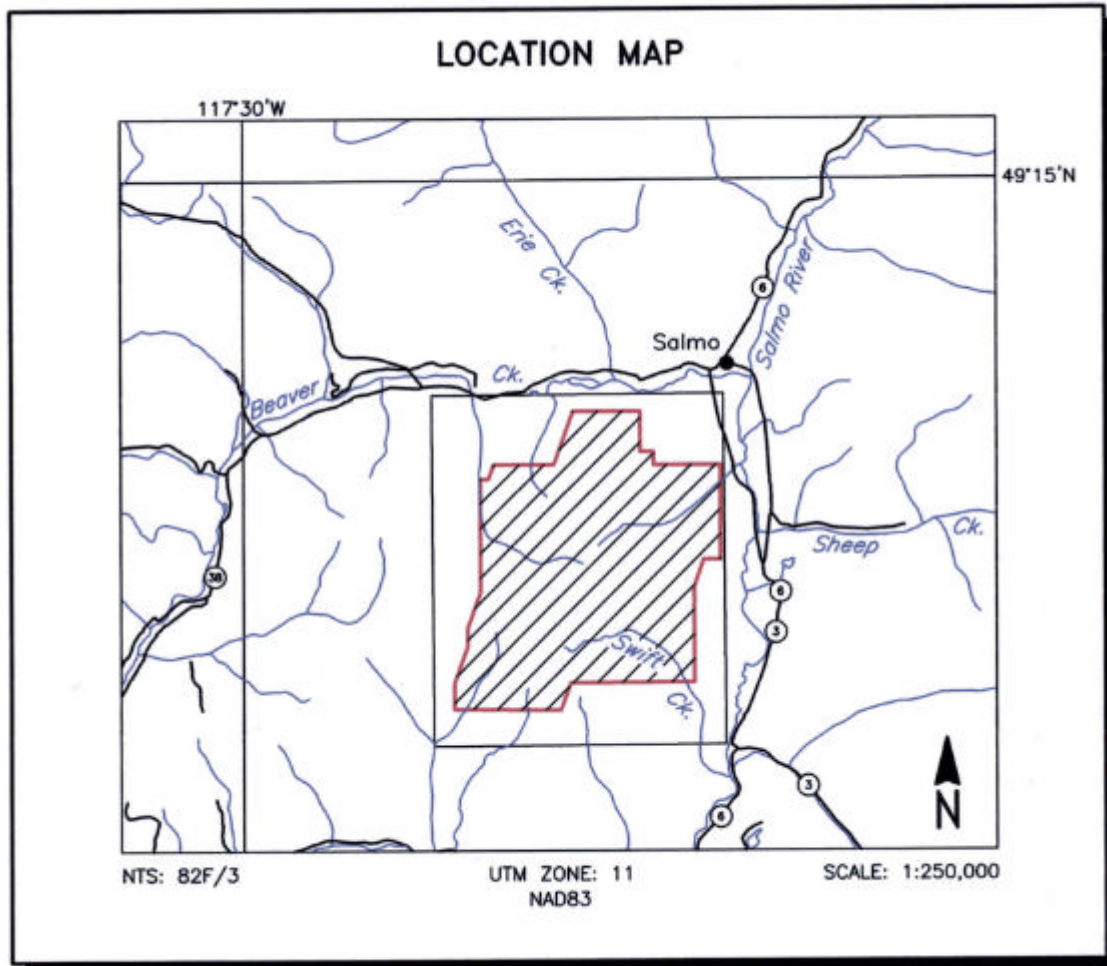


Figure 2
Location Map and Sheet Layout
Swift Katie Block, British Columbia
Job # 07114

The survey specifications were as follows:

Parameter	Specifications
Traverse line direction	20°/200°
Traverse line spacing	200 m
Tie line direction	110°/290°,
Tie line spacing	400 m
Sample interval	10 Hz, 2.0 m @ 72 km/h
Aircraft mean terrain clearance	58 m
EM sensor mean terrain clearance	30 m
Mag sensor mean terrain clearance	30 m
Average speed	72 km/h
Navigation (guidance)	±5 m, Real-time GPS
Post-survey flight path	±2 m, Differential GPS

3. SURVEY EQUIPMENT

This section provides a brief description of the geophysical instruments used to acquire the survey data and the calibration procedures employed. The geophysical equipment was installed in an AS350B3 helicopter. This aircraft provides a safe and efficient platform for surveys of this type.

Electromagnetic System

Model: DIGHEM V – BKS54

Type: Towed bird, symmetric dipole configuration operated at a nominal survey altitude of 30 metres. Coil separation is 8 metres for 900 Hz, 1000 Hz, 5500 Hz and 7200 Hz, and 6.3 metres for the 56,000 Hz coil-pair.

Coil orientations, frequencies and dipole moments	<u>Atm²</u>	<u>orientation</u>	<u>nominal</u>	<u>actual</u>
	211	coaxial /	1000 Hz	1120 Hz
	211	coplanar /	900 Hz	870 Hz
	67	coaxial /	5500 Hz	5440 Hz
	56	coplanar /	7200 Hz	7130 Hz
	15	coplanar /	56,000 Hz	56,000 Hz

Channels recorded: 5 in-phase channels
5 quadrature channels
2 monitor channels

Sensitivity: 0.06 ppm at 1000 Hz Cx
0.12 ppm at 900 Hz Cp
0.12 ppm at 5,500 Hz Cx
0.24 ppm at 7,200 Hz Cp
0.60 ppm at 56,000 Hz Cp

Sample rate: 10 per second, equivalent to 1 sample every 2.0 m,
at a survey speed of 72 km/h.

The electromagnetic system utilizes a multi-coil coaxial/coplanar technique to energize conductors in different directions. The coaxial coils are vertical with their axes in the flight direction. The coplanar coils are horizontal. The secondary fields are sensed simultaneously by means of receiver coils that are maximum coupled to their respective transmitter coils. The system yields an in-phase and a quadrature channel from each transmitter-receiver coil-pair.

In-Flight EM System Calibration

Calibration of the system during the survey uses the Fugro AutoCal automatic, internal calibration process. At the beginning and end of each flight, and at intervals during the flight, the system is flown up to high altitude to remove it from any “ground effect” (response from the earth). Any remaining signal from the receiver coils (base level) is measured as the zero level, and is removed from the data collected until the time of the next calibration. Following the zero level setting, internal calibration coils, for which the response phase and amplitude have been determined at the factory, are automatically triggered – one for each frequency. The on-time of the coils is sufficient to determine an accurate response through any ambient noise. The receiver response to each calibration coil “event” is compared to the expected response (from the factory calibration) for both phase angle and amplitude, and any phase and gain corrections are automatically applied to bring the data to the correct value.

In addition, the outputs of the transmitter coils are continuously monitored during the survey, and the gains are adjusted to correct for any change in transmitter output.

Because the internal calibration coils are calibrated at the factory (on a resistive half-space) ground calibrations using external calibration coils on-site are not necessary for system calibration. A check calibration may be carried out on-site to ensure all systems are working correctly. All system calibrations will be carried out in the air, at sufficient altitude that there will be no measurable response from the ground. The internal calibration coils are rigidly positioned and mounted in the system relative to the transmitter and receiver coils. In addition, when the internal calibration coils are calibrated at the factory, a rigid jig is employed to ensure accurate response from the external coils.

Using real time Fast Fourier Transforms and the calibration procedures outlined above, the data are processed in real time, from measured total field at a high sampling rate, to in-phase and quadrature values at 10 samples per second.

Airborne Magnetometer

Model:	Geometrics G822A
Type:	Optically pumped cesium vapour
Sensitivity:	0.01 nT
Sample rate:	10 per second

The magnetometer sensor was mounted inside the centre of the EM bird, 28 m below the helicopter.

Magnetic Base Station

Primary

Model: Fugro CF1 base station with timing
provided by integrated GPS

Sensor type: Geometrics G822A

Counter specifications: Accuracy: ± 0.1 nT
Resolution: 0.01 nT
Sample rate: 1 Hz

GPS specifications: Model: Marconi Allstar
Type: Code and carrier tracking of L1 band,
12-channel, C/A code at 1575.42 MHz
Sensitivity: -90 dBm, 1.0 second update
Accuracy: Manufacturer's stated accuracy for differential
corrected GPS is 2 metres

Environmental

Monitor specifications: Temperature:

- Accuracy: $\pm 1.5^{\circ}\text{C}$ max
- Resolution: 0.0305°C
- Sample rate: 1 Hz
- Range: -40°C to $+75^{\circ}\text{C}$

Barometric pressure:

- Model: Motorola MPXA4115A
- Accuracy: $\pm 3.0^{\circ}$ kPa max (-20°C to 105°C temp. ranges)
- Resolution: 0.013 kPa
- Sample rate: 1 Hz
- Range: 55 kPa to 108 kPa

A digital recorder is operated in conjunction with the base station magnetometer to record the diurnal variations of the earth's magnetic field. The clock of the base station is synchronized with that of the airborne system, using GPS time, to permit subsequent removal of diurnal drift. The Fugro CF1 was the primary magnetic base station. For the 2007 flying, it was located in Castlegar, BC, at latitude 49° 17' 36.929" N, longitude 117° 38' 02.967" W, at an elevation of 442.4 metres above the ellipsoid. In 2008, the CF1 was moved to Nelson, BC, latitude 49° 29' 28.871" N, longitude 117° 18' 23.148" W, at an elevation of 488.7 metres above the ellipsoid.



Figure 3-1: Fugro CF1

Navigation (Global Positioning System)

Airborne Receiver for Real-time Navigation & Guidance

Model:	Novatel OEM IV.
Type:	Code and carrier tracking of L1-C/A code at 1575.42 MHz and L2-P code at 1227.0 MHz. Dual frequency, 24-channel.
Sample rate:	10 Hz update.
Accuracy:	Better than 1 metre in differential mode.
Antenna:	Aero AT1675 mounted on tail of aircraft

Primary Base Station for Post-Survey Differential Correction

Model:	Novatel OEM IV
Type:	Code and carrier tracking of L1-C/A code at 1575.42 MHz and L2-P code at 1227.0 MHz. Dual frequency, 24-channel.
Sample rate:	10 Hz update.
Accuracy:	Better than 1 metre in differential mode.

Secondary GPS Base Station

Model:	Marconi Allstar OEM, CMT-1200
Type:	Code and carrier tracking of L1 band, 12-channel, C/A code

at 1575.42 MHz

Sensitivity: -90 dBm, 1.0 second update

Accuracy: Manufacturer's stated accuracy for differential corrected GPS is 2 metres.

The Novatel OEM IV is a line of sight, satellite navigation system that utilizes time-coded signals from at least four of forty-eight available satellites. Both Russian GLONASS and American NAVSTAR satellite constellations are used to calculate the position and to provide real time guidance to the helicopter. A similar system was used as the primary base station receiver. The mobile and base station raw XYZ data were recorded, thereby permitting post-survey differential corrections for theoretical accuracies of better than one metre. A Marconi Allstar GPS unit, part of the CF-1, was used as a secondary (back-up) base station.

Each base station receiver is able to calculate its own latitude and longitude. For the 2007 portion of the survey, the primary GPS station was located at Castlegar airport, latitude 49° 17' 35.934" N, longitude 117° 38' 02.822" W, at an elevation of 483.3 metres above the ellipsoid. In 2008, the GPS station was moved to Nelson, BC at latitude 49° 29' 28.818" N, longitude 117° 18' 22.391" W, at an elevation of 522.7 metres above the ellipsoid. The GPS records data relative to the WGS84 ellipsoid, which is the basis of the revised North American Datum (NAD83). Conversion software is used to transform the WGS84 coordinates to the NAD83 UTM system displayed on the maps.



Figure 3-2: Fugro Primary GPS base station

Radar Altimeter

Manufacturer:	Sperry
Model:	RT220
Type:	Short pulse modulation, 4.3 GHz
Sensitivity:	0.3 m
Sample rate:	2 per second

The radar altimeter measures the vertical distance between the helicopter and the ground.

This information is used in the processing algorithm that determines conductor depth.

Barometric Pressure and Temperature Sensors

Model:	DIGHEM D 1300		
Type:	Motorola MPX4115AP analog pressure sensor AD592AN high-impedance remote temperature sensors		
Sensitivity:	Pressure:	150 mV/kPa	
	Temperature:	100 mV/°C or 10 mV/°C (selectable)	
Sample rate:	10 per second		

The D1300 circuit is used in conjunction with one barometric sensor and up to three temperature sensors. Two sensors (baro and temp) are installed in the EM console in the aircraft, to monitor pressure (KPA), and internal (TEMP_INT) operating temperature. A third sensor is installed in the bird to monitor the external (TEMP_EXT) temperature.

Digital Data Acquisition System

Manufacturer:	Fugro
Model:	HeliDAS
Recorder:	Ultra II Compact Flash Memory Card

The stored data are downloaded to the field workstation PC at the survey base, for verification, backup and preparation of in-field products.

Video Flight Path Recording System

Type:	Axis 2420 Digital Network Camera
Recorder:	Axis 214S Video Server & Tablet Computer
Format:	Digital Video (*.BIN/ *.BDX)

Fiducial numbers are recorded continuously and are displayed on the margin of each image. This procedure ensures accurate correlation of data with respect to visible features on the ground.

4. QUALITY CONTROL AND IN-FIELD PROCESSING

Digital data for each flight were transferred to the field workstation, in order to verify data quality and completeness. A database was created and updated using Geosoft Oasis Montaj and proprietary Fugro Atlas software. This allowed the field personnel to calculate, display and verify both the positional (flight path) and geophysical data on a screen or printer. Records were examined as a preliminary assessment of the data acquired for each flight.

In-field processing of Fugro survey data consists of differential corrections to the airborne GPS data, verification of EM calibrations, drift correction of the raw airborne EM data, spike rejection and filtering of all geophysical and ancillary data, verification of flight videos, calculation of preliminary resistivity data, diurnal correction, and preliminary leveling of magnetic data.

All data, including base station records, were checked on a daily basis, to ensure compliance with the survey contract specifications. Reflights were required if any of the following specifications were not met.

Navigation - Positional (x,y) accuracy of better than 10 m, with a CEP (circular error of probability) of 95%.

- 4.2 -

- Flight Path - No lines to exceed $\pm 25\%$ departure from nominal line spacing over a continuous distance of more than 1 km, except for reasons of safety.
- Clearance - Mean terrain sensor clearance of 30 m, except where precluded by safety considerations, e.g., restricted or populated areas, severe topography, obstructions, tree canopy, aerodynamic limitations, etc.
- Airborne Mag - The non-normalized 4th difference will not exceed 1.6 nT over a continuous distance of 1 kilometre excluding areas where this specification is exceeded due to natural anomalies.
- Base Mag - Diurnal variations not to exceed 10 nT over a straight-line time chord of 1 minute.
- EM - Spheric pulses may occur having strong peaks but narrow widths. The EM data area considered acceptable when their occurrence is less than 10 spheric events exceeding the stated noise specification for a given frequency per 100 samples continuously over a distance of 2,000 metres.

- 4.3 -

Frequency	Coil Orientation	Peak to Peak Noise Envelope (ppm)
900 Hz	horizontal coplanar	10.0
1000 Hz	vertical coaxial	5.0
5500 Hz	vertical coaxial	10.0
7200 Hz	horizontal coplanar	20.0
56,000 Hz	horizontal coplanar	40.0

5. DATA PROCESSING

Flight Path Recovery

The raw range data from at least four satellites are simultaneously recorded by both the base and mobile GPS units. The geographic positions of both units, relative to the model ellipsoid, are calculated from this information. Differential corrections, which are obtained from the base station, are applied to the mobile unit data to provide a post-flight track of the aircraft, accurate to within 2 m. Speed checks of the flight path are also carried out to determine if there are any spikes or gaps in the data.

The corrected WGS84 latitude/longitude coordinates are transformed to the coordinate system used on the final maps. Images or plots are then created to provide a visual check of the flight path.

Electromagnetic Data

EM data are processed at the recorded sample rate of 10 samples/second. Spheric rejection median and Hanning filters are then applied to reduce noise to acceptable levels. EM test profiles are then created to allow the interpreter to select the most appropriate EM anomaly picking controls for a given survey area. The EM picking parameters depend on several factors but are primarily based on the dynamic range of the resistivities within the

survey area, and the types and expected geophysical responses of the targets being sought.

Anomalous electromagnetic responses are selected and analysed by computer to provide a preliminary electromagnetic anomaly map. The automatic selection algorithm is intentionally oversensitive to assure that no meaningful responses are missed. Using the preliminary map in conjunction with the multi-parameter stacked profiles, the interpreter then classifies the anomalies according to their source and eliminates those that are not substantiated by the data. The final interpreted EM anomaly map includes bedrock, surficial and cultural conductors. A map containing only bedrock conductors can be generated, if desired.

Apparent Resistivity

The apparent resistivities in ohm-m are generated from the in-phase and quadrature EM components for all of the coplanar frequencies, using a pseudo-layer half-space model. The inputs to the resistivity algorithm are the in-phase and quadrature amplitudes of the secondary field. The algorithm calculates the apparent resistivity in ohm-m, and the apparent height of the bird above the conductive source. Any difference between the apparent height and the true height, as measured by the radar altimeter, is called the pseudo-layer and reflects the difference between the real geology and a homogeneous half space. This difference is often attributed to the presence of a highly resistive upper layer. Any errors in the altimeter reading, caused by heavy tree cover, are included in the

pseudo-layer and do not affect the resistivity calculation. The apparent depth estimates, however, will reflect the altimeter errors. Apparent resistivities calculated in this manner may differ from those calculated using other models.

In areas where the effects of magnetic permeability or dielectric permittivity have suppressed the in-phase responses, the calculated resistivities will be erroneously high. Various algorithms and inversion techniques can be used to partially correct for the effects of permeability and permittivity.

Apparent resistivity maps portray all of the information for a given frequency over the entire survey area. This full coverage contrasts with the electromagnetic anomaly map, which provides information only over interpreted conductors. The large dynamic range afforded by the multiple frequencies makes the apparent resistivity parameter an excellent mapping tool.

The preliminary apparent resistivity maps and images are carefully inspected to identify any lines or line segments that might require base level adjustments. Subtle changes between in-flight calibrations of the system can result in line-to-line differences that are more recognizable in resistive (low signal amplitude) areas. If required, manual level adjustments are carried out to eliminate or minimize resistivity differences that can be attributed, in part, to changes in operating temperatures. These leveling adjustments are usually very subtle, and do not result in the degradation of discrete anomalies.

After the manual leveling process is complete, revised resistivity grids are created. The resulting grids can be subjected to a microleveling technique in order to smooth the data for contouring. The coplanar resistivity parameter has a broad 'footprint' that requires very little filtering.

The calculated resistivities for the 900 Hz, 7200 Hz and 56000 Hz coplanar frequencies are included in the XYZ and grid archives. Values are in ohm-metres on all final products.

Dielectric Permittivity and Magnetic Permeability Corrections¹

In resistive areas having magnetic rocks, the magnetic and dielectric effects will both generally be present in high-frequency EM data, whereas only the magnetic effect will exist in low-frequency data.

The magnetic permeability is first obtained from the EM data at the lowest frequency, because the ratio of the magnetic response to conductive response is maximized and because displacement currents are negligible. The homogeneous half-space model is used. The computed magnetic permeability is then used along with the in-phase and quadrature response at the highest frequency to obtain the relative dielectric permittivity, again using the homogeneous half-space model. The highest frequency is used because the ratio of dielectric response to conductive response is maximized. The resistivity can

⁴_____

¹ Huang, H. and Fraser, D.C., 2001 Mapping of the Resistivity, Susceptibility, and Permittivity of the Earth Using a Helicopter-borne Electromagnetic System: Geophysics 106 pg 148-157.

then be determined from the measured in-phase and quadrature components of each frequency, given the relative magnetic permeability and relative dielectric permittivity.

Resistivity-depth Sections (optional)

The apparent resistivities for all frequencies can be displayed simultaneously as coloured resistivity-depth sections. Usually, only the coplanar data are displayed as the close frequency separation between the coplanar and adjacent coaxial data tends to distort the section. The sections can be plotted using the topographic elevation profile as the surface. The digital terrain values, in metres a.m.s.l., can be calculated from the GPS Z-value or barometric altimeter, minus the aircraft radar altimeter.

Resistivity-depth sections can be generated in three formats:

- (1) Sengpiel resistivity sections, where the apparent resistivity for each frequency is plotted at the depth of the centroid of the in-phase current flow²; and,
- (2) Differential resistivity sections, where the differential resistivity is plotted at the differential depth³.
- (3) Occam⁴ or Multi-layer⁵ inversion.

² Sengpiel, K.P., 1988, Approximate Inversion of Airborne EM Data from Multilayered Ground: Geophysical Prospecting 36, 446-459.

³ Huang, H. and Fraser, D.C., 1993, Differential Resistivity Method for Multi-frequency Airborne EM Sounding: presented at Intern. Airb. EM Workshop, Tucson, Ariz.

Both the Sengpiel and differential methods are derived from the pseudo-layer half-space model. Both yield a coloured resistivity-depth section that attempts to portray a smoothed approximation of the true resistivity distribution with depth. Resistivity-depth sections are most useful in conductive layered situations, but may be unreliable in areas of moderate to high resistivity where signal amplitudes are weak. In areas where in-phase responses have been suppressed by the effects of magnetite, or adversely affected by cultural features, the computed resistivities shown on the sections may be unreliable.

Both the Occam and multi-layer inversions compute the layered earth resistivity model that would best match the measured EM data. The Occam inversion uses a series of thin, fixed layers (usually 20 x 5m and 10 x 10m layers) and computes resistivities to fit the EM data. The multi-layer inversion computes the resistivity and thickness for each of a defined number of layers (typically 3-5 layers) to best fit the data.

Total Magnetic Field

A fourth difference editing routine was applied to the magnetic data to remove any spikes. The aeromagnetic data were corrected for diurnal variation using the magnetic base station data. The results were then leveled using tie and traverse line intercepts. Manual adjustments were applied to any lines that required leveling, as indicated by shadowed

⁴ Constable et al, 1987, Occam's inversion: a practical algorithm for generating smooth models from electromagnetic sounding data: *Geophysics*, 52, 289-300.

⁵ Huang H., and Palacky, G.J., 1991, Damped least-squares inversion of time domain airborne EM data based on singular value decomposition: *Geophysical Prospecting*, 39, 827-844.

images of the gridded magnetic data. The manually leveled data were then subjected to a microleveling filter.

Calculated Vertical Magnetic Gradient

The diurnally-corrected total magnetic field data were subjected to a processing algorithm that enhances the response of magnetic bodies in the upper 500 m and attenuates the response of deeper bodies. The resulting vertical gradient map provides better definition and resolution of near-surface magnetic units. It also identifies weak magnetic features that may not be evident on the total field map. However, regional magnetic variations and changes in lithology may be better defined on the total magnetic field map.

EM Magnetite (optional)

The apparent percent magnetite by weight is computed wherever magnetite produces a negative in-phase EM response. This calculation is more meaningful in resistive areas.

Magnetic Derivatives (optional)

The total magnetic field data can be subjected to a variety of filtering techniques to yield maps or images of the following:

- enhanced magnetics
- second vertical derivative
- reduction to the pole/equator
- magnetic susceptibility with reduction to the pole
- upward/downward continuations
- analytic signal

All of these filtering techniques improve the recognition of near-surface magnetic bodies, with the exception of upward continuation. Any of these parameters can be produced on request.

Digital Elevation (optional)

The radar altimeter values (ALTR – aircraft to ground clearance) are subtracted from the differentially corrected and de-spiked GPS-Z values to produce profiles of the height above the ellipsoid along the survey lines. These values are gridded to produce contour maps showing approximate elevations within the survey area. The calculated digital terrain data are then tie-line leveled and adjusted to mean sea level. Any remaining subtle line-to-line discrepancies are manually removed. After the manual corrections are applied, the digital terrain data are filtered with a microleveling algorithm.

The accuracy of the elevation calculation is directly dependent on the accuracy of the two input parameters, ALTR and GPS-Z. The ALTR value may be erroneous in areas of

heavy tree cover, where the altimeter reflects the distance to the tree canopy rather than the ground. The GPS-Z value is primarily dependent on the number of available satellites.

Although post-processing of GPS data will yield X and Y accuracies in the order of 1-2 metres, the accuracy of the Z value is usually much less, sometimes in the ± 10 metre range. Further inaccuracies may be introduced during the interpolation and gridding process.

Because of the inherent inaccuracies of this method, no guarantee is made or implied that the information displayed is a true representation of the height above sea level. Although this product may be of some use as a general reference, THIS PRODUCT MUST NOT BE USED FOR NAVIGATION PURPOSES.

Contour, Colour and Shadow Map Displays

The geophysical data are interpolated onto a regular grid using a modified Akima spline technique. The resulting grid is suitable for image processing and generation of contour maps. The grid cell size is 20% of the line interval.

Colour maps are produced by interpolating the grid down to the pixel size. The parameter is then incremented with respect to specific amplitude ranges to provide colour "contour" maps.

Monochromatic shadow maps or images are generated by employing an artificial sun to cast shadows on a surface defined by the geophysical grid. There are many variations in the shadowing technique. These techniques can be applied to total field or enhanced magnetic data, magnetic derivatives, resistivity, etc. The shadowing technique is also used as a quality control method to detect subtle changes between lines.

Multi-channel Stacked Profiles

Distance-based profiles of the digitally recorded geophysical data are generated and plotted at an appropriate scale. These profiles also contain the calculated parameters that are used in the interpretation process. These are produced as worksheets prior to interpretation, and are also presented in the final corrected form after interpretation. The profiles display electromagnetic anomalies with their respective interpretive symbols. Table 5-1 shows the parameters and scales for the multi-channel stacked profiles.

In Table 5-1, the log resistivity scale of 0.06 decade/mm means that the resistivity changes by an order of magnitude in 16.6 mm. The resistivities at 0, 33 and 67 mm up from the bottom of the digital profile are respectively 1, 100 and 10,000 ohm-m.

Table 5-1. Multi-channel Stacked Profiles

Channel Name (Freq)	Observed Parameters	Scale Units/mm
MAG	total magnetic field (fine)	5 nT
MAG	total magnetic field (coarse)	20 nT
ALTRAD_BIRD	EM sensor height above ground	6 m
CXI1000	vertical coaxial coil-pair in-phase (1000 Hz)	2 ppm
CXQ1000	vertical coaxial coil-pair quadrature (1000 Hz)	2 ppm
CPI900	horizontal coplanar coil-pair in-phase (900 Hz)	4 ppm
CPQ900	horizontal coplanar coil-pair quadrature (900 Hz)	4 ppm
CXI5500	vertical coaxial coil-pair in-phase (5500 Hz)	4 ppm
CXQ5500	vertical coaxial coil-pair quadrature (5500 Hz)	4 ppm
CPI7200	horizontal coplanar coil-pair in-phase (7200 Hz)	10 ppm
CPQ7200	horizontal coplanar coil-pair quadrature (7200 Hz)	10 ppm
CPI56K	horizontal coplanar coil-pair in-phase (56,000 Hz)	10 ppm
CPQ56K	horizontal coplanar coil-pair quadrature (56,000 Hz)	10 ppm
CXSP	coaxial spherics monitor	
	Computed Parameters	
DIFI (mid freq.)	difference function in-phase from CXI and CPI	9 ppm
DIFQ (mid freq.)	difference function quadrature from CXQ and CPQ	9 ppm
RES900	log resistivity	.06 decade
RES7200	log resistivity	.06 decade
RES56K	log resistivity	.06 decade
DEP900	apparent depth	6 m
DEP7200	apparent depth	6 m
DEP56K	apparent depth	6 m

6. PRODUCTS

This section lists the final maps and products that have been provided under the terms of the survey agreement. Other products can be prepared from the existing dataset, if requested. These include magnetic enhancements or derivatives, percent magnetite, resistivities corrected for magnetic permeability and/or dielectric permittivity, digital terrain, resistivity-depth sections, inversions, and overburden thickness. Most parameters can be displayed as contours, profiles, or in colour.

Base Maps

Base maps of the survey area were produced by scanning published topographic maps to a bitmap (.bmp) format. This process provides a relatively accurate, distortion-free base that facilitates correlation of the navigation data to the map coordinate system. The topographic files were combined with geophysical data for plotting the final maps. All maps were created using the following parameters:

Projection Description:

Datum:	NAD 83
Ellipsoid:	GRS80
Projection:	UTM (Zone: 11 North)
Central Meridian:	117 ° West
False Northing:	0
False Easting:	500000
Scale Factor:	0.9996
WGS84 to Local Conversion:	Molodensky
Datum Shifts:	DX: 0 DY: -0 DZ: -0

The following parameters are presented on 1 map sheet, at a scale of 1:20,000. All maps include flight lines and topography, unless otherwise indicated. Preliminary products are not listed.

Final Products

	No. of Map Sets = 2		
	Mylar	Blackline	Colour
EM Anomalies		1 x 2	
Total Magnetic Field			1 x 2
Calculated Vertical Magnetic Gradient			1 x 2
Apparent Resistivity 7200 Hz			1 x 2
Apparent Resistivity 56,000 Hz			1 x 2

Additional Products

Digital Archive (see Archive Description)	1 CD-ROM
Survey Report	2 copies
Multi-channel Stacked Profiles	All lines
Digital Video (Flights 4-6)	1 DVD

7. SURVEY RESULTS

General Discussion

Table 7-1 summarizes the EM responses in the survey area, with respect to conductance grade and interpretation. The apparent conductance and depth values shown in the EM Anomaly list appended to this report have been calculated from "local" in-phase and quadrature amplitudes of the Coaxial 5500 Hz frequency. The picking and interpretation procedure relies on several parameters and calculated functions. For this survey, the Coaxial 5500 Hz responses and the mid-frequency difference channels were used as two of the main picking criteria. The 7200 Hz coplanar results were also weighted to provide picks over wider or flat-dipping sources. The quadrature channels provided picks in areas where the in-phase responses might have been suppressed by magnetite.

The anomalies shown on the electromagnetic anomaly maps are based on a near-vertical, half plane model. This model best reflects "discrete" bedrock conductors. Wide bedrock conductors or flat-lying conductive units, whether from surficial or bedrock sources, may give rise to very broad anomalous responses on the EM profiles. These may not appear on the electromagnetic anomaly map if they have a regional character rather than a locally anomalous character.

TABLE 7-1 EM ANOMALY STATISTICS

SWIFT KATIE BLOCK

CONDUCTOR GRADE	CONDUCTANCE RANGE SIEMENS (MHOS)	NUMBER OF RESPONSES
7	>100	6
6	50 - 100	3
5	20 - 50	27
4	10 - 20	55
3	5 - 10	51
2	1 - 5	148
1	<1	125
*	INDETERMINATE	23
TOTAL		438

CONDUCTOR MODEL	MOST LIKELY SOURCE	NUMBER OF RESPONSES
D	DISCRETE BEDROCK CONDUCTOR	55
B	DISCRETE BEDROCK CONDUCTOR	165
S	CONDUCTIVE COVER	67
H	ROCK UNIT OR THICK COVER	70
E	EDGE OF WIDE CONDUCTOR	36
L	CULTURE	45
TOTAL		438

(SEE EM MAP LEGEND FOR EXPLANATIONS)

- 7.3 -

These broad conductors, which more closely approximate a half-space model, will be maximum coupled to the horizontal (coplanar) coil-pair and should be more evident on the resistivity parameter. Resistivity maps, therefore, may be more valuable than the electromagnetic anomaly maps, in areas where broad or flat-lying conductors are considered to be of importance. Contoured resistivity maps, based on the 7200 Hz and 56kHz coplanar data are included with this report.

Excellent resolution and discrimination of conductors was accomplished by using a fast sampling rate of 0.1 sec and by employing a “common” frequency (5500/7200 Hz) on two orthogonal coil-pairs (coaxial and coplanar). The resulting difference channel parameters often permit differentiation of bedrock and surficial conductors, even though they may exhibit similar conductance values.

Anomalies that occur near the ends of the survey lines (i.e., outside the survey area), should be viewed with caution. Some of the weaker anomalies could be due to aerodynamic noise, i.e., bird bending, which is created by abnormal stresses to which the bird is subjected during the climb and turn of the aircraft between lines. Such aerodynamic noise is usually manifested by an anomaly on the coaxial in-phase channel only, although severe stresses can affect the coplanar in-phase channels as well.

Magnetic Data

A Fugro CF-1 cesium vapour magnetometer was set up near the survey block to record diurnal variations of the earth's magnetic field. The clock of the base station was synchronized with that of the airborne system to permit subsequent removal of diurnal drift.

The total magnetic field data have been presented as contours on the base map using a contour interval of 5 nT where gradients permit. The map shows the magnetic properties of the rock units underlying the survey area.

The total magnetic field data have been subjected to a processing algorithm to produce maps of the calculated vertical gradient. This procedure enhances near-surface magnetic units and suppresses regional gradients. It also provides better definition and resolution of magnetic units and displays weak magnetic features that may not be clearly evident on the total field maps.

There is some evidence on the magnetic maps that suggests that the survey area has been subjected to deformation and/or alteration. These structural complexities are evident on the contour maps as variations in magnetic intensity, irregular patterns, and as offsets or changes in strike direction. If a specific magnetic intensity can be assigned to the rock type that is believed to host the target mineralization, it may be possible to select areas of

higher priority on the basis of the total field magnetic data. This is based on the assumption that the magnetite content of the host rocks will give rise to a limited range of contour values that will permit differentiation of various lithological units.

The magnetic results, in conjunction with the other geophysical parameters, have provided valuable information that can be used to effectively map the geology and structure in the survey area.

Apparent Resistivity

Apparent resistivity maps, which display the conductive properties of the survey area, were produced from the 7200 Hz and 56,000 Hz coplanar data. The maximum resistivity values, which are calculated for each frequency, are 8,100 and 20,800 ohm-m respectively. These cut-offs eliminate the erratic higher resistivities that would result from unstable ratios of very small EM amplitudes.

Electromagnetic Anomalies

The EM anomalies resulting from this survey appear to fall within one of four general categories. The first type consists of discrete, well-defined anomalies that yield marked inflections on the difference channels. These anomalies are usually attributed to

conductive sulphides or graphite and are generally given a "B", "T" or "D" interpretive symbol, denoting a bedrock source.

The second class of anomalies comprises moderately broad responses that exhibit the characteristics of a half-space and do not yield well-defined inflections on the difference channels. Anomalies in this category are usually given an "S" or "H" interpretive symbol. The lack of a difference channel response usually implies a broad or flat-lying conductive source such as overburden. Some of these anomalies could reflect conductive rock units, zones of deep weathering, the weathered tops of plugs or pipes, or broad alteration zones, all of which can yield "non-discrete" signatures.

The effects of conductive overburden are evident over portions of the survey area. Although the difference channels (DIFI and DIFQ) are extremely valuable in detecting bedrock conductors that are partially masked by conductive overburden, sharp undulations in the bedrock/overburden interface can yield anomalies in the difference channels which may be interpreted as possible bedrock conductors. Such anomalies usually fall into the "S?" or "B?" classification but may also be given an "E" interpretive symbol, denoting a resistivity contrast at the edge of a conductive unit.

The "?" symbol does not question the validity of an anomaly, but instead indicates some degree of uncertainty as to which is the most appropriate EM source model. This ambiguity results from the combination of effects from two or more conductive sources, such as overburden and bedrock, gradational changes, or moderately shallow dips. The

presence of a conductive upper layer has a tendency to mask or alter the characteristics of bedrock conductors, making interpretation difficult. This problem is further exacerbated in the presence of magnetite.

The third anomaly category includes responses that are associated with magnetite. Magnetite can cause suppression or polarity reversals of the in-phase components, particularly at the lower frequencies in resistive areas. The effects of magnetite-rich rock units are usually evident on the multi-parameter geophysical data profiles as negative excursions of the lower frequency in-phase channels.

In areas where EM responses are evident primarily on the quadrature components, zones of poor conductivity are indicated. Where these responses are coincident with magnetic anomalies, it is possible that the in-phase component amplitudes have been suppressed by the effects of magnetite. Poorly conductive magnetic features can give rise to resistivity anomalies that are only slightly below or slightly above background. If it is expected that poorly conductive economic mineralization could be associated with magnetite-rich units, most of these weakly anomalous features will be of interest. In areas where magnetite causes the in-phase components to become negative, the apparent conductance and depth of EM anomalies will be unreliable. Magnetite effects usually give rise to overstated (higher) resistivity values and understated (shallow) depth calculations.

The fourth class consists of cultural anomalies which are usually given the symbol "L" or "L?". Anomalies in this category can include telephone or power lines, pipelines, railways, fences, metal bridges or culverts, buildings and other metallic structures. There is a line

source that crosses the property from the west end of line 19220 to the east end of 19180.

This linear feature could be due to a pipeline, as there is no 60Hz response on the power line monitor, nor is there any evidence of poles or towers along the cleared swath. Snow cover has obscured any cultural feature that might be on surface, and there is no line source shown on the 1988 topographic map, Salmo sheet 82F/3.

Potential Targets in the Survey Area

As potential targets within the survey area may be associated with massive to weakly disseminated sulphides, which may or may not be hosted by magnetite-rich rocks, it is impractical to assess the relative merits of EM anomalies on the basis of conductance or direct magnetic correlation. It is recommended that an attempt be made to compile a suite of geophysical "signatures" over any known mines and current areas of interest. Anomaly characteristics are clearly defined on the multi-parameter geophysical data profiles that are supplied as one of the survey products.

The electromagnetic anomaly maps show the anomaly locations with the interpreted conductor type, dip, conductance and depth being indicated by symbols. Direct magnetic correlation is also shown if it exists. The strike direction and length of the conductors are indicated only where anomalies can be correlated from line to line with a reasonable degree of confidence.

In areas where several conductors or conductive trends appear to be related to a common geological unit, these have been outlined as "zones" on the EM anomaly maps. The zone outlines approximate the limits of conductive units defined by the 250 ohm-m resistivity contour. Most of the bedrock conductors on the property are contained within one of these five highly conductive zones, which are outlined on the EM Anomaly map as Zones A through E.

Although concentrations of massive sulphide mineralization on the property should yield distinct EM anomalies, any disseminated (porphyry) zones might not be conductive or resistive enough to exhibit a well-defined contrast with the surrounding units. At least some of the porphyry deposits in B.C. yield relative resistivity highs, rather than lows. The Mt. Milligan deposit is one such example. The Mt. Milligan zone also hosts three areas of slightly elevated magnetic susceptibility. Therefore, any plug-like resistive units in the project area should obviously be considered potential targets, particularly those that exhibit weak to moderate magnetic correlation.

Any vein-type mineralization on the property may not be conductive enough to override the opposing effects of the more resistive quartz-carbonate host, and would be unlikely to yield resistivity lows. However, if the unweathered quartz-rich units are thick enough, it is possible that they could give rise to relative resistivity highs. Conversely, faults and shear zones can often be moderately conductive due to the increased porosity or development of alteration products. Because of these factors, it is impractical to assess the relative merits

of EM anomalies on the basis of conductance. It is also quite likely that zones of quartz-vein hosted auriferous mineralization might not yield discernable EM responses.

Many of the magnetite associated responses will also give rise to resistivity highs. These are usually evident on the low frequency 900Hz profiles as negative excursions of the in-phase component. If these negatives correlate with anomalous (positive) responses on the quadrature parameter or high frequencies, they often carry an "S?" symbol. However, they could reflect skarn-type mineralization, rather than conductive overburden.

Magnetic relief varies from a low of 54,093 nT to a high of more than 57,930 nT. The central portion of the survey area is underlain by a block-like unit of higher susceptibility that strikes roughly SSW. The eastern contact of this unit is clearly defined by the 55,750 nT contour, which strikes SSE from the northern end of line 10210.

This magnetic zone appears to be interrupted or intruded by non-magnetic units that strike roughly east to east-southeast, in the vicinity of fiducials 4370, 4436, 4495, 4597, 4664 and 4705, on line 10240. There are several other possible breaks that can be inferred from the vertical gradient data, east of the main contact that parallels line 10270.

The magnetic patterns show moderately poor agreement with resistivity lows, suggesting that the two parameters are responding to different causative sources. The resistivity lows are generally associated with units of lower magnetic susceptibility, and only a few of the bedrock anomalies yield magnetic correlation. The highly conductive and non-magnetic

nature of most of the stronger anomalies suggests that they are likely due to graphitic sediments. The few bedrock conductors that do yield magnetic correlation could be due to pods of magnetic sulphides, such as pyrrhotite, or possible concentrations of magnetite within, or underlying, the conductive zones.

It is beyond the scope of this report to attempt to describe the 438 anomalies detected by the survey. The following paragraphs provide a very brief description of some of the more discrete (sulphide-type) conductors, and a few other responses that appear to be associated with possible faults, shears or non-magnetic intrusions that can be inferred from the magnetic data. The discussion does not include any of the plug-like resistive or weakly conductive units that could reflect porphyritic intrusions. These larger zones should be more evident on the high frequency resistivity maps.

Zone A comprises two pods of moderately conductive material on the northern half of line 10020. The strongest conductivity occurs in the northern lobe, near 10020I. Although both lobes appear to be associated with relatively non-magnetic units, the tie lines show that at least two of the conductive sources in this zone are weakly magnetic, as evidenced by anomalies 19090D and 19110C. Zones A1 and A2 appear to be separated by a more resistive, more magnetic unit on the 10020.

Zone B does not host any thin, discrete conductors, but indicates a moderately broad, weakly conductive buried source that is associated with a north-trending creek and adjacent road.

Anomaly 19050A is a very weak response that is associated with the western contact of a prominent magnetic low that strikes NNE, parallel to line 10140. This isolated response gives rise to a weak, poorly-defined resistivity low and yields a similar response on traverse line 10140.

Anomaly 10070C reflects a probable thin source of limited strike length, that occurs near the north-trending Diavik Creek. It coincides with a small magnetic high, yielding a direct magnetic correlation of 107 nT.

Zone C is the more conductive portion of a U-shaped resistivity low in the northern part of the survey block. The western lobe of this zone follows Gilliam Creek, while the northeastern portion is on higher ground. Zone C hosts one, thin, west-dipping source at 19020D, while line 19010 suggests as many as four possible sources. The most conductive area is associated with a plug-like magnetic low that tends to enhance the significance of the poorly defined responses from 19010A to 19010D. The apparently broad response on line 10220 is probably due to the fact that this NE-trending conductor is nearly parallel to the traverse line.

Anomalies 19020A&B, 19030B, 19030D, 19040A and 19040B are all within the western lobe of the northern resistivity low that hosts Zone C. Anomaly 19020B suggests a thin, west-dipping source, east of Gilliam Creek. Anomaly 19030D also indicates a narrow source near the eastern contact of a weak magnetic anomaly. Anomaly 19040A occurs near the contact of a weak magnetic high, and could be due to an edge effect, rather than a discrete bedrock source.

Zone D is a >12km-long resistivity low that strikes SSE from the north end of line 10350 to the south end of line 10160. This prominent feature is not restricted to low-lying topography, and has been attributed to a moderately wide, highly conductive, bedrock source. This unit often abuts a magnetic contact, but is generally non-magnetic, suggesting graphitic shales or argillites as a likely cause.

Although most of the anomalies comprising Zone D are non-magnetic, there are a few, such as 10210A, 10230B&E, 10270B, 10280D, 10310E&G, 10330K&N, 19050E, 19100I, 19120C, 19250D and 19260B, that exhibit magnetic correlation. These anomalies are generally considered to be of higher priority than the non-magnetic conductors, as the former are more likely to be due to magnetic sulphides such as pyrrhotite, rather than graphite or varved clays that do not yield magnetic correlation.

It is very difficult to assign priorities to the numerous conductors comprising Zone D. Apart from those with magnetic correlation, the anomalies that exhibit pods of more conductive material or those that appear to be related to zones of structural deformation, are considered to be of higher priority in the search for massive sulphides. The following table lists some of the more attractive geophysical responses in Zone D.

Anomaly	Type	Mag	Comments
10170B	B	Low	Rtes less than 2 ohm-m. Coincident with interesting, circular magnetic low.
19260B	B	555	Less than 1 ohm-m. In close proximity to NE-trending contact.

Anomaly	Type	Mag	Comments
10240B	B		On local mag high near a faulted offset of the NE-trending contact. Less than 2 ohm-m.
10270B	B	87	Strong, 1 ohm-m source at an estimated depth of about 25 m. Near eastern contact of a magnetic unit close to an inferred ESE-trending non-magnetic narrow unit.
10300B	B?	-	Broad, buried source near a subtle magnetic low.
19180C	B?	-	A possible broad source at an approximate depth of 50-60 m. In close proximity to a magnetic contact near an inferred SE-trending break. Caution: could be (partially?) due to interference from nearby line source.
10340G	B	-	Moderate response near a probable SE-trending break.
10360F	B	-	Extremely strong broad conductor at a depth of about 25 m. This anomaly is associated with a pronounced magnetic low, near the eastern contact of a strong magnetic high. The high appears to be interrupted or truncated by a SE-trending non-magnetic unit through 10360G. The main axis of Zone D swings to the NW, north of 10360G, through anomaly 10320I, beyond which it changes direction towards the NE.
19120F	D	Low	A highly conductive thin source at depth that coincides with a sharp magnetic low.
10340I	D	18	This anomaly suggests a thin source within the larger, highly-conductive buried unit.
10350O	B		Both the 900 Hz and 7200 Hz indicate a highly conductive zone (<1 ohm-m) at a probable depth of about 30 m. This is located near the contact of a _____ trending magnetic low.
10350R 10350S	B? B		These two anomalies near the north end of line 10350 are both associated with a possible circular magnetic low. The actual shape of the magnetic low is uncertain, as this feature is open to the NNE.

Zone E is an irregularly-shaped resistivity low that hosts multiple conductors. Although this zone is located within a broad unit of relatively low magnetic susceptibility, the vertical gradient shows that several of the anomalous responses correlate with magnetic highs. The conductive responses in Zone E should be subjected to further investigation in order

to determine their causative sources. Both magnetic and non-magnetic thin sources are evident at 10410B, C and D, 10420D and F, 10430B, and 10430B and C.

In addition to the conductive zones described in the foregoing test, there are several shorter, more isolated conductors of probable bedrock origin that are considered to be of interest. Anomalies 19130A and 19130B are very weak, but they occur in a non-magnetic unit near an inferred SE-trending break, near a NNE-trending contact.

Anomalies 10290A and 19210D define a thin conductor with a probable NE strike length of more than 350 m. Anomaly 19210D is weakly magnetic and suggests a probable dip towards the northwest. Anomaly 10290A could be related to a fault or non-magnetic intrusion that strikes east ($\sim 80^\circ$) from this vicinity.

Anomaly 19210I is a weak, isolated conductor of limited strike extent, with a magnetic correlation of 80 nT. Similarly, anomaly 19200D suggests a short, weak, thin source, that flanks a very weak magnetic contact.

Anomalies 19100N and 19100O are both non-magnetic and are associated with a deep, conductive unit at the eastern end of line 19100, beyond the survey boundary. Anomalies 19050J and 19060F give rise to a very strong resistivity low near the eastern edge of the property. This incomplete anomaly remains open to the east.

Although this report refers to conductors or conductive zones, some of the circular or ovate resistivity highs could also represent plug-like intrusions. One such example is the resistive unit centered near the intersection of line 10380 and tie line 19170.

8. CONCLUSIONS AND RECOMMENDATIONS

This report describes the equipment, data processing procedures, anomaly interpretation and logistics of a survey over the Swift Katie Block, British Columbia, flown from December 5th, 2007, to January 16th, 2008.

Numerous highly conductive sources have been detected by the airborne survey. Many of the interpreted bedrock conductors and anomalous targets defined by the survey should be subjected to further investigation, using appropriate surface exploration techniques. Anomalies that are currently considered to be of moderately low priority may require upgrading if follow-up results are favourable.

Most of the highly conductive zones are non-magnetic, suggesting graphite or argillaceous shales as likely causative sources. However, several of the moderate to strong responses yield magnetic correlation, which tends to enhance their potential as possible sulphide sources. Other anomalies appear to be related to contacts or zones of structural deformation, which may have influenced mineral deposition in the area.

In the search for porphyritic intrusions, empirical results have indicated that these can be either more resistive, less resistive, or indistinguishable from the surrounding host rocks. Any subtle resistivity anomalies, therefore, may be of interest, particularly if they exhibit a circular or plug-like shape with fairly large dimensions. Such features may be evident on

the resistivity parameter, even though they do not yield discrete EM anomalies. It should be noted that magnetite-rich (skarn) zones can also yield resistivity highs.

It is also recommended that additional processing of existing geophysical data be considered, in order to extract the maximum amount of information from the survey results.

Current software and imaging techniques often provide valuable information on structure and lithology, which may not be clearly evident on the contour and colour maps. These techniques can yield images that define subtle, but significant, structural details.

Respectfully submitted,

FUGRO AIRBORNE SURVEYS CORP.

R07114MAR.08

APPENDIX A

LIST OF PERSONNEL

The following personnel were involved in the acquisition, processing, interpretation and presentation of data, relating to a DIGHEM airborne geophysical survey carried out for Valterra Resource Corporation over the Swift Katie Block, in the Salmo area of British Columbia.

David Miles	Manager, Helicopter Operations
Emily Farquhar	Manager, Data Processing and Interpretation
Parag Paliwal	Geophysical Operator
Laura Quigley	Field Geophysicist
Tai-chyi Shei	Field Geophysicist
Guy Lajoie	Helicopter Pilot
Ed Howel	Helicopter Mechanic
Robert Chatman	Helicopter Mechanic
Igor Sram	Geophysicist
Paul Smith	Geophysicist
Lyn Vanderstarren	Drafting Supervisor
Susan Pothiah	Word Processing Operator
Albina Tonello	Secretary/Expeditor

The survey consisted of 505 km of coverage, flown from December 5th, 2007, to January 16th, 2008.

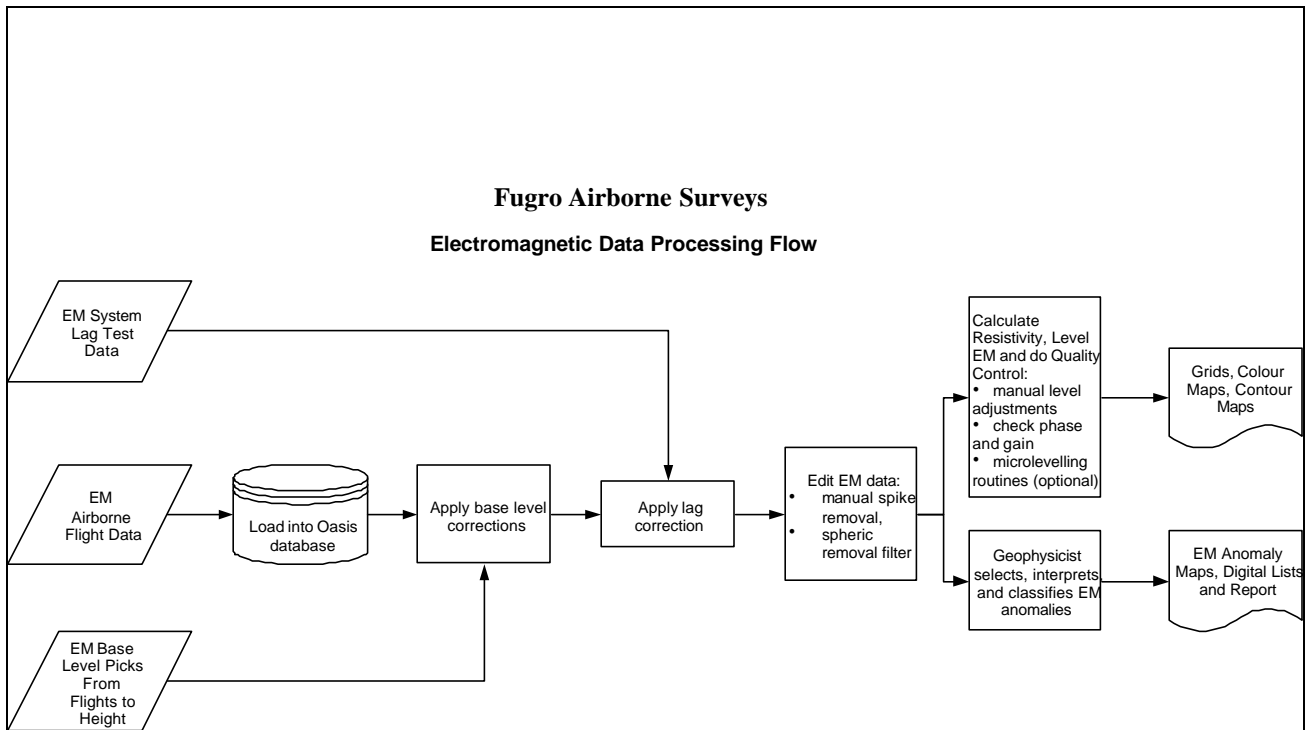
All personnel are employees of Fugro Airborne Surveys, except for the pilot and engineer who are employees of Questral Helicopters Ltd.

APPENDIX B

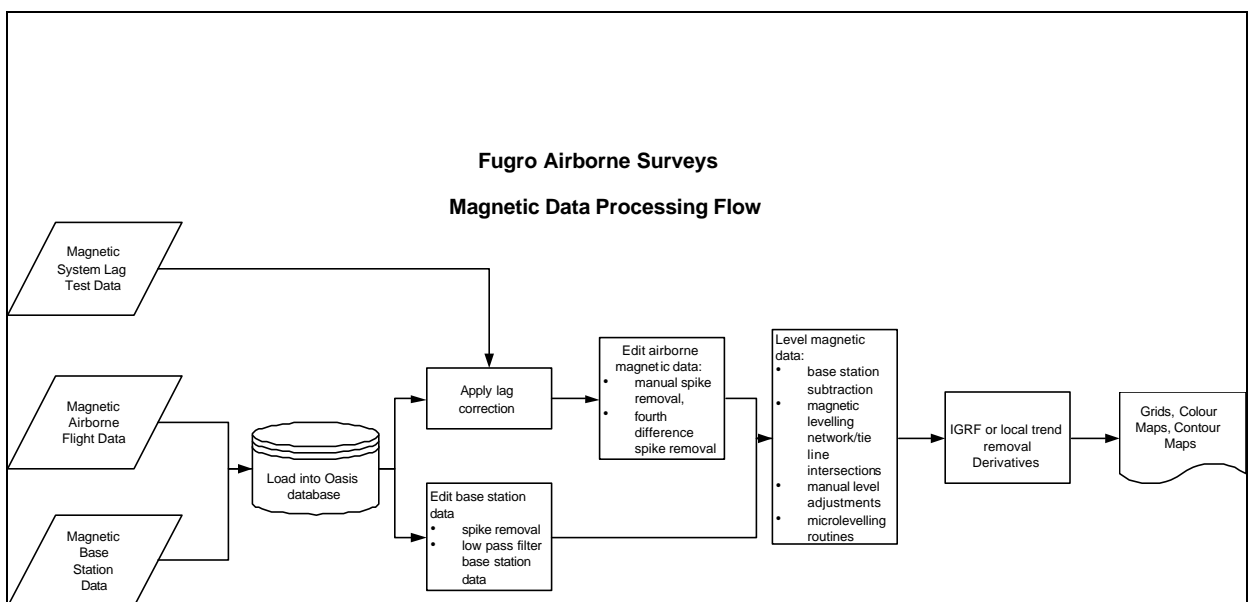
DATA PROCESSING FLOWCHARTS

APPENDIX B

Processing Flow Chart - Electromagnetic Data



Processing Flow Chart - Magnetic Data



APPENDIX C

BACKGROUND INFORMATION

BACKGROUND INFORMATION

Electromagnetics

Fugro electromagnetic responses fall into two general classes, discrete and broad. The discrete class consists of sharp, well-defined anomalies from discrete conductors such as sulphide lenses and steeply dipping sheets of graphite and sulphides. The broad class consists of wide anomalies from conductors having a large horizontal surface such as flatly dipping graphite or sulphide sheets, saline water-saturated sedimentary formations, conductive overburden and rock, kimberlite pipes and geothermal zones. A vertical conductive slab with a width of 200 m would straddle these two classes.

The vertical sheet (half plane) is the most common model used for the analysis of discrete conductors. All anomalies plotted on the geophysical maps are analyzed according to this model. The following section entitled **Discrete Conductor Analysis** describes this model in detail, including the effect of using it on anomalies caused by broad conductors such as conductive overburden.

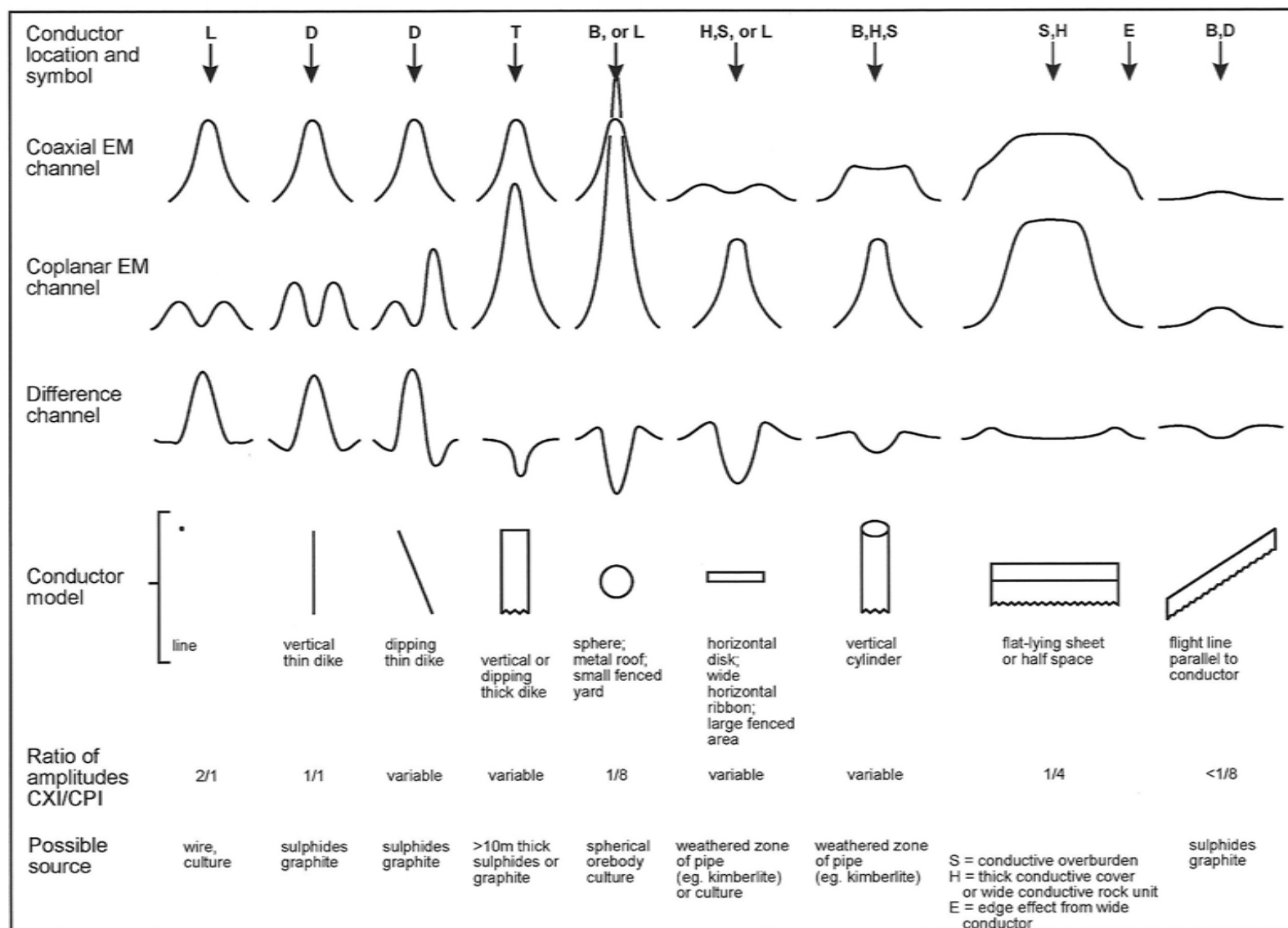
The conductive earth (half-space) model is suitable for broad conductors. Resistivity contour maps result from the use of this model. A later section entitled **Resistivity Mapping** describes the method further, including the effect of using it on anomalies caused by discrete conductors such as sulphide bodies.

Geometric Interpretation

The geophysical interpreter attempts to determine the geometric shape and dip of the conductor. Figure C-1 shows typical HEM anomaly shapes which are used to guide the geometric interpretation.

Discrete Conductor Analysis

The EM anomalies appearing on the electromagnetic map are analyzed by computer to give the conductance (i.e., conductivity-thickness product) in siemens (mhos) of a vertical sheet model. This is done regardless of the interpreted geometric shape of the conductor. This is not an unreasonable procedure, because the computed conductance increases as the electrical quality of the conductor increases, regardless of its true shape. DIGHEM anomalies are divided into seven grades of conductance, as shown in Table C-1. The conductance in siemens (mhos) is the reciprocal of resistance in ohms.



Typical HEM anomaly shapes

Figure C-1

- Appendix C.3 -

The conductance value is a geological parameter because it is a characteristic of the conductor alone. It generally is independent of frequency, flying height or depth of burial, apart from the averaging over a greater portion of the conductor as height increases. Small anomalies from deeply buried strong conductors are not confused with small anomalies from shallow weak conductors because the former will have larger conductance values.

Table C-1. EM Anomaly Grades

Anomaly Grade	Siemens
7	> 100
6	50 - 100
5	20 - 50
4	10 - 20
3	5 - 10
2	1 - 5
1	< 1

Conductive overburden generally produces broad EM responses which may not be shown as anomalies on the geophysical maps. However, patchy conductive overburden in otherwise resistive areas can yield discrete anomalies with a conductance grade (cf. Table C-1) of 1, 2 or even 3 for conducting clays which have resistivities as low as 50 ohm-m. In areas where ground resistivities are below 10 ohm-m, anomalies caused by weathering variations and similar causes can have any conductance grade. The anomaly shapes from the multiple coils often allow such conductors to be recognized, and these are indicated by the letters S, H, and sometimes E on the geophysical maps (see EM legend on maps).

For bedrock conductors, the higher anomaly grades indicate increasingly higher conductances. Examples: the New Insco copper discovery (Noranda, Canada) yielded a grade 5 anomaly, as did the neighbouring copper-zinc Magusi River ore body; Mattabi (copper-zinc, Sturgeon Lake, Canada) and Whistle (nickel, Sudbury, Canada) gave grade 6; and the Montcalm nickel-copper discovery (Timmins, Canada) yielded a grade 7 anomaly. Graphite and sulphides can span all grades but, in any particular survey area, field work may show that the different grades indicate different types of conductors.

Strong conductors (i.e., grades 6 and 7) are characteristic of massive sulphides or graphite. Moderate conductors (grades 4 and 5) typically reflect graphite or sulphides of a less massive character, while weak bedrock conductors (grades 1 to 3) can signify poorly connected graphite or heavily disseminated sulphides. Grades 1 and 2 conductors may not respond to ground EM equipment using frequencies less than 2000 Hz.

- Appendix C.4 -

The presence of sphalerite or gangue can result in ore deposits having weak to moderate conductances. As an example, the three million ton lead-zinc deposit of Restigouche Mining Corporation near Bathurst, Canada, yielded a well-defined grade 2 conductor. The 10 percent by volume of sphalerite occurs as a coating around the fine grained massive pyrite, thereby inhibiting electrical conduction. Faults, fractures and shear zones may produce anomalies that typically have low conductances (e.g., grades 1 to 3). Conductive rock formations can yield anomalies of any conductance grade. The conductive materials in such rock formations can be salt water, weathered products such as clays, original depositional clays, and carbonaceous material.

For each interpreted electromagnetic anomaly on the geophysical maps, a letter identifier and an interpretive symbol are plotted beside the EM grade symbol. The horizontal rows of dots, under the interpretive symbol, indicate the anomaly amplitude on the flight record. The vertical column of dots, under the anomaly letter, gives the estimated depth. In areas where anomalies are crowded, the letter identifiers, interpretive symbols and dots may be obliterated. The EM grade symbols, however, will always be discernible, and the obliterated information can be obtained from the anomaly listing appended to this report.

The purpose of indicating the anomaly amplitude by dots is to provide an estimate of the reliability of the conductance calculation. Thus, a conductance value obtained from a large ppm anomaly (3 or 4 dots) will tend to be accurate whereas one obtained from a small ppm anomaly (no dots) could be quite inaccurate. The absence of amplitude dots indicates that the anomaly from the coaxial coil-pair is 5 ppm or less on both the in-phase and quadrature channels. Such small anomalies could reflect a weak conductor at the surface or a stronger conductor at depth. The conductance grade and depth estimate illustrates which of these possibilities fits the recorded data best.

The conductance measurement is considered more reliable than the depth estimate. There are a number of factors that can produce an error in the depth estimate, including the averaging of topographic variations by the altimeter, overlying conductive overburden, and the location and attitude of the conductor relative to the flight line. Conductor location and attitude can provide an erroneous depth estimate because the stronger part of the conductor may be deeper or to one side of the flight line, or because it has a shallow dip. A heavy tree cover can also produce errors in depth estimates. This is because the depth estimate is computed as the distance of bird from conductor, minus the altimeter reading. The altimeter can lock onto the top of a dense forest canopy. This situation yields an erroneously large depth estimate but does not affect the conductance estimate.

Dip symbols are used to indicate the direction of dip of conductors. These symbols are used only when the anomaly shapes are unambiguous, which usually requires a fairly resistive environment.

A further interpretation is presented on the EM map by means of the line-to-line correlation of bedrock anomalies, which is based on a comparison of anomaly shapes on adjacent lines. This provides conductor axes that may define the geological structure over portions

- Appendix C.5 -

of the survey area. The absence of conductor axes in an area implies that anomalies could not be correlated from line to line with reasonable confidence.

The electromagnetic anomalies are designed to provide a correct impression of conductor quality by means of the conductance grade symbols. The symbols can stand alone with geology when planning a follow-up program. The actual conductance values are printed in the attached anomaly list for those who wish quantitative data. The anomaly ppm and depth are indicated by inconspicuous dots which should not distract from the conductor patterns, while being helpful to those who wish this information. The map provides an interpretation of conductors in terms of length, strike and dip, geometric shape, conductance, depth, and thickness. The accuracy is comparable to an interpretation from a high quality ground EM survey having the same line spacing.

The appended EM anomaly list provides a tabulation of anomalies in ppm, conductance, and depth for the vertical sheet model. No conductance or depth estimates are shown for weak anomalous responses that are not of sufficient amplitude to yield reliable calculations.

Since discrete bodies normally are the targets of EM surveys, local base (or zero) levels are used to compute local anomaly amplitudes. This contrasts with the use of true zero levels which are used to compute true EM amplitudes. Local anomaly amplitudes are shown in the EM anomaly list and these are used to compute the vertical sheet parameters of conductance and depth.

Questionable Anomalies

The EM maps may contain anomalous responses that are displayed as asterisks (*). These responses denote weak anomalies of indeterminate conductance, which may reflect one of the following: a weak conductor near the surface, a strong conductor at depth (e.g., 100 to 120 m below surface) or to one side of the flight line, or aerodynamic noise. Those responses that have the appearance of valid bedrock anomalies on the flight profiles are indicated by appropriate interpretive symbols (see EM legend on maps). The others probably do not warrant further investigation unless their locations are of considerable geological interest.

The Thickness Parameter

A comparison of coaxial and coplanar shapes can provide an indication of the thickness of a steeply dipping conductor. The amplitude of the coplanar anomaly (e.g., CPI channel) increases relative to the coaxial anomaly (e.g., CXI) as the apparent thickness increases, i.e., the thickness in the horizontal plane. (The thickness is equal to the conductor width if the conductor dips at 90 degrees and strikes at right angles to the flight line.) This report refers to a conductor as thin when the thickness is likely to be less than 3 m, and thick when in excess of 10 m. Thick conductors are indicated on the EM map by parentheses "(

)". For base metal exploration in steeply dipping geology, thick conductors can be high priority targets because many massive sulphide ore bodies are thick. The system cannot sense the thickness when the strike of the conductor is subparallel to the flight line, when the conductor has a shallow dip, when the anomaly amplitudes are small, or when the resistivity of the environment is below 100 ohm-m.

Resistivity Mapping

Resistivity mapping is useful in areas where broad or flat lying conductive units are of interest. One example of this is the clay alteration which is associated with Carlin-type deposits in the south west United States. The resistivity parameter was able to identify the clay alteration zone over the Cove deposit. The alteration zone appeared as a strong resistivity low on the 900 Hz resistivity parameter. The 7,200 Hz and 56,000 Hz resistivities showed more detail in the covering sediments, and delineated a range front fault. This is typical in many areas of the south west United States, where conductive near surface sediments, which may sometimes be alkaline, attenuate the higher frequencies.

Resistivity mapping has proven successful for locating diatremes in diamond exploration. Weathering products from relatively soft kimberlite pipes produce a resistivity contrast with the unaltered host rock. In many cases weathered kimberlite pipes were associated with thick conductive layers that contrasted with overlying or adjacent relatively thin layers of lake bottom sediments or overburden.

Areas of widespread conductivity are commonly encountered during surveys. These conductive zones may reflect alteration zones, shallow-dipping sulphide or graphite-rich units, saline ground water, or conductive overburden. In such areas, EM amplitude changes can be generated by decreases of only 5 m in survey altitude, as well as by increases in conductivity. The typical flight record in conductive areas is characterized by in-phase and quadrature channels that are continuously active. Local EM peaks reflect either increases in conductivity of the earth or decreases in survey altitude. For such conductive areas, apparent resistivity profiles and contour maps are necessary for the correct interpretation of the airborne data. The advantage of the resistivity parameter is that anomalies caused by altitude changes are virtually eliminated, so the resistivity data reflect only those anomalies caused by conductivity changes. The resistivity analysis also helps the interpreter to differentiate between conductive bedrock and conductive overburden. For example, discrete conductors will generally appear as narrow lows on the contour map and broad conductors (e.g., overburden) will appear as wide lows.

The apparent resistivity is calculated using the pseudo-layer (or buried) half-space model defined by Fraser (1978)⁶. This model consists of a resistive layer overlying a conductive

⁶ Resistivity mapping with an airborne multicoil electromagnetic system: Geophysics, v. 43, p.144-172

- Appendix C.7 -

half-space. The depth channels give the apparent depth below surface of the conductive material. The apparent depth is simply the apparent thickness of the overlying resistive layer. The apparent depth (or thickness) parameter will be positive when the upper layer is more resistive than the underlying material, in which case the apparent depth may be quite close to the true depth.

The apparent depth will be negative when the upper layer is more conductive than the underlying material, and will be zero when a homogeneous half-space exists. The apparent depth parameter must be interpreted cautiously because it will contain any errors that might exist in the measured altitude of the EM bird (e.g., as caused by a dense tree cover). The inputs to the resistivity algorithm are the in-phase and quadrature components of the coplanar coil-pair. The outputs are the apparent resistivity of the conductive half-space (the source) and the sensor-source distance. The flying height is not an input variable, and the output resistivity and sensor-source distance are independent of the flying height when the conductivity of the measured material is sufficient to yield significant in-phase as well as quadrature responses. The apparent depth, discussed above, is simply the sensor-source distance minus the measured altitude or flying height. Consequently, errors in the measured altitude will affect the apparent depth parameter but not the apparent resistivity parameter.

The apparent depth parameter is a useful indicator of simple layering in areas lacking a heavy tree cover. Depth information has been used for permafrost mapping, where positive apparent depths were used as a measure of permafrost thickness. However, little quantitative use has been made of negative apparent depths because the absolute value of the negative depth is not a measure of the thickness of the conductive upper layer and, therefore, is not meaningful physically. Qualitatively, a negative apparent depth estimate usually shows that the EM anomaly is caused by conductive overburden. Consequently, the apparent depth channel can be of significant help in distinguishing between overburden and bedrock conductors.

Interpretation in Conductive Environments

Environments having low background resistivities (e.g., below 30 ohm-m for a 900 Hz system) yield very large responses from the conductive ground. This usually prohibits the recognition of discrete bedrock conductors. However, Fugro data processing techniques produce three parameters that contribute significantly to the recognition of bedrock conductors in conductive environments. These are the in-phase and quadrature difference channels (DIFI and DIFQ, which are available only on systems with "common" frequencies on orthogonal coil pairs), and the resistivity and depth channels (RES and DEP) for each coplanar frequency.

- Appendix C.8 -

The EM difference channels (DIFI and DIFQ) eliminate most of the responses from conductive ground, leaving responses from bedrock conductors, cultural features (e.g., telephone lines, fences, etc.) and edge effects. Edge effects often occur near the perimeter of broad conductive zones. This can be a source of geologic noise. While edge effects yield anomalies on the EM difference channels, they do not produce resistivity anomalies. Consequently, the resistivity channel aids in eliminating anomalies due to edge effects. On the other hand, resistivity anomalies will coincide with the most highly conductive sections of conductive ground, and this is another source of geologic noise. The recognition of a bedrock conductor in a conductive environment therefore is based on the anomalous responses of the two difference channels (DIFI and DIFQ) and the resistivity channels (RES). The most favourable situation is where anomalies coincide on all channels.

The DEP channels, which give the apparent depth to the conductive material, also help to determine whether a conductive response arises from surficial material or from a conductive zone in the bedrock. When these channels ride above the zero level on the depth profiles (i.e., depth is negative), it implies that the EM and resistivity profiles are responding primarily to a conductive upper layer, i.e., conductive overburden. If the DEP channels are below the zero level, it indicates that a resistive upper layer exists, and this usually implies the existence of a bedrock conductor. If the low frequency DEP channel is below the zero level and the high frequency DEP is above, this suggests that a bedrock conductor occurs beneath conductive cover.

Reduction of Geologic Noise

Geologic noise refers to unwanted geophysical responses. For purposes of airborne EM surveying, geologic noise refers to EM responses caused by conductive overburden and magnetic permeability. It was mentioned previously that the EM difference channels (i.e., channel DIFI for in-phase and DIFQ for quadrature) tend to eliminate the response of conductive overburden.

Magnetite produces a form of geological noise on the in-phase channels. Rocks containing less than 1% magnetite can yield negative in-phase anomalies caused by magnetic permeability. When magnetite is widely distributed throughout a survey area, the in-phase EM channels may continuously rise and fall, reflecting variations in the magnetite percentage, flying height, and overburden thickness. This can lead to difficulties in recognizing deeply buried bedrock conductors, particularly if conductive overburden also exists. However, the response of broadly distributed magnetite generally vanishes on the in-phase difference channel DIFI. This feature can be a significant aid in the recognition of conductors that occur in rocks containing accessory magnetite.

EM Magnetite Mapping

- Appendix C.9 -

The information content of HEM data consists of a combination of conductive eddy current responses and magnetic permeability responses. The secondary field resulting from conductive eddy current flow is frequency-dependent and consists of both in-phase and quadrature components, which are positive in sign. On the other hand, the secondary field resulting from magnetic permeability is independent of frequency and consists of only an in-phase component which is negative in sign. When magnetic permeability manifests itself by decreasing the measured amount of positive in-phase, its presence may be difficult to recognize. However, when it manifests itself by yielding a negative in-phase anomaly (e.g., in the absence of eddy current flow), its presence is assured. In this latter case, the negative component can be used to estimate the percent magnetite content.

A magnetite mapping technique, based on the low frequency coplanar data, can be complementary to magnetometer mapping in certain cases. Compared to magnetometry, it is far less sensitive but is more able to resolve closely spaced magnetite zones, as well as providing an estimate of the amount of magnetite in the rock. The method is sensitive to 1/4% magnetite by weight when the EM sensor is at a height of 30 m above a magnetitic half-space. It can individually resolve steep dipping narrow magnetite-rich bands which are separated by 60 m. Unlike magnetometry, the EM magnetite method is unaffected by remanent magnetism or magnetic latitude.

The EM magnetite mapping technique provides estimates of magnetite content which are usually correct within a factor of 2 when the magnetite is fairly uniformly distributed. EM magnetite maps can be generated when magnetic permeability is evident as negative in-phase responses on the data profiles.

Like magnetometry, the EM magnetite method maps only bedrock features, provided that the overburden is characterized by a general lack of magnetite. This contrasts with resistivity mapping which portrays the combined effect of bedrock and overburden.

The Susceptibility Effect

When the host rock is conductive, the positive conductivity response will usually dominate the secondary field, and the susceptibility effect⁷ will appear as a reduction in the in-phase, rather than as a negative value. The in-phase response will be lower than would be predicted by a model using zero susceptibility. At higher frequencies the in-phase conductivity response also gets larger, so a negative magnetite effect observed on the low frequency might not be observable on the higher frequencies, over the same body. The

⁷ Magnetic susceptibility and permeability are two measures of the same physical property. Permeability is generally given as relative permeability, μ_r , which is the permeability of the substance divided by the permeability of free space ($4 \pi \times 10^{-7}$). Magnetic susceptibility k is related to permeability by $k = \mu_r - 1$. Susceptibility is a unitless measurement, and is usually reported in units of 10^{-6} . The typical range of susceptibilities is -1 for quartz, 130 for pyrite, and up to 5×10^5 for magnetite, in 10^{-6} units (Telford et al, 1986).

susceptibility effect is most obvious over discrete magnetite-rich zones, but also occurs over uniform geology such as a homogeneous half-space.

High magnetic susceptibility will affect the calculated apparent resistivity, if only conductivity is considered. Standard apparent resistivity algorithms use a homogeneous half-space model, with zero susceptibility. For these algorithms, the reduced in-phase response will, in most cases, make the apparent resistivity higher than it should be. It is important to note that there is nothing wrong with the data, nor is there anything wrong with the processing algorithms. The apparent difference results from the fact that the simple geological model used in processing does not match the complex geology.

Measuring and Correcting the Magnetite Effect

Theoretically, it is possible to calculate (forward model) the combined effect of electrical conductivity and magnetic susceptibility on an EM response in all environments. The difficulty lies, however, in separating out the susceptibility effect from other geological effects when deriving resistivity and susceptibility from EM data.

Over a homogeneous half-space, there is a precise relationship between in-phase, quadrature, and altitude. These are often resolved as phase angle, amplitude, and altitude. Within a reasonable range, any two of these three parameters can be used to calculate the half space resistivity. If the rock has a positive magnetic susceptibility, the in-phase component will be reduced and this departure can be recognized by comparison to the other parameters.

The algorithm used to calculate apparent susceptibility and apparent resistivity from HEM data, uses a homogeneous half-space geological model. Non half-space geology, such as horizontal layers or dipping sources, can also distort the perfect half-space relationship of the three data parameters. While it may be possible to use more complex models to calculate both rock parameters, this procedure becomes very complex and time-consuming. For basic HEM data processing, it is most practical to stick to the simplest geological model.

Magnetite reversals (reversed in-phase anomalies) have been used for many years to calculate an “FeO” or magnetite response from HEM data (Fraser, 1981). However, this technique could only be applied to data where the in-phase was observed to be negative, which happens when susceptibility is high and conductivity is low.

Applying Susceptibility Corrections

Resistivity calculations done with susceptibility correction may change the apparent resistivity. High-susceptibility conductors, that were previously masked by the susceptibility effect in standard resistivity algorithms, may become evident. In this case the susceptibility corrected apparent resistivity is a better measure of the actual resistivity of

the earth. However, other geological variations, such as a deep resistive layer, can also reduce the in-phase by the same amount. In this case, susceptibility correction would not be the best method. Different geological models can apply in different areas of the same data set. The effects of susceptibility, and other effects that can create a similar response, must be considered when selecting the resistivity algorithm.

Susceptibility from EM vs Magnetic Field Data

The response of the EM system to magnetite may not match that from a magnetometer survey. First, HEM-derived susceptibility is a rock property measurement, like resistivity. Magnetic data show the total magnetic field, a measure of the potential field, not the rock property. Secondly, the shape of an anomaly depends on the shape and direction of the source magnetic field. The electromagnetic field of HEM is much different in shape from the earth's magnetic field. Total field magnetic anomalies are different at different magnetic latitudes; HEM susceptibility anomalies have the same shape regardless of their location on the earth.

In far northern latitudes, where the magnetic field is nearly vertical, the total magnetic field measurement over a thin vertical dike is very similar in shape to the anomaly from the HEM-derived susceptibility (a sharp peak over the body). The same vertical dike at the magnetic equator would yield a negative magnetic anomaly, but the HEM susceptibility anomaly would show a positive susceptibility peak.

Effects of Permeability and Dielectric Permittivity

Resistivity algorithms that assume free-space magnetic permeability and dielectric permittivity, do not yield reliable values in highly magnetic or highly resistive areas. Both magnetic polarization and displacement currents cause a decrease in the in-phase component, often resulting in negative values that yield erroneously high apparent resistivities. The effects of magnetite occur at all frequencies, but are most evident at the lowest frequency. Conversely, the negative effects of dielectric permittivity are most evident at the higher frequencies, in resistive areas.

The table below shows the effects of varying permittivity over a resistive (10,000 ohm-m) half space, at frequencies of 56,000 Hz (DIGHEM^V) and 102,000 Hz (RESOLVE).

Apparent Resistivity Calculations

Effects of Permittivity on In-phase/Quadrature/Resistivity

Freq (Hz)	Coil	Sep (m)	Thres (ppm)	Alt (m)	In Phase	Quad Phase	App Res	App Depth (m)	Permittivity
56,000	CP	6.3	0.1	30	7.3	35.3	10118	-1.0	1 Air

- Appendix C.12 -

56,000	CP	6.3	0.1	30	3.6	36.6	19838	-13.2	5 Quartz
56,000	CP	6.3	0.1	30	-1.1	38.3	81832	-25.7	10 Epidote
56,000	CP	6.3	0.1	30	-10.4	42.3	76620	-25.8	20 Granite
56,000	CP	6.3	0.1	30	-19.7	46.9	71550	-26.0	30 Diabase
56,000	CP	6.3	0.1	30	-28.7	52.0	66787	-26.1	40 Gabbro
102,000	CP	7.86	0.1	30	32.5	117.2	9409	-0.3	1 Air
102,000	CP	7.86	0.1	30	11.7	127.2	25956	-16.8	5 Quartz
102,000	CP	7.86	0.1	30	-14.0	141.6	97064	-26.5	10 Epidote
102,000	CP	7.86	0.1	30	-62.9	176.0	83995	-26.8	20 Granite
102,000	CP	7.86	0.1	30	-107.5	215.8	73320	-27.0	30 Diabase
102,000	CP	7.86	0.1	30	-147.1	259.2	64875	-27.2	40 Gabbro

Methods have been developed (Huang and Fraser, 2000, 2001) to correct apparent resistivities for the effects of permittivity and permeability. The corrected resistivities yield more credible values than if the effects of permittivity and permeability are disregarded.

Recognition of Culture

Cultural responses include all EM anomalies caused by man-made metallic objects. Such anomalies may be caused by inductive coupling or current gathering. The concern of the interpreter is to recognize when an EM response is due to culture. Points of consideration used by the interpreter, when coaxial and coplanar coil-pairs are operated at a common frequency, are as follows:

1. Channels CXPL and CPPL monitor 60 Hz radiation. An anomaly on these channels shows that the conductor is radiating power. Such an indication is normally a guarantee that the conductor is cultural. However, care must be taken to ensure that the conductor is not a geologic body that strikes across a power line, carrying leakage currents.
2. A flight that crosses a "line" (e.g., fence, telephone line, etc.) yields a centre-peaked coaxial anomaly and an m-shaped coplanar anomaly.⁸ When the flight crosses the cultural line at a high angle of intersection, the amplitude ratio of coaxial/coplanar response is 2. Such an EM anomaly can only be caused by a line. The geologic body that yields anomalies most closely resembling a line is the vertically dipping thin dike. Such a body, however, yields an amplitude ratio of 1 rather than 2. Consequently, an m-shaped coplanar anomaly with a CXI/CPI amplitude ratio of 2 is virtually a guarantee that the source is a cultural line.
3. A flight that crosses a sphere or horizontal disk yields centre-peaked coaxial and coplanar anomalies with a CXI/CPI amplitude ratio (i.e., coaxial/coplanar) of 1/8. In

12
⁸ See Figure C-1 presented earlier.

- Appendix C.13 -

- the absence of geologic bodies of this geometry, the most likely conductor is a metal roof or small fenced yard.⁹ Anomalies of this type are virtually certain to be cultural if they occur in an area of culture.
4. A flight that crosses a horizontal rectangular body or wide ribbon yields an m-shaped coaxial anomaly and a centre-peaked coplanar anomaly. In the absence of geologic bodies of this geometry, the most likely conductor is a large fenced area.⁵ Anomalies of this type are virtually certain to be cultural if they occur in an area of culture.
 5. EM anomalies that coincide with culture, as seen on the camera film or video display, are usually caused by culture. However, care is taken with such coincidences because a geologic conductor could occur beneath a fence, for example. In this example, the fence would be expected to yield an m-shaped coplanar anomaly as in case #2 above. If, instead, a centre-peaked coplanar anomaly occurred, there would be concern that a thick geologic conductor coincided with the cultural line.
 6. The above description of anomaly shapes is valid when the culture is not conductively coupled to the environment. In this case, the anomalies arise from inductive coupling to the EM transmitter. However, when the environment is quite conductive (e.g., less than 100 ohm-m at 900 Hz), the cultural conductor may be conductively coupled to the environment. In this latter case, the anomaly shapes tend to be governed by current gathering. Current gathering can completely distort the anomaly shapes, thereby complicating the identification of cultural anomalies. In such circumstances, the interpreter can only rely on the radiation channels and on the camera film or video records.

Magnetic Responses

The measured total magnetic field provides information on the magnetic properties of the earth materials in the survey area. The information can be used to locate magnetic bodies of direct interest for exploration, and for structural and lithological mapping.

The total magnetic field response reflects the abundance of magnetic material in the source. Magnetite is the most common magnetic mineral. Other minerals such as ilmenite, pyrrhotite, franklinite, chromite, hematite, arsenopyrite, limonite and pyrite are also magnetic, but to a lesser extent than magnetite on average.

13

⁹ It is a characteristic of EM that geometrically similar anomalies are obtained from: (1) a planar conductor, and (2) a wire which forms a loop having dimensions identical to the perimeter of the equivalent planar conductor.

- Appendix C.14 -

In some geological environments, an EM anomaly with magnetic correlation has a greater likelihood of being produced by sulphides than one which is non-magnetic. However, sulphide ore bodies may be non-magnetic (e.g., the Kidd Creek deposit near Timmins, Canada) as well as magnetic (e.g., the Mattabi deposit near Sturgeon Lake, Canada).

Iron ore deposits will be anomalously magnetic in comparison to surrounding rock due to the concentration of iron minerals such as magnetite, ilmenite and hematite.

Changes in magnetic susceptibility often allow rock units to be differentiated based on the total field magnetic response. Geophysical classifications may differ from geological classifications if various magnetite levels exist within one general geological classification. Geometric considerations of the source such as shape, dip and depth, inclination of the earth's field and remanent magnetization will complicate such an analysis.

In general, mafic lithologies contain more magnetite and are therefore more magnetic than many sediments which tend to be weakly magnetic. Metamorphism and alteration can also increase or decrease the magnetization of a rock unit.

Textural differences on a total field magnetic contour, colour or shadow map due to the frequency of activity of the magnetic parameter resulting from inhomogeneities in the distribution of magnetite within the rock, may define certain lithologies. For example, near surface volcanics may display highly complex contour patterns with little line-to-line correlation.

Rock units may be differentiated based on the plan shapes of their total field magnetic responses. Mafic intrusive plugs can appear as isolated "bulls-eye" anomalies. Granitic intrusives appear as sub-circular zones, and may have contrasting rings due to contact metamorphism. Generally, granitic terrain will lack a pronounced strike direction, although granite gneiss may display strike.

Linear north-south units are theoretically not well-defined on total field magnetic maps in equatorial regions due to the low inclination of the earth's magnetic field. However, most stratigraphic units will have variations in composition along strike that will cause the units to appear as a series of alternating magnetic highs and lows.

Faults and shear zones may be characterized by alteration that causes destruction of magnetite (e.g., weathering) that produces a contrast with surrounding rock. Structural breaks may be filled by magnetite-rich, fracture filling material as is the case with diabase dikes, or by non-magnetic felsic material.

Faulting can also be identified by patterns in the magnetic total field contours or colours. Faults and dikes tend to appear as lineaments and often have strike lengths of several kilometres. Offsets in narrow, magnetic, stratigraphic trends also delineate structure. Sharp contrasts in magnetic lithologies may arise due to large displacements along strike-slip or dip-slip faults.

APPENDIX D

DATA ARCHIVE DESCRIPTION

APPENDIX D

ARCHIVE DESCRIPTION

Reference # : CCD02566
Number of CD's : 1
Archive Date : 2008-March-17

This archive contains final data archives, grids and map files of an airborne geophysical survey conducted by FUGRO AIRBORNE SURVEYS CORP. on behalf of Valterra Resources Corporation over the Swift Katie Block, British Columbia.

Job # 07114

***** Disc 1 of 1 *****

This archive comprises 22 files in four directories

Grids\ grids in Geosoft float (.grd) format

cvg_swift-katie	- calculated vertical gradient (nT/m)
mag_swift-katie	- total magnetic field (nT)
res900_swift-katie	- apparent resistivity 900 Hz (ohm.m)
res7200_swift-katie	- apparent resistivity 7200 Hz (ohm.m)
res56k_swift-katie	- apparent resistivity 56K Hz (ohm.m)

Linedata\ databases in Geosoft ASCII/binary format

anomalies.txt	- anomaly archive description file
ArchiveSummary.txt	- archive description file
anSwift-Katie.xyz	- anomaly archive in Geosoft ASCII format
Swift-Katie.xyz	- linedata archive in Geosoft ASCII format
Swift-Katie.gdb	- linedata archive in Geosoft binary format

Maps\ map files in Adobe Acrobat (.pdf) format v1.3

SwiftKatie_aem.pdf	- Electromagnetic Anomalies
SwiftKatie_cvg .pdf	- Calculated Vertical Gradient (nT/m)
SwiftKatie_mag.pdf	- Total Magnetic Field (nT)
SwiftKatie_res56k.pdf	- Apparent Resistivity 56K Hz (ohm.m)
SwiftKatie_res7200.pdf	- Apparent Resistivity 7200 Hz (ohm.m)

Report\ report in Adobe Acrobat (.pdf) format v1.3

- Appendix D.2 -

r07114_mar.pdf - final report

- Appendix D.3 -

The coordinate system for all grids and the data archive is projected as follows

Datum	NAD83
Spheroid	Clarke 1866
Projection	UTM Zone 11
Central meridian	-117 West
False easting	500000
False northing	0
Scale factor	0.9996
Northern parallel	N/A
Base parallel	N/A
WGS84 to local conversion method	Molodensky
Delta X shift	+0
Delta Y shift	-0
Delta Z shift	-0

If you have any problems with this archive please contact

Processing Manager
FUGRO AIRBORNE SURVEYS CORP.
2270 Argentia Road, Unit 2
Mississauga, Ontario
Canada L5N 6A6
Tel (905) 812-0212
Fax (905) 812-1504
E-mail toronto@fugroairborne.com

- Appendix D.4 -

Geosoft ARCHIVE SUMMARY

JOB TITLE:

JOB # :07114
TYPE OF SURVEY :FUGRO Dighem and Magnetics
AREA :Swift Katie Project, BC
CLIENT :Valterra Resource Corp.

SURVEY DATA FORMAT: 45 CHANNELS

#	CHANNAME	TIME	UNITS /	DESCRIPTION
1	X	0.1	m	easting utme-nad83 (UTM Zone 11)
2	Y	0.1	m	northing utmn-nad83 (UTM Zone 11)
3	fid	0.1		fiducial increment
4	lat	0.1	degrees	latitude WGS84
5	lon	0.1	degrees	longitude WGS84
6	flight	0.1		flight number
7	date	0.1		flight date (yyyy/mm/dd)
8	altrad_bird	0.1	m	bird height from radar altimeter
9	altrad_heli	0.1	m	helicopter height from radar altimeter
10	gpsz	0.1	m	survey height above spheroid
11	dem	0.1	m	digital elevation model
12	diurnal	1.0	nt	diurnal variation
13	diurnal_cor	0.1	nt	diurnal correction applied - base removed
14	mag_raw	0.1	nt	total magnetic field - raw
15	mag_lag	0.1	nt	total magnetic field - corrected for lag
16	mag_diu	0.1	nt	total magnetic field - diurnal variation removed
17	mag	0.1	nt	total magnetic field - final
18	cpi900_r	0.1	ppm	unleveled inphase-coplanar 870 hz
19	cpq900_r	0.1	ppm	unleveled quadrature- coplanar 870 hz
20	cxil1000_r	0.1	ppm	unleveled inphase-coaxial 1120 hz
21	cxql1000_r	0.1	ppm	unleveled quadrature- coaxial 1120 hz
22	cxil5500_r	0.1	ppm	unleveled inphase -coaxial 5470 hz
23	cxql5500_r	0.1	ppm	unleveled quadrature -coaxial 5470 hz
24	cpi7200_r	0.1	ppm	unleveled inphase -coplanar 7130 hz
25	cpq7200_r	0.1	ppm	unleveled quadrature -coplanar 7130 hz
26	cpi56k_r	0.1	ppm	unleveled inphase-coplanar 56 000 hz
27	cpq56k_r	0.1	ppm	unleveled quadrature-coplanar 56 000 hz
28	cpi900	0.1	ppm	inphase-coplanar 870 hz
29	cpq900	0.1	ppm	quadrature- coplanar 870 hz
30	cxil1000	0.1	ppm	inphase-coaxial 1120 hz
31	cxql1000	0.1	ppm	quadrature- coaxial 1120 hz
32	cxil5500	0.1	ppm	inphase -coaxial 5470 hz
33	cxql5500	0.1	ppm	quadrature -coaxial 5470 hz
34	cpi7200	0.1	ppm	inphase -coplanar 7130 hz
35	cpq7200	0.1	ppm	quadrature -coplanar 7130 hz
36	cpi56k	0.1	ppm	inphase-coplanar 56 000 hz

- Appendix D.5 -

37	cpq56k	0.1	ppm	quadrature-coplanar	56 000	hz
38	res900	0.1	ohm-m	resistivity -	900	hz
39	res7200	0.1	ohm-m	resistivity -	7200	hz
40	res56k	0.1	ohm-m	resistivity -	56K	hz
41	dep900	0.1	m	depth	- 900	hz
42	dep7200	0.1	m	depth	- 7200	hz
43	dep56k	0.1	m	depth	- 56K	hz
44	cxsp	0.1		coaxial spherics	monitor	
45	cppl	0.1		coplanar powerline	monitor	

ISSUE DATE :March 17, 2008
FOR WHOM :Valterra Resource Corp.
BY WHOM :FUGRO AIRBORNE SURVEYS
2270 ARGENTIA ROAD, UNIT 2
MISSISSAUGA, ONTARIO,
CANADA L5N 6A6
TEL. (905) 812-0212
FAX (905) 812-1504

APPENDIX E

EM ANOMALY LIST

EM Anomaly List

Label	Fid	Interp	XUTM m	YUTM m	CX 5500 HZ Real ppm	Quad ppm	CP 7200 HZ Real ppm	Quad ppm	CP 900 HZ Real ppm	Quad ppm	Vertical Dike COND siemens	DEPTH* m	Mag. Corr NT
LINE 10010			FLIGHT	1									
A	1641.8	H	471677	5444862	4.5	5.1	43.9	41.4	4.9	18.3	0.9	38	0
LINE 10020			FLIGHT	1									
A	1790.9	E	471830	5444732	14.0	13.8	98.2	113.4	15.2	47.8	1.5	15	39
B	1788.5	B?	471852	5444793	5.9	7.3	98.2	113.5	15.2	47.8	0.9	22	0
C	1783.1	D	471903	5444927	10.2	14.4	99.7	103.0	13.7	39.3	0.9	11	0
D	1779.8	B?	471928	5445007	7.0	11.1	99.7	103.0	13.7	39.3	0.7	17	33
E	1777.1	D	471950	5445071	9.9	11.0	99.7	103.0	13.7	39.3	1.2	24	31
F	1772.3	B?	471998	5445180	0.0	0.0	69.8	52.5	8.4	25.5	---	---	0
G	1769.5	B?	472026	5445245	15.8	4.7	69.8	52.5	8.4	25.5	7.5	18	262
H	1752.8	E	472194	5445624	23.3	8.4	130.2	1.2	14.1	25.7	6.5	11	0
I	1748.4	B	472222	5445718	23.5	8.6	152.4	41.9	49.6	73.5	6.4	14	0
LINE 10050			FLIGHT	1									
A	2324.2	H	471941	5443259	3.6	4.3	14.5	29.7	2.0	6.4	0.8	46	13
LINE 10070			FLIGHT	2									
A	1577.3	L	471273	5440265	13.2	6.9	13.1	9.4	5.8	5.0	3.3	23	0
B	1640.1	S	471736	5441537	5.0	20.3	42.9	130.0	2.5	21.2	0.3	0	0
C	1894.8	D	473076	5445187	8.3	7.8	57.2	44.6	10.1	25.2	1.4	22	107
D	1900.0	E	473119	5445298	6.5	8.1	25.6	26.0	3.0	12.0	0.9	30	0
LINE 10080			FLIGHT	2									
A	2559.8	S	470799	5438363	5.6	25.3	17.2	130.0	3.8	20.7	0.3	0	0
B	2488.2	L	471510	5440321	17.0	11.6	16.4	16.6	5.5	8.1	2.5	5	0
C	2407.3	S	472078	5441882	1.6	8.5	67.3	155.5	0.1	26.1	0.2	10	0
D	2377.0	H	472189	5442196	5.7	6.3	14.2	48.8	1.1	6.7	1.0	41	0
E	2340.1	H	472439	5442838	3.9	10.8	18.9	58.0	1.9	9.3	0.4	11	0
F	2320.3	H	472595	5443320	5.3	9.4	9.3	26.5	1.4	5.3	0.6	29	15
LINE 10090			FLIGHT	2									
A	2717.6	H	470844	5437904	2.5	4.9	23.8	46.4	2.4	9.2	0.4	39	0
B	2737.0	S	471013	5438341	3.7	16.5	19.4	112.5	1.2	17.7	0.3	2	0
C	2842.7	L	471710	5440302	21.0	17.2	11.7	23.7	4.0	6.6	2.2	1	0
LINE 10100			FLIGHT	2									
A	3540.2	L	471941	5440324	23.9	17.5	17.3	28.0	4.8	8.6	2.6	2	0

CX = COAXIAL
CP = COPLANAR

Note: EM values shown above
are local amplitudes

*Estimated Depth may be unreliable because the
stronger part of the conductor may be deeper or
to one side of the flight line, or because of a

EM Anomaly List

					CX 5500 HZ	CP 7200 HZ	CP 900 HZ	Vertical Dike		Mag. Corr			
Label	Fid	Interp	XUTM m	YUTM m	Real ppm	Quad ppm	Real ppm	Quad ppm	Real ppm	Quad ppm	COND siemens	DEPTH* m	NT
LINE 10110			FLIGHT	2									
A	4025.1	L	472148	5440305	33.2	30.6	22.7	49.9	6.1	11.4	2.2	4	94
LINE 10120			FLIGHT	2									
A	4858.7	L	472373	5440344	25.9	15.9	25.9	17.7	8.5	11.4	3.3	9	51
B	4561.4	H	474436	5446016	0.3	1.0	27.6	7.7	7.1	11.1	---	---	0
C	4557.5	E	474464	5446093	4.3	4.9	27.6	10.9	7.1	11.1	0.9	30	110
LINE 10130			FLIGHT	2									
A	5331.2	L	472577	5440325	34.2	22.8	29.3	18.1	10.7	13.8	3.3	10	71
B	5607.8	H	474464	5445507	6.2	5.5	36.8	25.7	4.9	16.3	1.3	30	0
LINE 10140			FLIGHT	2									
A	6258.3	H?	471705	5437356	3.9	14.2	52.2	122.2	5.2	21.5	0.3	4	266
B	6221.3	S	472045	5438254	4.6	5.9	11.1	42.6	6.1	6.6	0.8	24	0
C	6173.9	S	472501	5439524	3.5	9.3	21.6	63.4	0.6	11.3	0.4	0	0
D	6129.9	L	472806	5440383	26.8	21.6	25.2	46.1	7.8	12.8	2.4	6	0
E	5859.7	H	474961	5446279	2.6	4.0	43.8	61.2	0.9	14.2	0.5	45	0
LINE 10150			FLIGHT	2									
A	6630.4	L	473043	5440424	27.3	23.1	49.5	88.8	6.9	20.5	2.3	0	0
LINE 10160			FLIGHT	2									
A	7598.8	B	472046	5437109	6.0	0.9	62.7	0.0	74.6	29.8	14.4	46	0
B	7592.0	H?	472100	5437262	10.9	8.5	82.2	83.2	33.4	27.9	1.8	38	0
C	7586.1	E	472143	5437396	9.4	16.0	74.7	83.2	31.9	27.7	0.8	17	334
D	7451.4	L	473270	5440482	31.5	40.8	77.7	155.8	5.9	35.2	1.5	0	104
E	7125.0	S?	475570	5446808	4.8	16.7	41.3	115.7	0.1	20.1	0.3	0	0
F	7104.1	H?	475744	5447271	5.5	4.9	28.7	27.7	3.0	12.6	1.2	39	104
LINE 10170			FLIGHT	2									
A	7821.5	B	472255	5437099	18.9	12.3	184.9	52.6	37.6	92.2	2.8	25	0
B	7827.1	B	472291	5437196	21.2	8.5	184.9	52.6	121.7	92.2	5.4	33	0
C	7838.9	B	472368	5437414	49.1	24.6	420.3	52.6	360.8	171.8	5.4	9	760
D	7965.5	S	473391	5440215	3.3	5.9	24.3	64.5	11.1	11.3	0.5	26	80
E	7978.0	L	473502	5440515	43.7	28.1	30.1	47.7	9.7	17.4	3.7	6	222
F	8337.9	S	475714	5446578	3.7	11.6	32.3	83.4	1.6	16.0	0.3	0	0
G	8370.6	H	475953	5447249	4.4	7.0	28.6	34.6	5.0	12.5	0.6	33	0

CX = COAXIAL
CP = COPLANAR

Note: EM values shown above
are local amplitudes

*Estimated Depth may be unreliable because the
stronger part of the conductor may be deeper or
to one side of the flight line, or because of a
shallow dip or magnetite/overburden effects

Block A

EM Anomaly List

					CX 5500 HZ	CP 7200 HZ	CP 900 HZ	Vertical Dike		Mag. Corr			
Label	Fid	Interp	XUTM m	YUTM m	Real ppm	Quad ppm	Real ppm	Quad ppm	Real ppm	Quad ppm	COND siemens	DEPTH* m	NT
LINE	10180		FLIGHT	2									
A	8973.4	B	472449	5437062	53.9	15.3	300.5	72.7	245.8	109.9	12.1	12	0
B	8935.5	H	472718	5437830	1.0	4.6	6.7	0.0	3.0	3.0	0.2	16	0
C	8816.0	L	473739	5440599	31.2	21.3	26.8	16.3	4.8	14.9	3.1	9	0
D	8524.3	S?	475887	5446521	3.3	5.3	22.7	37.0	0.9	8.5	0.6	6	0
LINE	10190		FLIGHT	2									
A	9384.1	H	472893	5437683	8.6	12.3	26.7	35.8	4.0	10.1	0.9	12	0
B	9493.2	S	473616	5439674	3.9	7.2	25.4	42.6	19.6	7.2	0.5	29	0
C	9537.5	L	473963	5440623	58.2	63.5	68.1	112.2	24.2	26.5	2.2	0	0
D	9674.4	H	474985	5443444	3.4	8.8	12.9	44.1	2.7	7.8	0.4	24	0
E	9896.6	S?	476210	5446798	3.2	14.3	16.1	83.3	0.6	13.3	0.2	0	0
LINE	10200		FLIGHT	4									
A	1900.6	H	472891	5437102	6.1	4.3	7.0	16.3	2.8	2.3	1.7	35	0
B	1875.5	H?	473073	5437603	12.9	5.0	30.1	19.0	14.1	9.7	4.9	32	0
C	1770.3	S	473834	5439663	7.4	12.7	20.5	66.1	12.7	10.4	0.7	10	0
D	1737.0	L	474200	5440689	40.8	30.9	24.5	36.2	10.2	14.4	3.0	4	0
E	1476.6	H	476253	5446316	6.0	4.0	14.8	12.6	2.7	6.2	1.8	48	0
F	1463.8	H	476335	5446545	6.0	7.1	14.3	27.3	2.0	7.4	1.0	14	30
LINE	10210		FLIGHT	4									
A	2044.8	B	473234	5437467	5.3	6.3	40.3	18.1	26.4	17.7	0.9	29	186
B	2171.7	S	473986	5439526	9.0	20.6	20.9	32.6	20.8	6.3	---	---	0
C	2223.6	L	474407	5440676	57.6	37.5	36.0	37.3	21.5	17.9	4.0	6	0
D	2526.1	H	476714	5447002	6.1	9.3	29.5	35.9	3.2	11.3	0.7	25	10
E	2530.7	B?	476734	5447071	5.7	9.7	29.5	35.9	3.2	11.3	0.6	29	0
F	2537.9	D	476769	5447177	14.4	11.0	32.4	32.0	0.6	10.7	2.1	25	0
LINE	10220		FLIGHT	4									
A	3265.8	D	473495	5437620	13.8	5.0	121.8	33.7	96.5	51.7	5.5	23	0
B	3260.6	B	473528	5437706	13.6	10.4	121.9	30.9	106.7	46.9	2.0	18	391
C	3256.4	D	473554	5437768	18.2	5.4	121.9	56.0	106.7	35.1	7.9	20	0
D	3247.6	B	473593	5437890	7.4	6.9	32.2	143.2	25.4	4.5	1.3	36	0
E	3231.2	E	473674	5438100	4.2	0.7	26.7	29.5	33.0	9.5	---	---	69
F	3211.2	S	473795	5438405	2.9	9.8	13.8	19.7	14.2	2.5	---	---	0
G	3168.3	S	474176	5439466	5.3	25.7	29.9	101.9	5.9	16.7	0.3	0	0
H	3153.3	S?	474327	5439881	4.1	8.7	20.6	26.3	21.5	4.9	---	---	0

CX = COAXIAL

CP = COPLANAR

Note: EM values shown above
are local amplitudes*Estimated Depth may be unreliable because the
stronger part of the conductor may be deeper or
to one side of the flight line, or because of a
shallow dip or magnetite/overburden effects

Block A

EM Anomaly List

					CX	5500 HZ	CP	7200 HZ	CP	900 HZ	Vertical Dike		Mag. Corr
Label	Fid	Interp	XUTM m	YUTM m	Real ppm	Quad ppm	Real ppm	Quad ppm	Real ppm	Quad ppm	COND siemens	DEPTH* m	NT
LINE	10220		FLIGHT	4									
I	3124.9	L	474605	5440644	36.5	22.4	19.6	18.1	7.0	12.1	3.7	0	0
J	3090.9	S	474913	5441521	3.7	14.0	27.7	100.0	7.2	16.9	0.3	0	0
K	2979.1	S	475774	5443842	4.1	9.7	32.3	24.4	26.3	6.1	0.4	0	0
L	2971.2	S	475847	5444027	3.5	17.1	44.6	142.1	3.4	24.4	0.2	0	0
M	2841.3	H	476906	5446943	2.8	3.5	45.5	54.4	4.7	18.2	0.7	37	0
N	2817.5	H	477028	5447286	0.9	1.4	29.5	19.5	5.0	13.3	0.4	72	0
LINE	10230		FLIGHT	4									
A	3430.9	E	473799	5437847	101.8	28.9	214.7	64.9	155.7	96.4	15.0	3	0
B	3439.3	B	473845	5437982	421.1	173.8	2773.4	596.3	2155.0	1123.7	14.2	0	611
C	3447.7	B?	473895	5438107	102.7	48.6	676.3	193.2	493.9	295.2	7.4	7	0
D	3462.2	B	474001	5438364	61.4	64.9	493.8	166.3	249.0	247.2	---	---	187
E	3464.6	B	474019	5438414	98.9	64.9	493.8	166.3	249.0	247.2	4.8	0	187
F	3524.4	H?	474499	5439762	3.6	6.2	27.7	36.7	26.2	6.1	0.5	29	0
G	3561.2	L	474795	5440558	45.0	38.3	58.8	51.1	41.3	14.7	2.7	1	0
H	3771.1	S	476013	5443903	4.7	20.0	43.2	147.0	3.6	25.2	0.3	0	0
LINE	10240		FLIGHT	4									
A	4713.7	E	474217	5438392	148.1	69.5	943.1	291.9	591.6	440.1	8.5	0	829
B	4709.5	B	474251	5438489	111.8	49.4	943.1	291.9	591.6	440.1	8.3	1	0
C	4707.3	B	474270	5438542	101.2	53.7	943.1	291.9	591.6	440.1	---	---	0
D	4664.2	S	474679	5439652	5.6	14.4	26.6	91.1	6.4	14.9	0.5	3	0
E	4636.5	L	474981	5440531	73.2	62.6	92.5	78.4	60.2	25.4	3.1	3	0
F	4604.5	S	475251	5441245	3.9	4.9	12.7	34.1	4.0	6.7	0.8	22	0
G	4436.1	S	476149	5443693	3.2	1.1	29.0	14.7	13.3	4.7	3.9	62	340
LINE	10250		FLIGHT	4									
A	4933.0	D	474425	5438396	7.9	7.6	39.5	24.2	15.9	20.0	1.3	29	56
B	4949.4	B	474575	5438796	67.2	19.6	314.0	82.3	208.8	157.2	12.6	0	0
C	4952.2	E	474601	5438868	58.2	21.4	314.0	82.3	208.8	157.2	8.6	0	0
D	4967.3	H	474737	5439248	3.7	6.2	12.7	16.3	20.6	2.1	0.6	34	0
E	4981.1	S	474871	5439610	8.3	21.8	36.2	127.3	15.4	20.8	0.5	0	0
F	5023.3	L	475183	5440455	49.6	36.0	54.8	75.5	10.3	20.8	3.4	1	0
G	5053.4	S	475434	5441163	3.1	13.5	32.4	98.0	13.7	16.2	0.2	0	0
H	5208.7	S	476314	5443560	5.2	4.8	16.5	42.9	9.6	9.4	1.2	24	0
LINE	10260		FLIGHT	4									
A	5932.8	B	474842	5438965	114.7	32.5	709.7	96.2	627.7	271.5	15.6	0	0

CX = COAXIAL
CP = COPLANAR

Note: EM values shown above
are local amplitudes

*Estimated Depth may be unreliable because the
stronger part of the conductor may be deeper or
to one side of the flight line, or because of a

EM Anomaly List

					CX	5500 HZ	CP	7200 HZ	CP	900 HZ	Vertical Dike		Mag. Corr
Label	Fid	Interp	XUTM	YUTM	Real	Quad	Real	Quad	Real	Quad	COND	DEPTH*	
			m	m	ppm	ppm	ppm	ppm	ppm	ppm	siemens	m	NT
LINE	10260		FLIGHT	4									
B	5918.6	B	474939	5439197	15.4	4.7	168.0	47.1	142.0	58.7	7.3	15	0
C	5907.6	B	474993	5439348	16.0	3.5	111.0	47.4	84.0	46.8	11.6	39	0
D	5891.8	B?	475090	5439616	14.3	35.6	49.5	162.8	21.4	28.4	0.6	0	0
E	5869.2	S	475267	5440092	5.6	14.9	30.1	111.5	8.0	20.0	0.4	7	303
F	5851.0	L	475389	5440429	54.3	35.1	41.0	35.9	13.6	17.1	4.0	3	0
G	5815.5	S	475670	5441237	1.4	0.8	13.6	45.8	11.3	6.9	---	---	0
H	5669.1	S	476557	5443651	6.5	18.2	37.7	76.7	4.5	15.4	0.4	0	0
LINE	10270		FLIGHT	4									
A	6232.0	B?	475086	5439054	23.0	13.9	85.9	67.3	58.0	32.2	3.3	16	0
B	6246.8	B	475208	5439381	41.9	19.5	274.9	46.3	282.2	90.4	5.6	3	87
C	6255.5	B	475293	5439602	23.2	2.6	155.3	116.7	214.8	74.6	36.7	22	0
D	6263.1	B?	475362	5439789	18.8	17.2	84.9	116.7	12.1	32.6	1.8	7	0
E	6294.9	L	475565	5440356	66.8	43.7	44.9	43.9	17.3	20.1	4.2	1	31
F	6470.6	E	476641	5443309	2.0	9.5	8.0	34.9	4.1	7.3	0.2	12	44
G	6481.3	S	476706	5443486	4.0	19.4	50.0	102.0	0.8	20.9	0.2	0	107
H	6492.0	S?	476790	5443707	5.1	28.8	38.9	165.0	2.5	31.1	---	---	216
LINE	10280		FLIGHT	4									
A	7009.7	B	475395	5439290	27.7	12.0	290.8	28.0	235.9	116.5	5.4	12	0
B	7005.0	B	475423	5439367	20.0	2.7	174.5	28.0	145.3	116.5	25.7	15	0
C	6998.9	H	475460	5439473	12.2	0.5	96.2	1.8	87.2	35.1	122.3	22	0
D	6987.9	H	475550	5439713	5.3	13.4	56.0	76.0	43.5	18.9	0.4	0	49
E	6958.4	L	475762	5440314	71.5	56.7	53.8	97.7	15.4	31.7	3.4	3	0
F	6786.1	H	476974	5443616	2.6	10.3	18.9	48.3	2.0	9.1	0.2	14	0
LINE	10290		FLIGHT	4									
A	7312.0	D	475493	5438985	23.8	24.3	71.9	105.6	2.2	26.8	1.8	6	0
B	7354.2	B?	475721	5439632	8.6	11.8	169.5	138.1	143.9	51.6	0.9	5	0
C	7357.3	B	475756	5439717	27.1	24.1	169.5	138.1	143.9	55.5	2.2	6	0
D	7378.4	L	475963	5440257	40.3	34.5	36.2	72.5	15.6	22.0	2.6	1	0
E	7453.2	S	476425	5441553	3.0	6.3	33.4	103.0	1.9	16.7	0.4	25	0
F	7471.2	S	476603	5442013	10.9	16.5	73.8	82.0	6.0	26.4	0.9	11	0
G	7482.7	H	476706	5442315	4.6	5.2	34.6	45.5	5.4	15.9	0.9	44	0
H	7535.3	H	477146	5443532	4.0	6.4	17.0	49.2	2.5	9.0	0.6	27	42
LINE	10300		FLIGHT	4									
A	7975.7	H	475804	5439240	5.4	9.5	41.5	59.1	0.2	17.5	0.6	34	0

CX = COAXIAL
CP = COPLANAR

Note:EM values shown above
are local amplitudes

*Estimated Depth may be unreliable because the
stronger part of the conductor may be deeper or
to one side of the flight line, or because of a

EM Anomaly List

Label	Fid	Interp	XUTM m	YUTM m	CX Real ppm	5500 HZ Quad ppm	CP Real ppm	7200 HZ Quad ppm	CP Real ppm	900 HZ Quad ppm	Vertical Dike COND siemens	DEPTH* m	Mag. Corr NT
LINE	10300		FLIGHT	4									
B	7942.2	B?	476037	5439889	95.5	23.9	449.7	84.7	326.7	194.2	17.5	0	0
C	7937.4	H	476080	5440010	36.2	16.0	449.7	94.9	326.7	194.2	5.7	8	0
D	7923.9	L	476202	5440343	21.4	11.5	39.0	27.5	18.4	24.9	3.7	12	0
E	7779.3	S?	477349	5443485	1.9	2.9	23.0	59.4	2.2	10.7	0.5	38	0
LINE	10310		FLIGHT	4									
A	8203.0	S	476108	5439539	0.8	1.3	10.5	31.3	3.0	6.7	0.3	53	0
B	8221.6	B	476279	5439982	21.0	16.5	147.6	12.5	141.7	53.0	2.3	2	0
C	8226.2	B	476314	5440084	20.3	7.4	145.8	10.4	117.3	59.3	6.2	10	64
D	8249.2	B	476447	5440436	47.2	10.5	583.0	61.4	505.1	216.8	16.4	17	0
E	8253.9	B	476477	5440518	48.4	15.1	583.0	61.4	505.1	216.8	10.2	19	96
F	8262.5	D	476534	5440674	35.6	4.3	183.0	18.6	59.7	85.2	37.1	20	0
G	8270.0	B?	476585	5440807	14.6	7.1	55.4	20.4	171.0	24.2	3.7	24	139
H	8274.6	B	476616	5440885	27.5	6.6	192.0	65.2	171.0	58.4	12.3	22	182
I	8287.5	E	476688	5441101	36.8	17.7	111.6	38.8	16.7	9.6	5.1	24	284
J	8362.9	S	477391	5443031	3.4	7.1	22.4	79.5	1.4	11.7	0.5	15	77
K	8386.5	H	477568	5443523	4.5	6.7	13.8	10.2	5.3	5.9	0.7	25	56
L	8402.7	D	477735	5443957	6.9	21.9	68.9	94.9	7.9	28.2	0.4	0	0
LINE	10320		FLIGHT	4									
A	8898.3	E	476669	5440466	113.7	23.5	138.5	60.6	117.8	39.6	24.6	0	0
B	8893.1	B	476713	5440586	185.6	18.9	1109.9	60.6	1135.8	312.7	83.3	0	0
C	8873.0	B	476848	5440959	41.6	16.0	193.4	73.0	147.9	68.5	7.3	17	51
D	8865.4	B	476884	5441068	44.7	16.8	444.5	45.2	443.8	169.5	7.6	1	0
E	8773.0	D	477588	5442971	24.5	6.6	109.9	15.2	54.9	58.0	10.0	29	234
F	8767.4	B	477642	5443099	47.7	13.2	309.0	91.9	206.9	143.5	12.1	12	0
G	8763.2	B	477673	5443191	81.2	43.4	634.4	194.1	485.6	307.0	5.8	0	0
H	8753.3	H	477741	5443395	33.4	6.6	281.9	32.5	255.0	106.1	17.7	22	0
I	8749.7	B	477767	5443471	36.1	5.7	276.8	18.6	268.6	91.3	25.4	12	0
J	8728.2	H	477966	5444033	10.0	6.9	53.6	13.6	58.1	21.7	2.1	45	0
LINE	10330		FLIGHT	4									
A	9202.8	S	476637	5439793	3.5	9.9	8.1	51.6	2.6	7.8	0.4	0	10
B	9248.3	L?	476881	5440448	50.2	27.2	56.9	91.5	27.8	21.1	4.9	4	0
C	9258.2	B	476946	5440635	134.3	49.8	1056.4	117.8	959.7	405.4	11.3	0	15
D	9267.8	B?	476994	5440775	94.1	27.8	451.5	126.7	329.5	166.2	13.7	4	0
E	9273.8	B	477024	5440867	60.9	23.1	281.9	23.9	203.3	131.5	8.4	2	81
F	9283.6	B?	477090	5441038	37.7	10.1	161.7	43.5	229.7	104.6	11.7	22	0

CX = COAXIAL
CP = COPLANAR

Note:EM values shown above
are local amplitudes

*Estimated Depth may be unreliable because the
stronger part of the conductor may be deeper or
to one side of the flight line, or because of a

EM Anomaly List

					CX 5500 HZ	CP 7200 HZ	CP 900 HZ	Vertical Dike		Mag. Corr			
Label	Fid	Interp	XUTM	YUTM	Real	Quad	Real	Quad	Real	Quad	COND	DEPTH*	
			m	m	ppm	ppm	ppm	ppm	ppm	ppm	siemens	m	NT
LINE	10330		FLIGHT	4									
G	9286.7	B	477110	5441093	32.7	13.9	230.6	51.3	229.7	104.6	5.8	13	0
H	9289.4	B?	477126	5441138	70.3	8.8	230.6	51.3	209.7	104.6	44.3	4	0
I	9299.3	D	477179	5441290	14.0	5.8	72.5	58.0	23.8	36.0	4.5	35	0
J	9370.3	E	477775	5442900	42.5	9.1	398.0	25.0	290.2	174.0	16.9	23	0
K	9375.1	B?	477816	5443014	35.4	0.0	297.3	73.3	283.8	174.0	999.0	23	42
L	9380.0	D	477856	5443129	44.7	5.6	297.3	90.5	283.8	136.6	37.7	19	0
M	9385.4	D	477904	5443258	68.0	25.3	346.8	80.9	237.2	157.2	8.9	3	10
N	9394.9	B	477992	5443496	23.1	4.7	102.0	28.7	90.9	36.5	14.9	29	277
O	9426.4	B	478301	5444351	24.3	7.0	277.4	43.7	268.1	91.0	9.0	19	0
LINE	10340		FLIGHT	5									
A	1326.5	L	477059	5440347	28.5	19.9	28.2	39.5	12.6	15.5	2.9	0	35
B	1307.6	B	477212	5440783	12.2	5.7	153.3	6.5	175.5	40.5	3.7	38	118
C	1297.9	B?	477266	5440936	48.4	19.3	567.6	87.9	499.7	203.4	7.3	10	347
D	1293.2	B	477292	5441000	77.5	21.6	567.6	87.9	497.6	203.4	14.1	3	0
E	1284.4	B	477336	5441117	16.2	5.7	151.1	18.2	146.3	45.8	6.0	42	0
F	1272.1	B	477398	5441273	25.4	5.4	312.8	31.9	298.5	96.3	14.1	22	0
G	1259.8	B	477446	5441422	20.9	6.4	129.4	17.8	104.5	52.0	7.9	20	0
H	1200.7	B?	477903	5442650	11.8	1.7	61.7	35.0	65.2	28.4	19.3	52	0
I	1189.4	D	477967	5442856	52.3	28.4	262.9	90.2	165.5	128.6	4.9	9	18
J	1122.3	E	478527	5444350	8.7	3.0	77.9	0.3	79.5	21.7	5.0	40	0
K	1111.7	B	478611	5444557	22.2	8.3	216.7	26.6	207.6	69.3	6.1	24	0
L	1096.8	H?	478710	5444913	35.6	9.7	213.4	19.9	231.4	52.4	11.2	8	0
M	1092.4	B	478757	5445025	45.1	8.0	213.4	12.7	231.4	52.4	22.8	0	0
N	1081.0	B?	478858	5445259	2.3	4.2	123.8	29.0	103.7	49.5	0.4	33	0
O	1075.6	B	478910	5445359	22.5	7.1	175.0	29.0	147.0	73.3	7.8	16	0
LINE	10350		FLIGHT	5									
A	1659.6	L	477144	5440017	6.3	2.8	0.2	0.0	0.6	1.1	3.3	64	0
B	1702.6	H	477378	5440668	4.8	4.8	3.0	10.5	2.8	0.4	1.0	39	0
C	1712.5	H?	477423	5440803	6.7	2.3	31.6	27.9	9.8	12.7	4.6	43	48
D	1728.7	H	477509	5441003	4.2	2.1	15.0	11.4	17.9	4.6	2.4	49	0
E	1741.0	H	477567	5441159	6.9	2.8	22.0	11.6	27.9	3.4	3.8	34	92
F	1752.1	E	477619	5441336	76.6	18.3	150.5	160.8	126.2	55.7	17.5	10	0
G	1757.8	B	477649	5441436	160.3	56.8	924.8	164.4	781.4	343.0	12.7	0	0
H	1773.5	B	477752	5441701	232.3	64.8	815.5	265.2	436.1	400.0	20.2	11	0
I	1780.2	B	477795	5441811	59.4	32.5	762.5	32.3	788.7	324.7	5.1	9	109
J	1787.7	B?	477841	5441934	56.6	23.6	64.3	65.6	76.1	21.2	7.2	16	0

CX = COAXIAL
CP = COPLANAR

Note:EM values shown above
are local amplitudes

*Estimated Depth may be unreliable because the
stronger part of the conductor may be deeper or
to one side of the flight line, or because of a

EM Anomaly List

					CX 5500 HZ	CP 7200 HZ	CP 900 HZ	Vertical Dike		Mag. Corr			
Label	Fid	Interp	XUTM m	YUTM m	Real ppm	Quad ppm	Real ppm	Quad ppm	Real ppm	Quad ppm	COND siemens	DEPTH* m	NT
LINE	10350		FLIGHT	5									
K	1797.7	D	477909	5442099	52.7	26.8	241.4	103.6	78.5	114.3	5.4	9	0
L	1804.7	H?	477954	5442221	5.4	7.0	17.5	23.6	7.4	12.5	0.8	35	0
M	1824.3	B	478069	5442530	55.3	7.9	485.2	92.8	436.2	178.2	33.3	0	0
N	1911.4	E	478809	5444548	24.4	6.2	140.5	29.7	114.8	48.4	10.8	21	233
O	1922.6	B	478908	5444830	51.5	12.0	203.3	17.9	210.8	57.8	15.8	20	0
P	1936.8	H	478999	5445120	3.8	2.5	342.8	56.5	296.9	131.5	1.6	61	0
Q	1942.2	B	479041	5445228	46.0	16.4	342.8	62.6	296.9	131.5	8.3	22	0
R	1955.0	B?	479149	5445511	8.5	2.9	49.9	2.4	56.4	11.3	5.0	48	0
S	1964.0	B	479221	5445697	61.7	9.1	257.3	12.7	294.4	51.9	33.1	2	0
LINE	10360		FLIGHT	20007									
A	1591.7	L	477323	5439889	11.1	10.5	10.1	26.7	3.0	6.0	1.5	30	0
B	1518.2	D	477703	5440968	11.6	10.9	52.5	45.9	5.8	19.0	1.5	2	68
C	1514.4	H?	477734	5441057	4.3	8.3	52.5	45.9	5.8	19.0	0.5	5	60
D	1498.0	B	477888	5441461	25.8	7.0	178.6	44.6	190.5	61.4	10.1	22	0
E	1476.9	E	478046	5441896	38.4	11.5	339.3	69.8	294.9	122.4	10.1	20	0
F	1469.6	B	478098	5442033	46.3	9.5	421.3	53.8	386.4	150.5	18.5	18	0
G	1459.1	B	478169	5442224	21.7	4.2	221.3	10.4	279.4	61.5	15.9	36	0
H	1453.5	B?	478205	5442332	20.9	0.7	247.5	33.6	223.9	106.4	202.3	34	0
I	1434.2	H	478359	5442785	11.3	9.7	58.3	27.1	33.6	27.0	1.7	25	120
J	1323.5	D	479103	5444815	29.1	5.0	121.8	27.1	101.0	45.1	20.8	24	0
K	1310.9	B?	479194	5445065	6.5	2.5	47.4	10.4	39.6	13.7	3.9	57	324
L	1296.3	H	479281	5445296	1.7	0.8	13.3	2.6	12.8	4.4	1.9	97	0
LINE	10370		FLIGHT	20007									
A	1830.4	L	477441	5439652	13.1	8.2	7.3	7.5	4.6	2.9	2.6	23	0
B	1974.2	D	478325	5442090	24.3	11.5	126.1	72.5	71.5	48.4	4.6	3	0
C	1988.8	B	478461	5442463	18.4	3.7	98.8	12.1	108.0	35.3	13.7	33	0
D	1999.7	D	478543	5442696	10.8	12.3	75.8	64.1	27.2	31.2	1.2	25	0
LINE	10380		FLIGHT	20007									
A	2512.8	L	477599	5439496	5.7	3.5	19.8	8.8	7.8	7.7	2.0	50	48
B	2375.0	H?	478605	5442275	12.6	3.0	63.0	23.2	46.3	25.3	9.8	25	0
LINE	10390		FLIGHT	20007									
A	2849.3	L	477724	5439273	5.7	4.8	16.3	11.5	5.7	1.0	1.4	41	42
B	2980.0	H	478736	5442035	1.0	0.6	2.1	3.7	2.1	0.3	---	---	23

CX = COAXIAL
CP = COPLANAR

Note: EM values shown above
are local amplitudes

*Estimated Depth may be unreliable because the
stronger part of the conductor may be deeper or
to one side of the flight line, or because of a
shallow dip or magnetite/overburden effects

EM Anomaly List

Label	Fid	Interp	XUTM m	YUTM m	CX Real ppm	5500 HZ Quad ppm	CP Real ppm	7200 HZ Quad ppm	CP Real ppm	900 HZ Quad ppm	Vertical COND siemens	Dike DEPTH* m	Mag. Corr NT
LINE	10400		FLIGHT	20007									
A	3541.1	L?	477885	5439120	44.9	16.4	130.3	52.0	56.5	62.7	8.0	15	0
B	3521.8	E	477967	5439332	4.0	7.9	16.2	16.7	1.5	4.9	0.5	32	0
LINE	10410		FLIGHT	20007									
A	3729.3	L	478019	5438890	15.7	12.7	15.9	13.7	6.0	7.2	2.0	1	335
B	3775.2	D	478232	5439512	10.7	6.8	65.0	39.6	25.4	32.2	2.4	35	0
C	3789.7	B	478321	5439740	27.6	28.0	145.1	116.9	28.6	63.8	1.9	12	198
D	3801.5	D	478403	5439964	9.4	16.8	44.8	38.3	17.8	20.2	0.7	14	131
E	3822.4	H	478536	5440324	3.3	3.6	14.2	18.8	2.2	5.5	0.8	26	0
F	4003.7	B	479808	5443819	1.7	9.3	41.7	100.9	2.4	19.3	---	---	0
G	4020.2	B?	479913	5444100	27.1	3.9	360.8	79.9	259.3	157.7	26.2	23	0
H	4024.7	B	479937	5444173	55.0	24.3	360.8	79.9	259.3	157.7	6.6	10	0
LINE	10420		FLIGHT	20007									
A	4575.2	L	478197	5438802	16.2	10.1	13.8	8.4	13.0	5.0	2.8	27	0
B	4539.9	H	478437	5439473	3.1	3.5	6.3	6.6	3.6	4.8	0.8	48	19
C	4527.4	B?	478535	5439746	8.5	7.5	139.2	66.0	36.3	64.6	1.5	15	86
D	4521.8	D	478582	5439881	34.9	29.2	139.2	67.2	36.3	64.6	2.5	18	0
E	4518.9	H?	478608	5439948	6.0	0.9	92.8	73.3	16.7	42.0	14.5	61	0
F	4509.6	B	478683	5440149	17.3	20.7	198.2	131.6	96.1	87.8	1.3	12	248
G	4506.6	E	478707	5440218	21.1	18.2	198.2	131.6	96.1	87.8	2.1	17	261
LINE	10430		FLIGHT	20007									
A	4732.2	L	478418	5438833	10.3	8.0	12.5	9.7	7.2	5.3	1.8	15	123
B	4770.0	D	478781	5439825	23.3	37.0	89.0	111.6	17.6	44.3	1.1	9	0
C	4776.8	B?	478846	5440003	6.2	3.9	45.5	33.1	3.8	23.8	2.0	52	0
LINE	10440		FLIGHT	20007									
A	5124.4	L	478658	5438919	10.4	9.0	13.0	16.6	4.6	5.8	1.6	16	39
B	5081.6	D	479003	5439847	11.6	10.7	49.8	45.7	13.0	19.6	1.6	26	151
C	5077.2	D	479038	5439948	10.4	15.3	49.8	45.7	12.3	19.6	0.9	13	28
D	5072.5	E	479078	5440060	6.7	11.5	41.6	53.3	1.3	16.3	0.7	13	0
LINE	10450		FLIGHT	20007									
A	5306.9	L	478906	5439005	27.2	25.9	28.5	40.5	7.4	13.2	2.0	12	0

CX = COAXIAL
CP = COPLANAR

Note: EM values shown above
are local amplitudes

*Estimated Depth may be unreliable because the
stronger part of the conductor may be deeper or
to one side of the flight line, or because of a
shallow dip or magnetite/overburden effects

Block A

EM Anomaly List

					CX 5500 HZ	CP 7200 HZ	CP 900 HZ	Vertical Dike		Mag. Corr			
Label	Fid	Interp	XUTM m	YUTM m	Real ppm	Quad ppm	Real ppm	Quad ppm	Real ppm	Quad ppm	COND siemens	DEPTH* m	NT
LINE	19010		FLIGHT	20006									
A	1363.0	D	476904	5447263	15.6	18.8	55.2	56.7	7.6	24.5	1.3	20	0
B	1368.1	B?	476976	5447235	8.3	7.1	54.8	51.3	11.3	25.5	1.5	32	0
C	1371.7	B	477029	5447220	8.6	10.1	54.8	51.3	11.3	25.5	1.1	18	0
D	1377.5	B?	477106	5447197	7.5	8.7	54.8	9.9	11.3	24.8	1.0	35	0
LINE	19020		FLIGHT	20006									
A	1738.7	B?	475809	5447247	7.8	10.6	57.5	47.9	11.2	25.5	0.9	12	52
B	1734.0	D	475911	5447212	17.1	14.2	57.5	47.9	11.2	25.5	2.0	18	56
C	1691.2	H?	476538	5446984	4.1	10.1	8.6	9.4	0.9	0.9	0.4	20	29
D	1677.8	D	476719	5446915	11.6	11.2	40.7	52.5	3.2	16.6	1.5	22	0
LINE	19030		FLIGHT	20006									
A	1946.4	H	475906	5446786	5.7	5.3	3.2	12.1	1.9	1.4	1.2	34	134
B	1965.7	D	476177	5446688	7.7	12.5	11.7	42.1	1.6	8.3	0.7	10	0
C	1981.2	H	476333	5446628	11.9	25.4	32.0	123.8	0.9	18.9	0.7	5	47
D	1992.8	B?	476450	5446578	6.0	17.4	57.2	125.5	6.4	32.5	0.4	0	0
LINE	19040		FLIGHT	20006									
A	2539.9	D	476260	5446233	10.3	13.5	53.5	49.6	3.0	18.3	1.0	17	0
B	2530.0	B	476396	5446183	7.7	7.3	25.8	39.5	0.4	10.6	1.3	39	19
C	2451.8	H	477732	5445689	5.0	7.1	13.2	23.6	2.3	4.0	0.7	29	0
D	2373.8	E	478849	5445296	44.0	8.2	110.6	30.1	81.9	43.6	21.1	14	333
E	2364.5	B	478950	5445257	102.0	25.4	812.2	56.2	818.5	224.7	18.1	12	0
F	2352.6	B	479088	5445200	52.7	11.3	286.7	32.3	272.6	91.7	18.0	19	0
LINE	19050		FLIGHT	20006									
A	2935.7	B	474901	5446301	5.4	9.9	53.4	73.2	2.1	17.2	0.6	29	121
B	2949.1	B?	474959	5446279	5.3	6.9	26.0	47.3	1.8	9.6	0.8	30	0
C	3018.4	H	476219	5445827	4.3	7.5	15.1	32.3	0.9	6.9	0.6	21	0
D	3177.6	E	478669	5444922	39.5	21.0	196.1	76.4	171.4	79.9	4.6	14	0
E	3182.1	B	478730	5444905	41.0	28.4	196.1	76.4	171.4	79.9	3.3	14	182
F	3190.4	B	478860	5444864	2.9	0.1	4.2	0.6	65.2	0.0	56.8	81	0
G	3200.0	B	478984	5444811	23.5	5.1	213.8	43.6	187.2	68.7	---	---	0
H	3204.5	B	479043	5444789	66.2	13.4	213.8	43.6	187.2	68.7	21.1	8	0
I	3258.8	B	480021	5444429	77.4	44.6	411.7	129.7	261.0	188.0	5.2	11	0
J	3261.2	B	480059	5444415	63.2	44.6	411.7	129.7	261.0	188.0	3.8	8	0

CX = COAXIAL
CP = COPLANAR

Note: EM values shown above
are local amplitudes

*Estimated Depth may be unreliable because the
stronger part of the conductor may be deeper or
to one side of the flight line, or because of a
shallow dip or magnetite/overburden effects

Block A

EM Anomaly List

					CX	5500 HZ	CP	7200 HZ	CP	900 HZ	Vertical Dike		Mag. Corr
Label	Fid	Interp	XUTM m	YUTM m	Real ppm	Quad ppm	Real ppm	Quad ppm	Real ppm	Quad ppm	COND siemens	DEPTH* m	NT
LINE	19060		FLIGHT	20006									
A	3771.5	H?	474564	5445996	9.0	8.9	44.5	25.4	6.1	15.7	1.3	15	19
B	3539.5	B?	478178	5444683	5.0	2.5	15.7	12.8	1.8	6.5	2.5	55	0
C	3509.2	B	478552	5444542	43.6	16.6	412.8	65.1	359.7	144.7	7.5	16	0
D	3502.1	B?	478638	5444514	21.1	3.7	398.3	26.7	356.7	57.0	18.2	30	0
E	3494.6	B?	478732	5444484	14.7	6.3	144.4	16.1	140.8	46.0	4.4	19	0
F	3406.5	B	479862	5444060	24.2	11.1	165.3	46.1	89.4	87.5	4.8	23	0
LINE	19070		FLIGHT	20006									
A	4189.0	H	474492	5445609	9.4	3.6	35.5	13.7	7.1	12.3	4.5	27	0
B	4419.1	B?	477917	5444351	7.4	7.6	31.5	34.2	14.3	14.8	1.2	28	11
C	4439.2	B?	478197	5444243	38.9	9.7	170.1	13.5	179.6	53.2	13.1	14	0
D	4445.2	B	478281	5444216	14.8	0.9	167.7	1.1	179.6	30.3	83.5	36	0
LINE	19080		FLIGHT	20006									
A	5068.0	H	474436	5445184	4.2	1.5	25.8	34.3	3.7	9.3	3.8	38	0
B	4858.2	D	477745	5443987	30.4	47.3	78.3	172.6	21.7	39.5	1.2	4	0
C	4849.4	H?	477904	5443931	11.7	11.5	39.8	64.2	43.2	39.5	1.5	0	59
LINE	19090		FLIGHT	20006									
A	5388.8	E	472083	5445626	21.2	29.5	33.0	78.3	1.3	17.1	1.2	5	61
B	5395.6	B?	472129	5445610	7.9	7.2	78.9	70.2	6.0	28.8	1.4	31	0
C	5413.1	B	472223	5445575	26.2	17.3	253.3	56.7	133.2	130.8	3.1	13	0
D	5421.4	D	472266	5445560	26.7	22.3	146.2	177.0	22.1	63.3	2.3	11	222
E	5504.7	H	473044	5445272	9.2	6.8	29.1	15.3	5.8	12.7	1.8	17	168
F	5587.5	H	474221	5444839	4.4	5.5	22.1	18.8	6.0	3.8	0.8	33	0
G	5684.3	S	476094	5444154	3.8	38.0	40.1	204.1	0.7	32.8	---	---	91
H	5718.0	S?	476719	5443927	3.4	62.4	38.6	241.1	1.5	39.4	---	---	0
I	5784.2	B	477894	5443509	58.6	18.3	292.3	46.7	240.2	127.2	10.8	12	0
LINE	19100		FLIGHT	20006									
A	6580.4	B?	472002	5445215	10.2	15.9	79.8	81.0	7.7	31.3	0.9	6	0
B	6574.3	B?	472086	5445184	10.5	8.9	79.8	78.4	7.7	31.3	1.7	18	0
C	6454.0	H	473775	5444575	6.0	12.2	6.2	21.4	1.0	6.2	0.6	20	0
D	6315.4	E	476279	5443666	3.6	13.0	11.4	40.6	8.7	7.3	0.3	0	0
E	6308.1	S	476440	5443608	6.4	39.1	71.1	269.1	1.6	48.4	0.2	0	0
F	6297.0	S	476731	5443503	9.3	26.8	49.4	114.7	9.0	22.3	0.5	1	0
G	6273.9	S	477308	5443292	9.1	13.7	0.8	52.4	4.7	1.6	0.8	0	46

CX = COAXIAL
CP = COPLANAR

Note: EM values shown above
are local amplitudes

*Estimated Depth may be unreliable because the
stronger part of the conductor may be deeper or
to one side of the flight line, or because of a
shallow dip or magnetite/overburden effects

Block A

EM Anomaly List

					CX	5500 HZ	CP	7200 HZ	CP	900 HZ	Vertical Dike		Mag. Corr
Label	Fid	Interp	XUTM	YUTM	Real	Quad	Real	Quad	Real	Quad	COND	DEPTH*	
			m	m	ppm	ppm	ppm	ppm	ppm	ppm	siemens	m	NT
LINE	19100		FLIGHT	20006									
H	6259.0	B	477572	5443198	102.7	58.9	551.4	132.5	404.0	266.6	5.8	0	0
I	6255.7	B?	477639	5443172	115.4	64.8	551.4	613.7	404.0	266.6	6.1	0	246
J	6251.3	B	477723	5443140	299.2	154.0	1360.8	613.7	743.6	651.0	9.5	0	0
K	6238.5	B	477890	5443079	25.6	11.4	344.9	66.2	254.5	143.8	5.0	14	0
L	6204.0	D	478462	5442880	39.7	26.7	66.4	57.6	25.6	31.5	3.4	5	0
M	6062.9	E	479800	5442378	15.7	12.4	98.0	49.3	6.3	43.2	2.1	27	0
N	6055.2	D	479903	5442342	8.4	3.5	100.2	49.3	63.0	46.7	3.9	37	0
O	6050.9	B	479960	5442320	14.2	3.1	100.2	25.0	63.0	46.7	11.4	26	0
LINE	19110		FLIGHT	20006									
A	6771.8	H	471637	5444938	4.7	0.5	31.0	59.6	6.3	12.7	21.2	68	26
B	6787.3	D	471832	5444861	28.9	42.4	105.8	134.2	10.4	47.7	1.3	0	427
C	6798.1	B	471942	5444823	34.2	29.0	253.9	200.4	26.4	101.7	2.5	18	0
D	7150.1	B	478062	5442587	47.7	8.8	190.3	19.6	205.7	62.5	21.8	0	0
E	7166.7	B	478413	5442470	106.7	29.0	311.7	47.1	260.9	135.2	16.2	11	0
F	7174.8	D	478530	5442428	28.1	10.0	57.2	42.5	39.8	41.3	7.1	25	38
G	7179.1	E	478596	5442403	16.0	9.3	94.4	42.5	52.3	41.3	3.1	20	18
LINE	19120		FLIGHT	20006									
A	7823.6	S?	471824	5444438	2.8	16.4	22.5	67.6	2.2	12.1	0.2	0	59
B	7519.4	S?	477439	5442389	2.6	7.9	38.2	118.9	1.4	19.5	0.3	21	29
C	7494.2	E	477983	5442205	64.1	15.5	78.6	41.1	42.0	111.7	16.1	8	1010
D	7487.6	B	478115	5442150	79.7	13.9	479.1	36.5	464.0	157.7	28.4	7	0
E	7481.9	H?	478230	5442107	6.4	5.3	82.2	0.0	97.0	27.4	1.5	25	0
F	7477.6	D	478318	5442073	19.6	0.0	174.4	89.3	109.2	64.5	999.0	36	0
G	7475.0	E	478371	5442052	34.1	26.6	174.4	89.3	109.2	64.5	2.7	5	144
LINE	19130		FLIGHT	20006									
A	8344.3	B?	476537	5442296	5.0	10.9	66.4	64.9	6.9	24.8	0.5	16	0
B	8350.6	B?	476641	5442253	5.5	8.0	66.4	64.9	6.5	24.8	0.7	25	0
C	8383.5	S	477330	5442007	4.5	11.1	17.8	85.2	5.3	12.7	0.4	1	77
D	8398.2	E	477690	5441871	19.8	20.8	612.0	97.9	566.4	216.1	1.6	11	0
E	8403.5	B	477809	5441828	116.2	22.4	612.0	97.9	566.4	216.1	27.5	1	0
F	8405.3	B	477848	5441813	116.2	22.4	612.0	97.9	566.4	216.1	27.5	5	0
G	8491.7	B?	478959	5441404	2.5	10.8	51.8	59.0	3.1	15.5	0.2	5	0
LINE	19140		FLIGHT	20006									
A	8794.6	S	476647	5441828	4.6	8.0	20.2	66.6	2.8	12.6	0.6	23	0

CX = COAXIAL
CP = COPLANAR

Note:EM values shown above
are local amplitudes

*Estimated Depth may be unreliable because the
stronger part of the conductor may be deeper or
to one side of the flight line, or because of a

EM Anomaly List

					CX 5500 HZ	CP 7200 HZ	CP 900 HZ	Vertical Dike		Mag. Corr			
Label	Fid	Interp	XUTM m	YUTM m	Real ppm	Quad ppm	Real ppm	Quad ppm	Real ppm	Quad ppm	COND siemens	DEPTH* m	NT
LINE	19140		FLIGHT	20006									
B	8756.1	E	477549	5441497	137.6	22.7	118.3	22.4	751.2	37.3	36.7	0	0
C	8750.7	B	477666	5441454	155.2	51.4	891.7	171.7	751.2	331.5	13.8	0	92
D	8743.0	D	477811	5441405	59.8	3.9	292.1	70.5	211.0	127.1	111.8	11	0
LINE	19150		FLIGHT	5									
A	2548.8	S	474777	5442087	0.8	3.9	15.8	2.6	20.0	1.4	0.2	12	42
B	2522.9	S	475328	5441884	2.3	1.9	12.9	5.5	16.3	0.7	1.1	70	0
C	2468.1	S	476356	5441517	4.0	17.4	52.1	163.7	7.4	28.3	0.3	0	0
D	2440.4	B?	476895	5441315	14.4	10.0	62.0	18.2	4.4	15.6	2.3	1	271
E	2433.7	B?	477067	5441251	20.8	5.7	92.1	14.5	53.3	37.8	9.3	28	340
F	2423.1	B	477313	5441161	169.5	30.6	663.3	93.2	602.9	238.4	34.5	2	0
G	2405.6	D	477725	5441009	28.2	22.0	112.4	87.9	9.8	43.1	2.6	0	0
LINE	19160		FLIGHT	5									
A	2803.9	H	471670	5442796	6.6	12.8	4.1	25.0	1.1	3.6	0.6	20	0
B	2827.8	H	472201	5442601	4.5	5.9	27.2	45.5	1.2	10.7	0.8	40	0
C	2945.9	S	474951	5441592	2.8	16.0	16.2	72.6	2.9	12.3	0.2	0	0
D	3010.7	B	476708	5440959	118.7	29.4	676.3	98.7	599.3	254.9	19.2	0	0
E	3018.3	B?	476909	5440885	2.9	0.0	296.9	76.3	279.6	95.9	664.9	95	0
F	3024.4	B	477059	5440829	307.6	83.2	1162.2	264.4	1104.6	501.1	23.2	0	0
G	3028.8	B	477160	5440792	296.8	91.7	1162.2	264.4	1104.6	501.1	19.0	0	78
H	3143.5	B?	478751	5440210	14.6	13.6	96.2	61.6	34.7	46.6	1.7	9	0
I	3156.1	E	478915	5440155	9.9	9.2	5.0	6.3	2.6	2.4	1.5	22	0
LINE	19170		FLIGHT	5									
A	3691.9	H	471641	5442383	3.4	10.6	5.8	27.6	0.9	3.9	0.3	22	20
B	3658.1	H	472218	5442174	5.6	12.5	39.4	92.2	1.3	17.7	0.5	16	0
C	3434.9	B	476596	5440577	254.4	102.9	1097.7	314.5	887.4	579.3	12.4	0	0
D	3429.6	B?	476716	5440532	64.0	11.4	951.6	228.0	844.9	333.7	25.5	7	0
E	3425.4	B?	476804	5440499	206.2	71.0	903.0	228.0	622.1	385.4	14.4	0	0
F	3413.6	E	477076	5440408	5.3	8.9	91.0	109.0	8.2	33.4	0.6	7	22
G	3315.8	D	478437	5439903	104.3	37.9	346.7	215.0	95.4	160.0	10.7	5	0
H	3307.5	B	478526	5439870	2.3	0.0	45.1	23.3	1.1	13.1	---	---	0
I	3299.8	D	478587	5439846	39.0	49.9	224.6	147.5	38.5	99.0	1.6	4	147
J	3292.4	B	478648	5439823	39.5	38.6	224.6	163.9	33.1	99.0	2.2	7	108
K	3281.1	D	478753	5439789	24.3	19.3	73.2	63.2	15.6	36.0	2.4	15	0

CX = COAXIAL
CP = COPLANAR

Note: EM values shown above
are local amplitudes

*Estimated Depth may be unreliable because the
stronger part of the conductor may be deeper or
to one side of the flight line, or because of a
shallow dip or magnetite/overburden effects

EM Anomaly List

					CX 5500 HZ	CP 7200 HZ	CP 900 HZ	Vertical Dike		Mag. Corr			
Label	Fid	Interp	XUTM m	YUTM m	Real ppm	Quad ppm	Real ppm	Quad ppm	Real ppm	Quad ppm	COND siemens	DEPTH* m	NT
LINE	19180		FLIGHT	5									
A	4299.4	S	472020	5441813	12.3	38.2	46.1	121.0	2.2	22.9	0.5	0	0
B	4484.7	L?	476100	5440325	18.3	6.6	0.9	2.3	26.7	22.2	6.0	25	492
C	4492.6	B?	476287	5440255	24.6	18.0	80.5	38.6	45.1	31.1	2.6	19	0
D	4498.8	D	476421	5440209	14.9	9.1	80.5	26.6	45.1	16.8	2.8	15	0
E	4536.3	L	477242	5439909	6.0	6.3	8.4	20.1	4.6	3.5	1.1	33	0
F	4595.9	B?	478285	5439538	5.7	4.5	17.5	24.7	7.5	8.5	1.5	43	25
G	4602.6	D	478343	5439516	4.1	7.9	17.5	21.0	0.0	7.8	0.5	31	0
H	4611.4	D	478421	5439488	8.1	19.3	25.1	27.4	0.9	12.6	0.5	5	0
LINE	19190		FLIGHT	5									
A	5157.4	E	471673	5441514	3.9	48.5	39.6	235.4	2.2	35.9	0.1	0	0
B	5148.8	S	471806	5441461	5.0	23.1	52.6	233.2	1.5	35.6	0.3	0	0
C	5145.6	S	471852	5441446	5.4	33.9	50.8	219.5	1.5	20.3	0.2	0	0
D	5029.4	L	474068	5440636	23.6	22.4	65.9	152.4	47.0	32.8	1.9	14	0
E	4994.7	S	474787	5440381	6.2	5.5	13.8	20.8	15.6	3.5	1.3	23	0
F	4989.7	S	474914	5440333	1.7	1.7	11.0	4.6	21.7	0.5	0.8	61	0
G	4932.7	B	476048	5439925	76.3	18.1	297.6	17.6	242.8	116.6	17.6	0	0
H	4927.1	B	476187	5439885	39.9	18.6	297.6	30.2	242.8	116.6	5.5	0	0
I	4860.9	L	477718	5439320	10.7	6.5	16.9	0.0	6.8	6.2	2.5	31	0
J	4851.6	H?	477928	5439236	0.0	0.3	40.7	44.8	2.9	13.6	0.1	106	51
K	4786.7	L	478741	5438938	7.2	6.4	0.0	0.0	1.4	6.7	1.4	30	0
LINE	19200		FLIGHT	5									
A	5365.1	L	473319	5440492	16.8	10.9	59.0	110.2	5.7	33.2	2.7	27	224
B	5440.9	D	475348	5439745	29.9	10.3	132.0	90.3	118.3	47.8	7.5	7	0
C	5452.6	B	475718	5439619	28.7	4.3	199.9	53.0	181.6	68.2	25.2	12	0
D	5624.7	D	478948	5438443	7.5	12.8	9.5	21.3	3.1	6.1	0.7	20	0
LINE	19210		FLIGHT	5									
A	6136.5	L	472613	5440317	5.5	7.2	21.3	24.2	4.7	12.7	0.8	34	163
B	6102.0	S	473281	5440070	4.7	13.8	18.3	109.5	24.4	18.4	0.4	11	0
C	6083.3	S	473677	5439938	4.0	17.4	25.5	111.2	16.4	18.1	0.3	0	0
D	6071.2	S	473955	5439833	2.3	9.7	14.2	45.1	9.7	7.6	0.2	0	0
E	6034.9	S	474678	5439567	2.9	13.9	20.6	95.9	26.3	15.2	0.2	7	0
F	6017.6	B	475108	5439411	81.3	27.3	305.6	126.5	271.5	108.9	11.0	0	0
G	6007.1	B	475395	5439313	17.2	9.7	222.3	43.0	195.0	86.6	3.2	4	0
H	5992.5	D	475767	5439180	29.1	32.5	82.4	75.0	6.8	34.1	1.7	15	14

CX = COAXIAL
CP = COPLANAR

Note: EM values shown above
are local amplitudes

*Estimated Depth may be unreliable because the
stronger part of the conductor may be deeper or
to one side of the flight line, or because of a
shallow dip or magnetite/overburden effects

Block A

EM Anomaly List

Label	Fid	Interp	XUTM m	YUTM m	CX Real ppm	5500 HZ Quad ppm	CP Real ppm	7200 HZ Quad ppm	CP Real ppm	900 HZ Quad ppm	Vertical Dike COND DEPTH* siemens m		Mag. Corr NT	
LINE	19210		FLIGHT	5										
I	5913.9	D	477187	5438658	9.5	10.9	40.4	36.6	8.5	15.7	1.1	24	80	
LINE	19220		FLIGHT	5										
A	6362.4	L	471440	5440314	12.8	7.3	29.9	24.1	12.6	14.7	2.9	18	47	
B	6440.4	S	473290	5439648	3.2	9.8	25.8	79.1	10.4	13.0	0.3	4	13	
C	6474.4	S	474280	5439282	6.5	40.2	14.1	147.3	4.3	22.2	---	---	0	
D	6489.0	E	474659	5439154	5.5	5.0	9.4	2.1	20.3	0.4	1.2	26	0	
E	6499.3	B	474923	5439055	46.8	10.4	413.2	28.9	388.8	142.0	16.5	12	0	
F	6502.1	B?	474987	5439030	76.2	17.9	413.2	28.9	388.8	142.0	17.8	0	0	
G	6505.7	E	475064	5439000	7.0	11.0	27.3	22.3	17.3	9.1	0.7	14	0	
H	6519.1	S	475321	5438908	3.3	9.7	11.3	42.8	2.6	7.8	0.3	11	0	
LINE	19230		FLIGHT	5										
A	6967.4	S	472835	5439390	0.6	5.9	8.0	50.8	4.0	7.7	---	---	27	
B	6881.7	D	474387	5438826	49.2	56.9	18.0	80.9	3.5	18.9	2.0	0	0	
C	6874.4	B	474534	5438777	84.8	16.4	316.6	76.8	208.9	161.8	24.8	0	0	
D	6866.4	D	474701	5438713	35.3	7.9	274.1	8.3	217.3	116.2	---	---	0	
LINE	19240		FLIGHT	5										
A	7445.9	B	474167	5438478	329.3	102.2	1506.4	450.1	1030.7	688.0	19.5	0	0	
B	7450.5	B	474248	5438448	63.0	153.1	1506.4	450.1	1030.7	669.7	1.1	0	623	
C	7459.1	D	474403	5438394	12.2	14.2	137.3	110.7	36.9	57.7	1.2	18	188	
LINE	19250		FLIGHT	5										
A	7658.2	S	472999	5438478	4.4	10.1	11.2	64.3	8.3	10.0	---	---	0	
B	7617.7	D	473917	5438145	57.9	32.6	552.5	307.5	181.1	268.7	---	---	0	
C	7614.7	B	473992	5438117	95.0	68.6	552.5	307.5	181.1	268.7	4.2	0	0	
D	7611.9	B?	474060	5438092	83.4	65.1	552.5	307.5	181.1	268.7	3.7	2	591	
LINE	19260		FLIGHT	5										
A	7963.4	S	472864	5438104	4.1	15.0	24.3	76.6	11.5	12.7	---	---	0	
B	7998.8	B	473673	5437802	132.8	37.5	538.1	105.9	456.8	201.1	16.5	0	555	
LINE	19270		FLIGHT	5										
A	8204.0	D	473096	5437590	7.4	2.6	33.2	28.0	33.7	15.4	4.7	46	0	
B	8200.0	H	473187	5437557	1.5	2.1	33.2	10.4	33.7	15.4	---	---	0	

CX = COAXIAL
CP = COPLANAR

Note: EM values shown above
are local amplitudes

*Estimated Depth may be unreliable because the
stronger part of the conductor may be deeper or
to one side of the flight line, or because of a
shallow dip or magnetite/overburden effects

Block A

EM Anomaly List

					CX 5500 HZ		CP 7200 HZ		CP 900 HZ		Vertical Dike		Mag. Corr
Label	Fid	Interp	XUTM m	YUTM m	Real ppm	Quad ppm	Real ppm	Quad ppm	Real ppm	Quad ppm	COND siemens	DEPTH* m	NT
LINE	19280		FLIGHT	5									
A	8586.4	S	470994	5437917	5.6	7.0	30.5	53.6	4.3	10.9	0.9	11	246
B	8652.3	E	472302	5437451	83.2	27.2	563.3	90.3	443.6	231.8	11.4	6	222
C	8656.0	B	472363	5437428	80.1	25.4	563.3	90.3	443.6	231.8	11.8	5	307
D	8662.3	B	472445	5437396	76.4	19.0	391.0	35.5	350.7	149.3	16.5	8	0
LINE	19290		FLIGHT	5									
A	8828.4	B?	471775	5437218	10.8	14.7	111.7	159.9	4.0	35.5	1.0	19	35
B	8810.8	B?	472080	5437112	33.2	4.7	269.3	101.3	338.8	107.9	28.5	22	0
C	8805.3	B	472173	5437074	28.0	11.8	262.4	56.4	341.5	107.9	5.6	21	0

CX = COAXIAL
CP = COPLANAR

Note: EM values shown above
are local amplitudes

Block A

- 16 -

*Estimated Depth may be unreliable because the
stronger part of the conductor may be deeper or
to one side of the flight line, or because of a
shallow dip or magnetite/overburden effects

Anomalies Summary

Conductor Grade	No, of Responses
-----------------	------------------

7	6
6	3
5	27
4	55
3	51
2	148
1	125
0	23

Total	438
-------	-----

Conductor Model	No, of Responses
-----------------	------------------

E	36
B	165
D	55
S	67
L	45
H	70

Total	438
-------	-----

APPENDIX F

GLOSSARY

APPENDIX F

GLOSSARY OF AIRBORNE GEOPHYSICAL TERMS

Note: The definitions given in this glossary refer to the common terminology as used in airborne geophysics.

altitude attenuation: the absorption of gamma rays by the atmosphere between the earth and the detector. The number of gamma rays detected by a system decreases as the altitude increases.

apparent- : the *physical parameters* of the earth measured by a geophysical system are normally expressed as apparent, as in “apparent *resistivity*”. This means that the measurement is limited by assumptions made about the geology in calculating the response measured by the geophysical system. Apparent resistivity calculated with *HEM*, for example, generally assumes that the earth is a *homogeneous half-space* – not layered.

amplitude: The strength of the total electromagnetic field. In *frequency domain* it is most often the sum of the squares of *in-phase* and *quadrature* components. In multi-component electromagnetic surveys it is generally the sum of the squares of all three directional components.

analytic signal: The total amplitude of all the directions of magnetic *gradient*. Calculated as the sum of the squares.

anisotropy: Having different *physical parameters* in different directions. This can be caused by layering or fabric in the geology. Note that a unit can be anisotropic, but still **homogeneous**.

anomaly: A localized change in the geophysical data characteristic of a discrete source, such as a conductive or magnetic body: something locally different from the **background**.

B-field: In time-domain **electromagnetic** surveys, the magnetic field component of the (electromagnetic) **field**. This can be measured directly, although more commonly it is calculated by integrating the time rate of change of the magnetic field **dB/dt**, as measured with a receiver coil.

background: The “normal” response in the geophysical data – that response observed over most of the survey area. **Anomalies** are usually measured relative to the background. In airborne gamma-ray spectrometric surveys the term defines the **cosmic**, radon, and aircraft responses in the absence of a signal from the ground.

base-level: The measured values in a geophysical system in the absence of any outside signal. All geophysical data are measured relative to the system base level.

- Appendix F.2 -

base frequency: The frequency of the pulse repetition for a **time-domain electromagnetic** system. Measured between subsequent positive pulses.

bird: A common name for the pod towed beneath or behind an aircraft, carrying the geophysical sensor array.

bucking: The process of removing the strong **signal** from the **primary field** at the **receiver** from the data, to measure the **secondary field**. It can be done electronically or mathematically. This is done in **frequency-domain EM**, and to measure **on-time** in **time-domain EM**.

calibration coil: A wire coil of known size and dipole moment, which is used to generate a field of known **amplitude** and **phase** in the receiver, for system calibration. Calibration coils can be external, or internal to the system. Internal coils may be called Q-coils.

coaxial coils: [CX] Coaxial coils in an HEM system are in the vertical plane, with their axes horizontal and collinear in the flight direction. These are most sensitive to vertical conductive objects in the ground, such as thin, steeply dipping conductors perpendicular to the flight direction. Coaxial coils generally give the sharpest anomalies over localized conductors. (See also **coplanar coils**)

coil: A multi-turn wire loop used to transmit or detect electromagnetic fields. Time varying **electromagnetic** fields through a coil induce a voltage proportional to the strength of the field and the rate of change over time.

compensation: Correction of airborne geophysical data for the changing effect of the aircraft. This process is generally used to correct data in **fixed-wing time-domain electromagnetic** surveys (where the transmitter is on the aircraft and the receiver is moving), and magnetic surveys (where the sensor is on the aircraft, turning in the earth's magnetic field).

component: In **frequency domain electromagnetic** surveys this is one of the two **phase** measurements – **in-phase or quadrature**. In “multi-component” electromagnetic surveys it is also used to define the measurement in one geometric direction (vertical, horizontal in-line and horizontal transverse – the Z, X and Y components).

Compton scattering: gamma ray photons will bounce off electrons as they pass through the earth and atmosphere, reducing their energy and then being detected by **radiometric** sensors at lower energy levels. See also **stripping**.

conductance: See **conductivity thickness**

- Appendix F.3 -

conductivity: [s] The facility with which the earth or a geological formation conducts electricity. Conductivity is usually measured in milli-Siemens per metre (mS/m). It is the reciprocal of **resistivity**.

conductivity-depth imaging: see **conductivity-depth transform**.

conductivity-depth transform: A process for converting electromagnetic measurements to an approximation of the conductivity distribution vertically in the earth, assuming a **layered earth**. (Macnae and Lamontagne, 1987; Wolfgram and Karlik, 1995)

conductivity thickness: [st] The product of the **conductivity**, and thickness of a large, tabular body. (It is also called the “conductivity-thickness product”) In electromagnetic geophysics, the response of a thin plate-like conductor is proportional to the conductivity multiplied by thickness. For example a 10 metre thickness of 20 Siemens/m mineralization will be equivalent to 5 metres of 40 S/m; both have 200 S conductivity thickness. Sometimes referred to as conductance.

conductor: Used to describe anything in the ground more conductive than the surrounding geology. Conductors are most often clays or graphite, or hopefully some type of mineralization, but may also be man-made objects, such as fences or pipelines.

coplanar coils: [CP] In HEM, the coplanar coils lie in the horizontal plane with their axes vertical, and parallel. These coils are most sensitive to massive conductive bodies, horizontal layers, and the **halfspace**.

cosmic ray: High energy sub-atomic particles from outer space that collide with the earth's atmosphere to produce a shower of gamma rays (and other particles) at high energies.

counts (per second): The number of **gamma-rays** detected by a gamma-ray **spectrometer**. The rate depends on the geology, but also on the size and sensitivity of the detector.

culture: A term commonly used to denote any man-made object that creates a geophysical anomaly. Includes, but not limited to, power lines, pipelines, fences, and buildings.

current channelling: See current gathering.

current gathering: The tendency of electrical currents in the ground to channel into a conductive formation. This is particularly noticeable at higher frequencies or early time channels when the formation is long and parallel to the direction of current flow. This tends to enhance anomalies relative to inductive currents (see also **induction**). Also known as current channelling.

- Appendix F.4 -

daughter products: The radioactive natural sources of gamma-rays decay from the original “parent” element (commonly potassium, uranium, and thorium) to one or more lower-energy “daughter” elements. Some of these lower energy elements are also radioactive and decay further. **Gamma-ray spectrometry** surveys may measure the gamma rays given off by the original element or by the decay of the daughter products.

dB/dt: As the **secondary electromagnetic field** changes with time, the magnetic field [**B**] component induces a voltage in the receiving **coil**, which is proportional to the rate of change of the magnetic field over time.

decay: In **time-domain electromagnetic** theory, the weakening over time of the **eddy currents** in the ground, and hence the **secondary field** after the **primary field** electromagnetic pulse is turned off. In **gamma-ray spectrometry**, the radioactive breakdown of an element, generally potassium, uranium, thorium, or one of their **daughter products**.

decay constant: see time constant.

decay series: In **gamma-ray spectrometry**, a series of progressively lower energy **daughter products** produced by the radioactive breakdown of uranium or thorium.

depth of exploration: The maximum depth at which the geophysical system can detect the target. The depth of exploration depends very strongly on the type and size of the target, the contrast of the target with the surrounding geology, the homogeneity of the surrounding geology, and the type of geophysical system. One measure of the maximum depth of exploration for an electromagnetic system is the depth at which it can detect the strongest conductive target – generally a highly conductive horizontal layer.

differential resistivity: A process of transforming **apparent resistivity** to an approximation of layer resistivity at each depth. The method uses multi-frequency HEM data and approximates the effect of shallow layer **conductance** determined from higher frequencies to estimate the deeper conductivities (Huang and Fraser, 1996)

dipole moment: [NIA] For a transmitter, the product of the area of a **coil**, the number of turns of wire, and the current flowing in the coil. At a distance significantly larger than the size of the coil, the magnetic field from a coil will be the same if the dipole moment product is the same. For a receiver coil, this is the product of the area and the number of turns. The sensitivity to a magnetic field (assuming the source is far away) will be the same if the dipole moment is the same.

diurnal: The daily variation in a natural field, normally used to describe the natural fluctuations (over hours and days) of the earth’s magnetic field.

dielectric permittivity: [ϵ] The capacity of a material to store electrical charge, this is most often measured as the relative permittivity [ϵ_r], or ratio of the material dielectric to that

- Appendix F.5 -

of free space. The effect of high permittivity may be seen in HEM data at high frequencies over highly resistive geology as a reduced or negative ***in-phase***, and higher ***quadrature*** data.

drape: To fly a survey following the terrain contours, maintaining a constant altitude above the local ground surface. Also applied to re-processing data collected at varying altitudes above ground to simulate a survey flown at constant altitude.

drift: Long-time variations in the base-level or calibration of an instrument.

eddy currents: The electrical currents induced in the ground, or other conductors, by a time-varying ***electromagnetic field*** (usually the ***primary field***). Eddy currents are also induced in the aircraft's metal frame and skin; a source of ***noise*** in EM surveys.

electromagnetic: [EM] Comprised of a time-varying electrical and magnetic field. Radio waves are common electromagnetic fields. In geophysics, an electromagnetic system is one which transmits a time-varying ***primary field*** to induce ***eddy currents*** in the ground, and then measures the ***secondary field*** emitted by those eddy currents.

energy window: A broad spectrum of ***gamma-ray*** energies measured by a spectrometric survey. The energy of each gamma-ray is measured and divided up into numerous discrete energy levels, called windows.

equivalent (thorium or uranium): The amount of radioelement calculated to be present, based on the gamma-rays measured from a ***daughter*** element. This assumes that the ***decay series*** is in equilibrium – progressing normally.

exposure rate: in radiometric surveys, a calculation of the total exposure rate due to gamma rays at the ground surface. It is used as a measurement of the concentration of all the ***radioelements*** at the surface. See also: ***natural exposure rate***.

fiducial, or fid: Timing mark on a survey record. Originally these were timing marks on a profile or film; now the term is generally used to describe 1-second interval timing records in digital data, and on maps or profiles.

Figure of Merit: (FOM) A sum of the 12 distinct magnetic noise variations measured by each of four flight directions, and executing three aircraft attitude variations (yaw, pitch, and roll) for each direction. The flight directions are generally parallel and perpendicular to planned survey flight directions. The FOM is used as a measure of the ***manoeuvre noise*** before and after ***compensation***.

fixed-wing: Aircraft with wings, as opposed to “rotary wing” helicopters.

footprint: This is a measure of the area of sensitivity under the aircraft of an airborne geophysical system. The footprint of an ***electromagnetic*** system is dependent on the

- Appendix F.6 -

altitude of the system, the orientation of the transmitter and receiver and the separation between the receiver and transmitter, and the conductivity of the ground. The footprint of a **gamma-ray spectrometer** depends mostly on the altitude. For all geophysical systems, the footprint also depends on the strength of the contrasting **anomaly**.

frequency domain: An **electromagnetic** system which transmits a **primary field** that oscillates smoothly over time (sinusoidal), inducing a similarly varying electrical current in the ground. These systems generally measure the changes in the **amplitude** and **phase** of the **secondary field** from the ground at different frequencies by measuring the **in-phase** and **quadrature** phase components. See also **time-domain**.

full-stream data: Data collected and recorded continuously at the highest possible sampling rate. Normal data are stacked (see **stacking**) over some time interval before recording.

gamma-ray: A very high-energy photon, emitted from the nucleus of an atom as it undergoes a change in energy levels.

gamma-ray spectrometry: Measurement of the number and energy of natural (and sometimes man-made) gamma-rays across a range of photon energies.

gradient: In magnetic surveys, the gradient is the change of the magnetic field over a distance, either vertically or horizontally in either of two directions. Gradient data is often measured, or calculated from the total magnetic field data because it changes more quickly over distance than the **total magnetic field**, and so may provide a more precise measure of the location of a source. See also **analytic signal**.

ground effect: The response from the earth. A common calibration procedure in many geophysical surveys is to fly to altitude high enough to be beyond any measurable response from the ground, and there establish **base levels** or **backgrounds**.

half-space: A mathematical model used to describe the earth – as infinite in width, length, and depth below the surface. The most common halfspace models are **homogeneous** and **layered earth**.

heading error: A slight change in the magnetic field measured when flying in opposite directions.

HEM: Helicopter ElectroMagnetic, This designation is most commonly used for helicopter-borne, **frequency-domain** electromagnetic systems. At present, the transmitter and receivers are normally mounted in a **bird** carried on a sling line beneath the helicopter.

herringbone pattern: A pattern created in geophysical data by an asymmetric system, where the **anomaly** may be extended to either side of the source, in the direction of flight.

- Appendix F.7 -

Appears like fish bones, or like the teeth of a comb, extending either side of centre, each tooth an alternate flight line.

homogeneous: This is a geological unit that has the same **physical parameters** throughout its volume. This unit will create the same response to an HEM system anywhere, and the HEM system will measure the same apparent **resistivity** anywhere. The response may change with system direction (see **anisotropy**).

HTEM: Helicopter Time-domain ElectroMagnetic, This designation is used for the new generation of helicopter-borne, **time-domain** electromagnetic systems.

in-phase: the component of the measured **secondary field** that has the same phase as the transmitter and the **primary field**. The in-phase component is stronger than the **quadrature** phase over relatively higher **conductivity**.

induction: Any time-varying electromagnetic field will induce (cause) electrical currents to flow in any object with non-zero **conductivity**. (see **eddy currents**)

induction number: also called the “response parameter”, this number combines many of the most significant parameters affecting the **EM** response into one parameter against which to compare responses. For a **layered earth** the response parameter is $\mu w s h^2$ and for a large, flat, **conductor** it is $\mu w s t h$, where μ is the **magnetic permeability**, w is the angular **frequency**, s is the **conductivity**, t is the thickness (for the flat conductor) and h is the height of the system above the conductor.

inductive limit: When the frequency of an EM system is very high, or the **conductivity** of the target is very high, the response measured will be entirely **in-phase** with no **quadrature** (phase angle =0). The in-phase response will remain constant with further increase in conductivity or frequency. The system can no longer detect changes in conductivity of the target.

infinite: In geophysical terms, an “infinite” dimension is one much greater than the **footprint** of the system, so that the system does not detect changes at the edges of the object.

International Geomagnetic Reference Field: [IGRF] An approximation of the smooth magnetic field of the earth, in the absence of variations due to local geology. Once the IGRF is subtracted from the measured magnetic total field data, any remaining variations are assumed to be due to local geology. The IGRF also predicts the slow changes of the field up to five years in the future.

inversion, or inverse modeling: A process of converting geophysical data to an earth model, which compares theoretical models of the response of the earth to the data measured, and refines the model until the response closely fits the measured data (Huang and Palacky, 1991)

- Appendix F.8 -

layered earth: A common geophysical model which assumes that the earth is horizontally layered – the **physical parameters** are constant to **infinite** distance horizontally, but change vertically.

magnetic permeability: [μ] This is defined as the ratio of magnetic induction to the inducing magnetic field. The relative magnetic permeability [μ_r] is often quoted, which is the ratio of the rock permeability to the permeability of free space. In geology and geophysics, the **magnetic susceptibility** is more commonly used to describe rocks.

magnetic susceptibility: [k] A measure of the degree to which a body is magnetized. In SI units this is related to relative **magnetic permeability** by $k = \mu_r - 1$, and is a dimensionless unit. For most geological material, susceptibility is influenced primarily by the percentage of magnetite. It is most often quoted in units of 10^{-6} . In HEM data this is most often apparent as a negative **in-phase** component over high susceptibility, high **resistivity** geology such as diabase dikes.

manoeuvre noise: variations in the magnetic field measured caused by changes in the relative positions of the magnetic sensor and magnetic objects or electrical currents in the aircraft. This type of noise is generally corrected by magnetic **compensation**.

model: Geophysical theory and applications generally have to assume that the geology of the earth has a form that can be easily defined mathematically, called the model. For example steeply dipping **conductors** are generally modeled as being **infinite** in horizontal and depth extent, and very thin. The earth is generally modeled as horizontally layered, each layer infinite in extent and uniform in characteristic. These models make the mathematics to describe the response of the (normally very complex) earth practical. As theory advances, and computers become more powerful, the useful models can become more complex.

natural exposure rate: in radiometric surveys, a calculation of the total exposure rate due to natural-source gamma rays at the ground surface. It is used as a measurement of the concentration of all the natural **radioelements** at the surface. See also: **exposure rate**.

noise: That part of a geophysical measurement that the user does not want. Typically this includes electronic interference from the system, the atmosphere (**sferics**), and man-made sources. This can be a subjective judgment, as it may include the response from geology other than the target of interest. Commonly the term is used to refer to high frequency (short period) interference. See also **drift**.

Occam's inversion: an **inversion** process that matches the measured **electromagnetic** data to a theoretical model of many, thin layers with constant thickness and varying resistivity (Constable et al, 1987).

off-time: In a **time-domain electromagnetic** survey, the time after the end of the **primary field pulse**, and before the start of the next pulse.

- Appendix F.9 -

on-time: In a *time-domain electromagnetic* survey, the time during the *primary field pulse*.

overburden: In engineering and mineral exploration terms, this most often means the soil on top of the unweathered bedrock. It may be sand, glacial till, or weathered rock.

Phase, phase angle: The angular difference in time between a measured sinusoidal electromagnetic field and a reference – normally the primary field. The phase is calculated from $\tan^{-1}(\text{in-phase} / \text{quadrature})$.

physical parameters: These are the characteristics of a geological unit. For electromagnetic surveys, the important parameters are *conductivity*, *magnetic permeability* (or *susceptibility*) and *dielectric permittivity*; for magnetic surveys the parameter is magnetic susceptibility, and for gamma ray spectrometric surveys it is the concentration of the major radioactive elements: potassium, uranium, and thorium.

permittivity: see *dielectric permittivity*.

permeability: see *magnetic permeability*.

primary field: the EM field emitted by a transmitter. This field induces *eddy currents* in (energizes) the conductors in the ground, which then create their own *secondary fields*.

pulse: In time-domain EM surveys, the short period of intense *primary* field transmission. Most measurements (the *off-time*) are measured after the pulse. **On-time** measurements may be made during the pulse.

quadrature: that component of the measured *secondary field* that is phase-shifted 90° from the *primary field*. The quadrature component tends to be stronger than the *in-phase* over relatively weaker *conductivity*.

Q-coils: see *calibration coil*.

radioelements: This normally refers to the common, naturally-occurring radioactive elements: potassium (K), uranium (U), and thorium (Th). It can also refer to man-made radioelements, most often cobalt (Co) and cesium (Cs)

radiometric: Commonly used to refer to *gamma ray* spectrometry.

radon: A radioactive daughter product of uranium and thorium, radon is a gas which can leak into the atmosphere, adding to the non-geological background of a gamma-ray spectrometric survey.

- Appendix F.10 -

receiver: the **signal** detector of a geophysical system. This term is most often used in active geophysical systems – systems that transmit some kind of signal. In airborne **electromagnetic** surveys it is most often a **coil**. (see also, **transmitter**)

resistivity: [ρ] The strength with which the earth or a geological formation resists the flow of electricity, typically the flow induced by the **primary field** of the electromagnetic transmitter. Normally expressed in ohm-metres, it is the reciprocal of **conductivity**.

resistivity-depth transforms: similar to **conductivity depth transforms**, but the calculated **conductivity** has been converted to **resistivity**.

resistivity section: an approximate vertical section of the resistivity of the layers in the earth. The resistivities can be derived from the **apparent resistivity**, the **differential resistivities**, **resistivity-depth transforms**, or **inversions**.

Response parameter: another name for the **induction number**.

secondary field: The field created by conductors in the ground, as a result of electrical currents induced by the **primary field** from the **electromagnetic** transmitter. Airborne **electromagnetic** systems are designed to create and measure a secondary field.

Sengpiel section: a **resistivity section** derived using the **apparent resistivity** and an approximation of the depth of maximum sensitivity for each frequency.

sferic: Lightning, or the **electromagnetic** signal from lightning, it is an abbreviation of “atmospheric discharge”. These appear to magnetic and electromagnetic sensors as sharp “spikes” in the data. Under some conditions lightning storms can be detected from hundreds of kilometres away. (see **noise**)

signal: That component of a measurement that the user wants to see – the response from the targets, from the earth, etc. (See also **noise**)

skin depth: A measure of the depth of penetration of an electromagnetic field into a material. It is defined as the depth at which the primary field decreases to $1/e$ of the field at the surface. It is calculated by approximately $503 \times \sqrt{(\text{resistivity}/\text{frequency})}$. Note that depth of penetration is greater at higher **resistivity** and/or lower **frequency**.

spectrometry: Measurement across a range of energies, where **amplitude** and energy are defined for each measurement. In gamma-ray spectrometry, the number of gamma rays are measured for each energy **window**, to define the **spectrum**.

spectrum: In **gamma ray spectrometry**, the continuous range of energy over which gamma rays are measured. In **time-domain electromagnetic** surveys, the spectrum is the energy of the **pulse** distributed across an equivalent, continuous range of frequencies.

spheric: see *sferic*.

stacking: Summing repeat measurements over time to enhance the repeating *signal*, and minimize the random *noise*.

stripping: Estimation and correction for the gamma ray photons of higher and lower energy that are observed in a particular *energy window*. See also *Compton scattering*.

susceptibility: See *magnetic susceptibility*.

tau: [*t*] Often used as a name for the *time constant*.

TDEM: *time domain electromagnetic*.

thin sheet: A standard model for electromagnetic geophysical theory. It is usually defined as a thin, flat-lying conductive sheet, *infinite* in both horizontal directions. (see also *vertical plate*)

tie-line: A survey line flown across most of the *traverse lines*, generally perpendicular to them, to assist in measuring *drift* and *diurnal* variation. In the short time required to fly a tie-line it is assumed that the drift and/or diurnal will be minimal, or at least changing at a constant rate.

time constant: The time required for an *electromagnetic* field to decay to a value of 1/e of the original value. In *time-domain* electromagnetic data, the time constant is proportional to the size and *conductance* of a tabular conductive body. Also called the decay constant.

Time channel: In *time-domain electromagnetic* surveys the decaying *secondary field* is measured over a period of time, and the divided up into a series of consecutive discrete measurements over that time.

time-domain: *Electromagnetic* system which transmits a pulsed, or stepped *electromagnetic* field. These systems induce an electrical current (*eddy current*) in the ground that persists after the *primary field* is turned off, and measure the change over time of the *secondary field* created as the currents *decay*. See also *frequency-domain*.

total energy envelope: The sum of the squares of the three *components* of the *time-domain electromagnetic secondary field*. Equivalent to the *amplitude* of the secondary field.

transient: Time-varying. Usually used to describe a very short period pulse of *electromagnetic* field.

- Appendix F.12 -

transmitter: The source of the **signal** to be measured in a geophysical survey. In airborne **EM** it is most often a **coil** carrying a time-varying electrical current, transmitting the **primary field**. (see also **receiver**)

traverse line: A normal geophysical survey line. Normally parallel traverse lines are flown across the property in spacing of 50 m to 500 m, and generally perpendicular to the target geology.

vertical plate: A standard model for electromagnetic geophysical theory. It is usually defined as thin conductive sheet, **infinite** in horizontal dimension and depth extent. (see also **thin sheet**)

waveform: The shape of the **electromagnetic pulse** from a **time-domain** electromagnetic transmitter.

window: A discrete portion of a **gamma-ray spectrum** or **time-domain electromagnetic decay**. The continuous energy spectrum or **full-stream** data are grouped into windows to reduce the number of samples, and reduce **noise**.

Version 1.5, November 29, 2005
Greg Hodges,
Chief Geophysicist
Fugro Airborne Surveys, Toronto

Common Symbols and Acronyms

k	Magnetic susceptibility
e	Dielectric permittivity
m, m_r	Magnetic permeability, relative permeability
r, r_a	Resistivity, apparent resistivity
s, s_a	Conductivity, apparent conductivity
st	Conductivity thickness
t	Tau, or time constant
Wm	ohm-metres, units of resistivity
AGS	Airborne gamma ray spectrometry.
CDT	Conductivity-depth transform, conductivity-depth imaging (Macnae and Lamontagne, 1987; Wolfgram and Karlik, 1995)
CPI, CPQ	Coplanar in-phase, quadrature
CPS	Counts per second
CTP	Conductivity thickness product
CXI, CXQ	Coaxial, in-phase, quadrature
FOM	Figure of Merit
fT	femtoteslas, normal unit for measurement of B-Field
EM	Electromagnetic
keV	kilo electron volts – a measure of gamma-ray energy
MeV	mega electron volts – a measure of gamma-ray energy 1MeV = 1000keV
NIA	dipole moment: turns x current x Area
nT	nanotesla, a measure of the strength of a magnetic field
nG/h	nanoGreys/hour – gamma ray dose rate at ground level
ppm	parts per million – a measure of secondary field or noise relative to the primary or radioelement concentration.
pT/s	picoteslas per second: Units of decay of secondary field, dB/dt
S	siemens – a unit of conductance
x:	the horizontal component of an EM field parallel to the direction of flight.
y:	the horizontal component of an EM field perpendicular to the direction of flight.
z:	the vertical component of an EM field.

References:

Constable, S.C., Parker, R.L., And Constable, C.G., 1987, Occam's inversion: a practical algorithm for generating smooth models from electromagnetic sounding data: *Geophysics*, 52, 289-300

Huang, H. and Fraser, D.C, 1996. The differential parameter method for multifrequency airborne resistivity mapping. *Geophysics*, 55, 1327-1337

Huang, H. and Palacky, G.J., 1991, Damped least-squares inversion of time-domain airborne EM data based on singular value decomposition: *Geophysical Prospecting*, v.39, 827-844

Macnae, J. and Lamontagne, Y., 1987, Imaging quasi-layered conductive structures by simple processing of transient electromagnetic data: *Geophysics*, v52, 4, 545-554.

Sengpiel, K.P. 1988, Approximate inversion of airborne EM data from a multi-layered ground. *Geophysical Prospecting*, 36, 446-459

Wolfgram, P. and Karlik, G., 1995, Conductivity-depth transform of GEOTEM data: *Exploration Geophysics*, 26, 179-185.

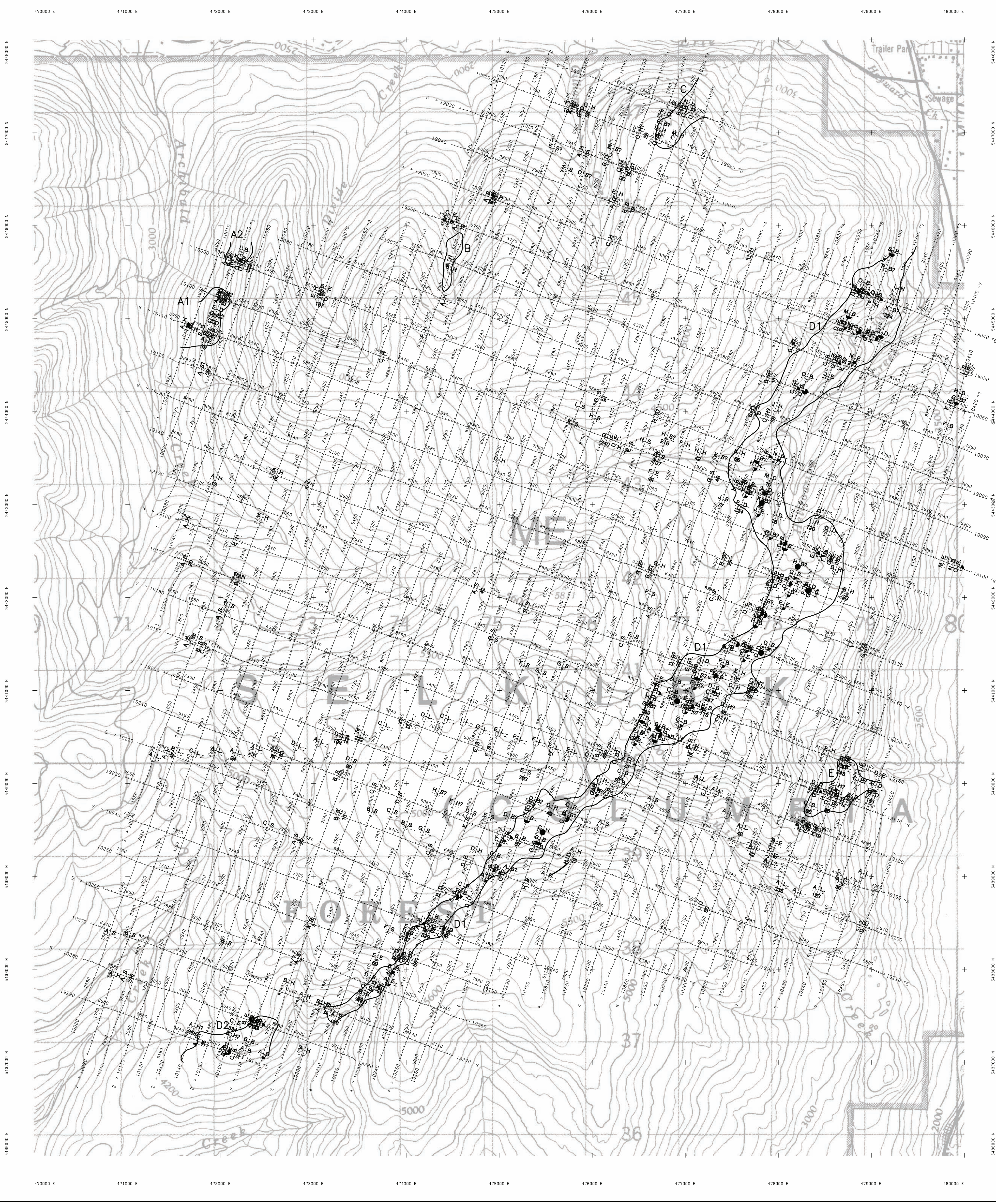
Yin, C. and Fraser, D.C. (2002), The effect of the electrical anisotropy on the responses of helicopter-borne frequency domain electromagnetic systems, Submitted to *Geophysical Prospecting*



APPENDIX B

Fugro Airborne Surveys Corp. DIGHEM Geophysical Base Maps

MAP 1:	ELECTROMAGNETIC ANOMALIES	SCALE 1:20,000
MAP 2:	APPARENT RESISTIVITY 7,200Hz COPLANAR	SCALE 1:20,000
MAP 3:	APPARENT RESISTIVITY 56,000Hz COPLANAR	SCALE 1:20,000
MAP 4:	TOTAL MAGNETIC FIELD	SCALE 1:20,000
MAP 5:	CALCULATED VERTICAL MAGNETIC GRADIENT	SCALE 1:20,000



TECHNICAL SUMMARY

Navigation Differentially-corrected GPS
Data reduction grid interval 40 metres
Terrain clearance Helicopter 57 m
Electromagnetic sensor 30 m
Magnetometer 30 m
Data sampling interval 0.1 second
Magnetometer / sensitivity Cesium / 0.01 nT
Electromagnetic system DIGHEM

Frequency	Sensitivity	Coil Orientation
1000 Hz	.06 ppm	Vertical coaxial
5500 Hz	.12 ppm	Vertical coaxial
900 Hz	.12 ppm	Horizontal coplanar
7200 Hz	.24 ppm	Horizontal coplanar
56000 Hz	.60 ppm	Horizontal coplanar

ELECTROMAGNETIC ANOMALIES

Grade	Anomaly	Conductance
7	●	>100 siemens
6	●	50-100 siemens
5	●	20-50 siemens
4	●	10-20 siemens
3	●	5-10 siemens
2	●	1-5 siemens
1	●	<1 siemens
	*	Questionable anomaly

Anomaly identifier: ●
Depth is greater than:
15 m
30 m
45 m
60 m

Interpretive symbol: ●
Conductor ("model"):
B Bedrock conductor
D Narrow bedrock conductor ("thin dike")
S Conductive cover ("horizontal thin sheet")
H Broad conductive rock unit, deep conductive weathering, thick conductive cover ("half space")
E Edge of broad conductor (edge of half space)
L Culture, e.g. power line, metal building or fence

FLIGHT LINES WITH EM ANOMALIES

Flight number
Flight direction
Flight line number
Refight Number
Line Number
Area Number
Fiducials identified on profiles
Dip direction
EM anomaly (see EM legend)
Conductor axis (on EM maps only)
Arcs indicate the conductor has a thickness > 10m
Magnetic correlation in nT (gammas)

INTERPRETATION LEGEND

Conductive Zone

LOCATION MAP

NTS: 82F/3 UTM ZONE: 11 NAD83 SCALE: 1:250,000

VALTERRA RESOURCE CORPORATION

SWIFT KATIE PROJECT, B.C.

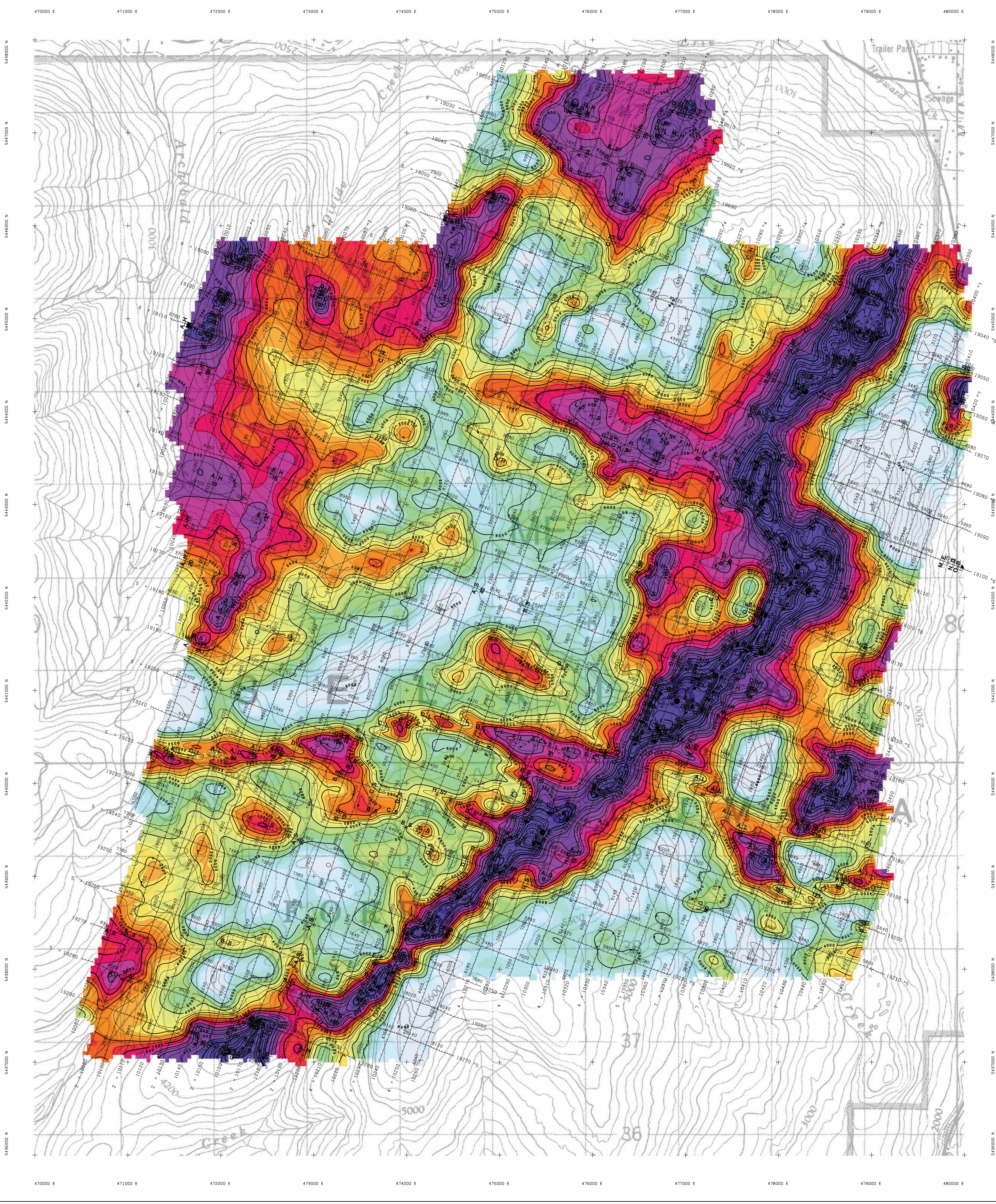
ELECTROMAGNETIC ANOMALIES

FUGRO DIGHEM® SURVEY	NTS: 82F/3	GEOPHYSICIST:
DATE: MARCH, 2008	JOB: 07114	SHEET: 1

Fugro Airborne Surveys

0 1 2 Km
0 1 Mi
Scale 1:20 000

FUGRO AIRBORNE SURVEYS



TECHNICAL SUMMARY

Navigation Differentially-corrected GPS
Data reduction grid interval 40 metres
Terrain clearance Helicopter 57 m
Electromagnetic sensor 30 m
Magnetometer 30 m
Data sampling interval 0.1 second
Magnetometer / sensitivity Cesium / 0.01 nT
Electromagnetic system DIGHEM

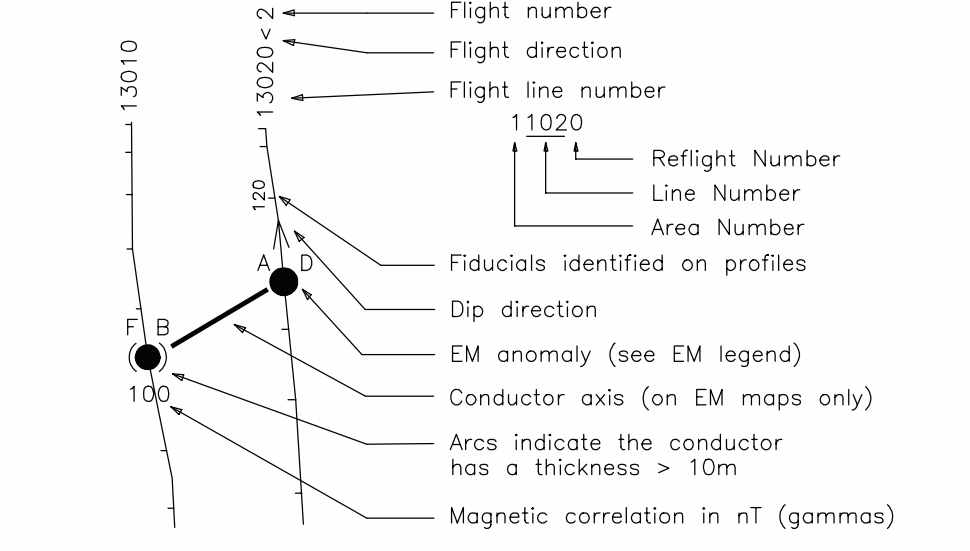
Frequency	Sensitivity	Coil Orientation
1000 Hz	.06 ppm	Vertical coaxial
5500 Hz	.12 ppm	Vertical coaxial
900 Hz	.12 ppm	Horizontal coplanar
7200 Hz	.24 ppm	Horizontal coplanar
56000 Hz	.60 ppm	Horizontal coplanar

ELECTROMAGNETIC ANOMALIES

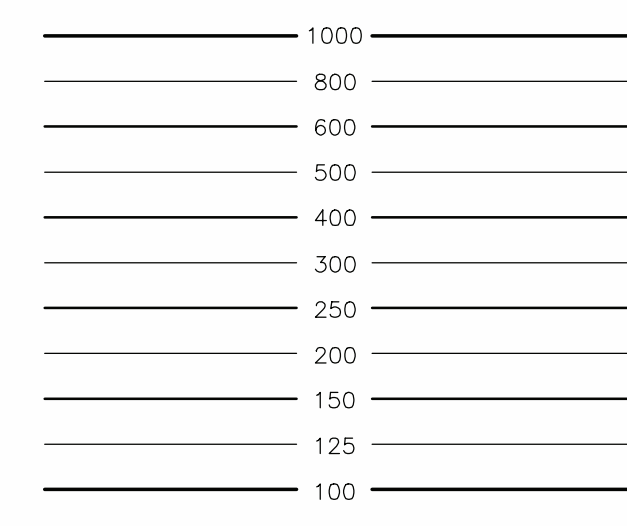
Grade	Anomaly	Conductance
7	●	>100 siemens
6	●	50-100 siemens
4	●	20-50 siemens
3	●	10-20 siemens
2	●	5-10 siemens
1	●	1-5 siemens
	*	<1 siemens
		Questionable anomaly

Interpretive symbol	Conductor ("model")
B	Bedrock conductor
D	Narrow bedrock conductor ("thin dike")
S	Conductive cover ("horizontal thin sheet")
H	Broad conductive rock unit, deep conductive weathering, thick conductive cover ("half space")
E	Edge of broad conductor ("edge of half space")
L	Culture, e.g. power line, metal building or fence

FLIGHT LINES WITH EM ANOMALIES

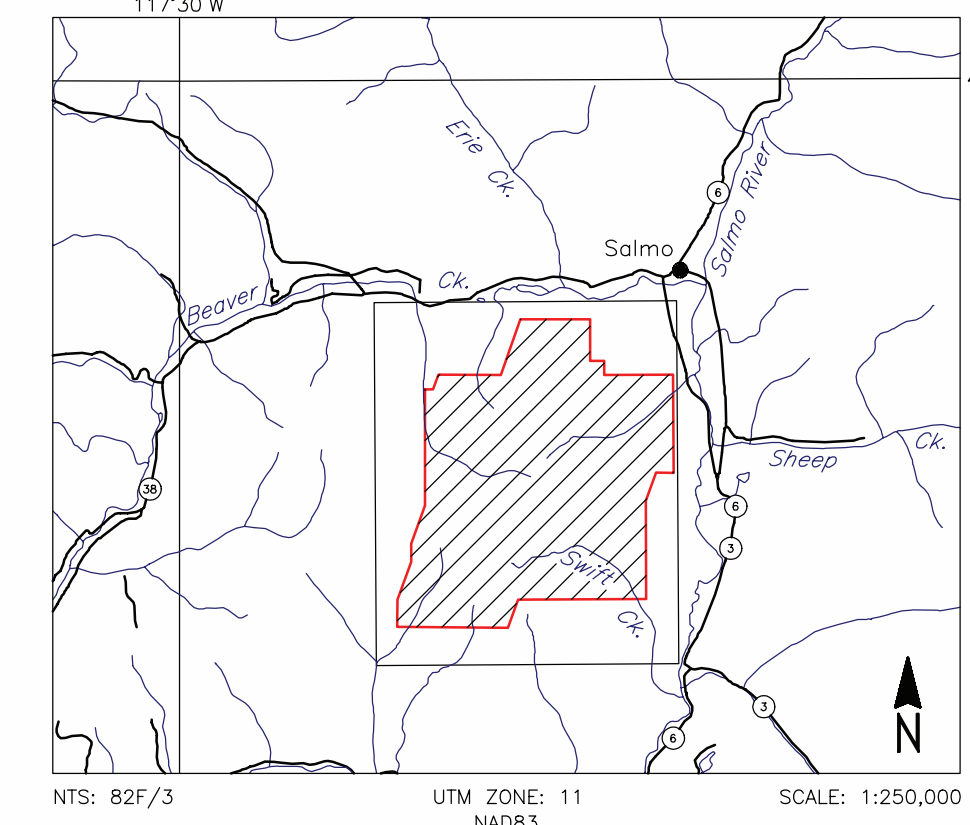


RESISTIVITY CONTOURS



Contours in ohm-m at 10 intervals per decade.
Apparent resistivity calculated using a pseudo-layer half-space model (Fraser 1978).

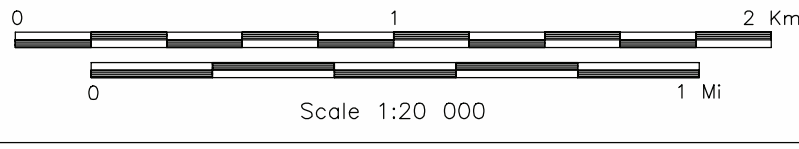
LOCATION MAP



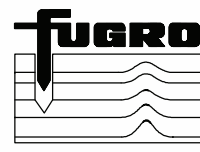
VALTERRA RESOURCE CORPORATION
SWIFT KATIE PROJECT, B.C.

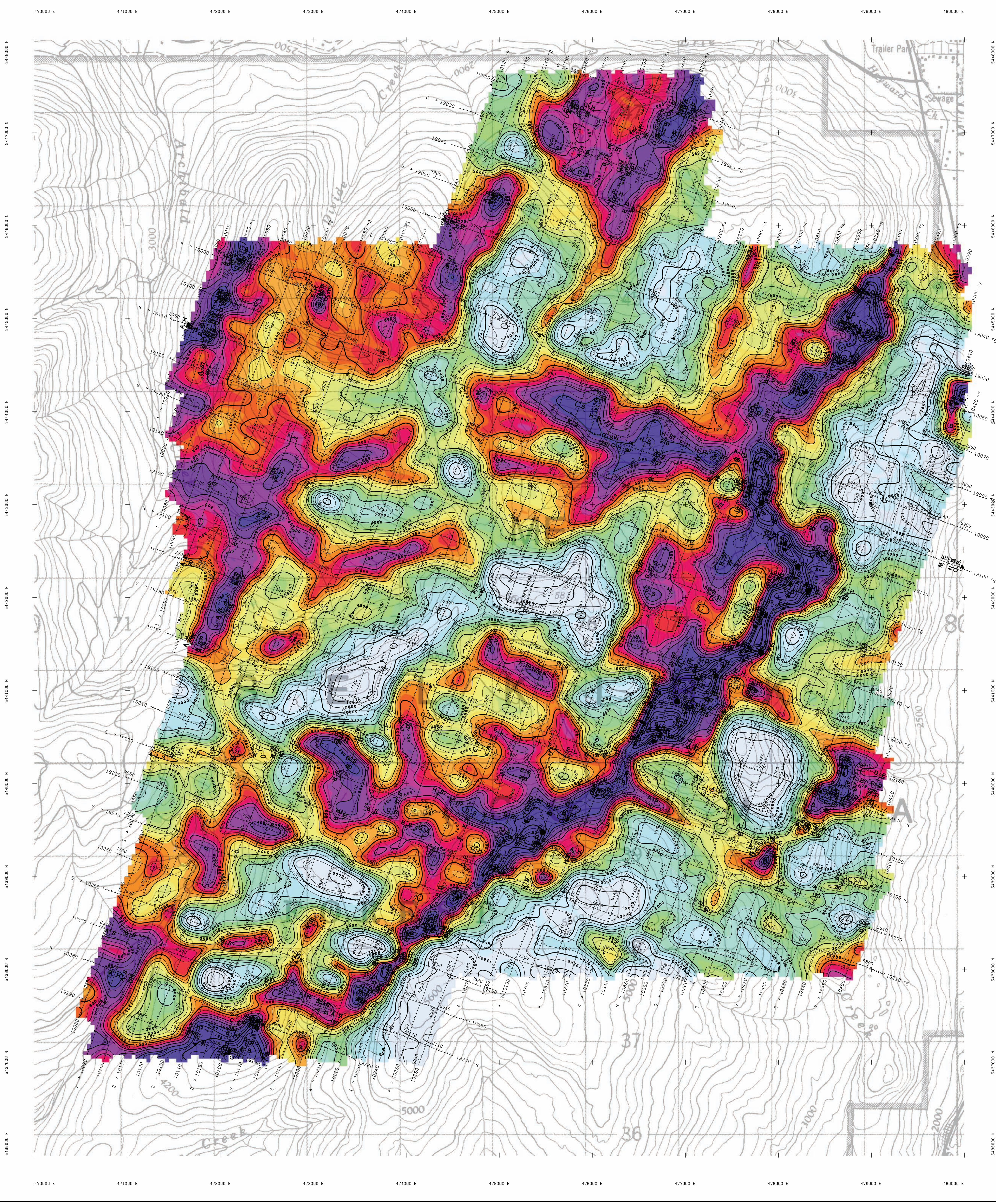
APPARENT RESISTIVITY
7200 Hz COPLANAR

FUGRO DIGHEM* SURVEY	NTS: 82F/3	GEOPHYSICIST:
DATE: MARCH, 2008	JOB: 07114	SHEET: 1
Fugro Airborne Surveys		



FUGRO AIRBORNE SURVEYS





TECHNICAL SUMMARY

Navigation Differentially-corrected GPS
Data reduction grid interval 40 metres
Terrain clearance Helicopter 57 m
Electromagnetic sensor 30 m
Magnetometer 30 m
Data sampling interval 0.1 second
Magnetometer / sensitivity Cesium / 0.01 nT
Electromagnetic system DIGHEM

Frequency	Sensitivity	Coil Orientation
1000 Hz	.06 ppm	Vertical coaxial
5500 Hz	.12 ppm	Vertical coaxial
900 Hz	.12 ppm	Horizontal coplanar
7200 Hz	.24 ppm	Horizontal coplanar
56000 Hz	.60 ppm	Horizontal coplanar

ELECTROMAGNETIC ANOMALIES

Grade	Anomaly	Conductance
7	●	>100 siemens
6	●	50-100 siemens
5	●	20-50 siemens
4	●	10-20 siemens
3	●	5-10 siemens
2	●	1-5 siemens
1	●	<1 siemens
	*	Questionable anomaly

Interpretive symbol Conductor ("model")

B Bedrock conductor
D Narrow bedrock conductor ("thin dike")
S Conductive cover ("horizontal thin sheet")
H Broad conductive rock unit, deep conductive weathering, thick conductive cover ("half space")
E Edge of broad conductor ("edge of half space")
L Culture, e.g. power line, metal building or fence

Anomaly identifier Inphase and Quadrature of coaxial coil is greater than
Depth is greater than
15 m
30 m
45 m
60 m
5 ppm
10 ppm
15 ppm
20 ppm

FLIGHT LINES WITH EM ANOMALIES

Flight number
Flight direction
Flight line number
11020
Refight Number
Line Number
Area Number
Fiducials identified on profiles
Dip direction
EM anomaly (see EM legend)
Conductor axis (on EM maps only)
Arcs indicate the conductor has a thickness > 10m
Magnetic correlation in nT (gammas)

RESISTIVITY CONTOURS

Contours in ohm-m at 10 intervals per decade.
Apparent resistivity calculated using a pseudo-layer half-space model (Fraser 1978).

1000
800
600
500
400
300
250
200
150
125
100

LOCATION MAP

117°30'W 49°15'N

Beaver Ck Salmo Sheep Ck Skeena River

NTS: 82F/3 UTM ZONE: 11 NAD83 SCALE: 1:250,000

VALTERRA RESOURCE CORPORATION

SWIFT KATIE PROJECT, B.C.

APPARENT RESISTIVITY

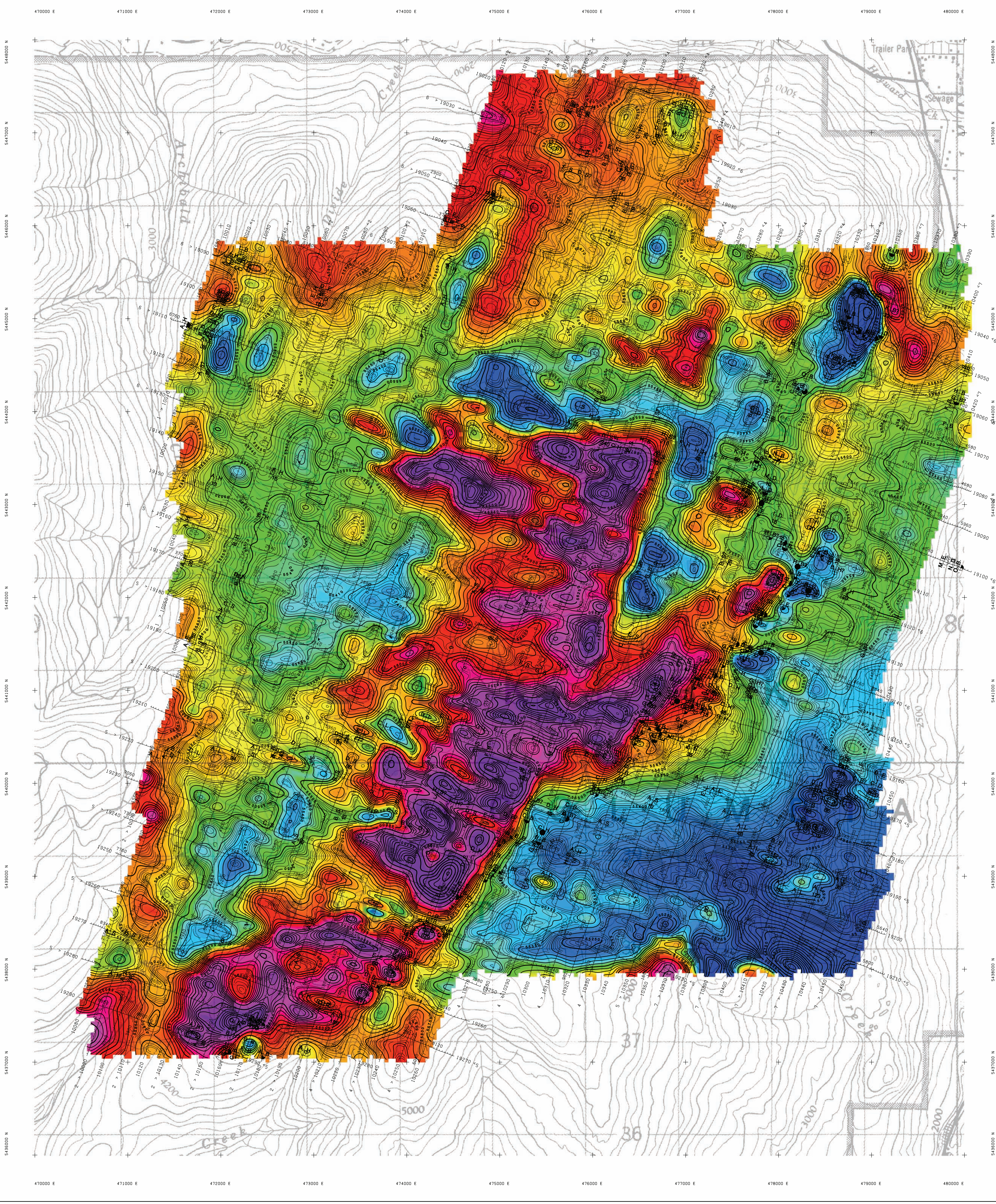
56,000 Hz COPLANAR

FUGRO DIGHEM* SURVEY	NTS: 82F/3	GEOPHYSICIST:
DATE: MARCH, 2008	JOB: 07114	SHEET: 1

Fugro Airborne Surveys

0 1 2 Km
0 1 Mi
Scale 1:20 000

FUGRO AIRBORNE SURVEYS



TECHNICAL SUMMARY

Navigation Differentially-corrected GPS
Data reduction grid interval 40 metres
Terrain clearance Helicopter 57 m
Electromagnetic sensor 30 m
Magnetometer 30 m
Data sampling interval 0.1 second
Magnetometer / sensitivity Cesium / 0.01 nT
Electromagnetic system DIGHEM

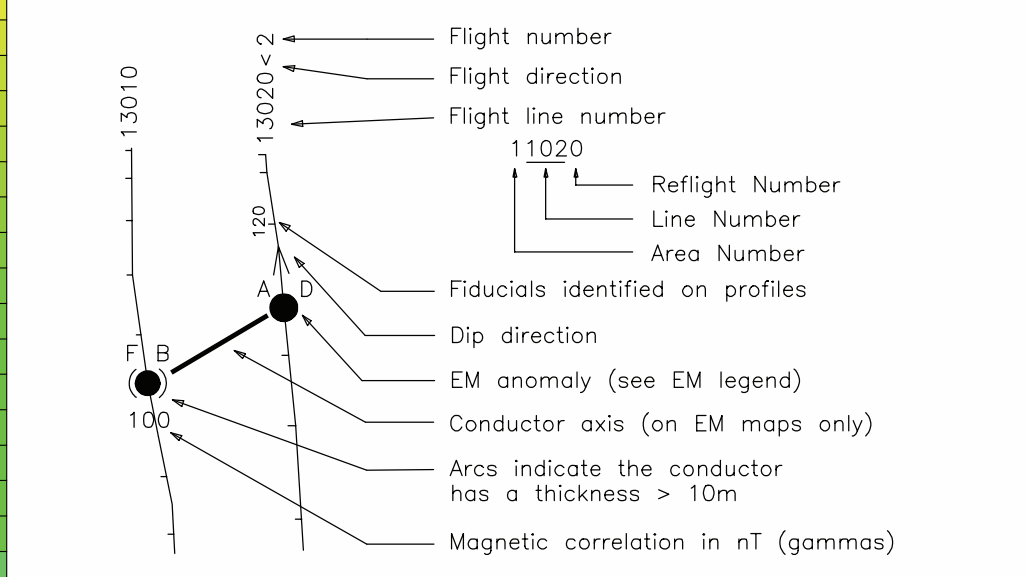
Frequency	Sensitivity	Coil Orientation
1000 Hz	.06 ppm	Vertical coaxial
5500 Hz	.12 ppm	Vertical coaxial
900 Hz	.12 ppm	Horizontal coplanar
7200 Hz	.24 ppm	Horizontal coplanar
56000 Hz	.60 ppm	Horizontal coplanar

ELECTROMAGNETIC ANOMALIES

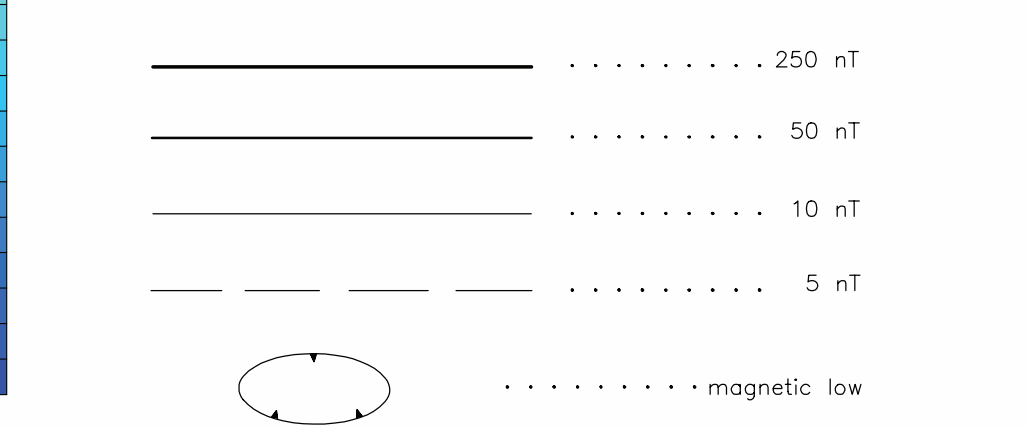
Grade	Anomaly	Conductance
7	●	>100 siemens
6	●	50-100 siemens
5	●	20-50 siemens
4	●	10-20 siemens
3	●	5-10 siemens
2	●	1-5 siemens
1	●	<1 siemens
	*	Questionable anomaly

Interpretive symbol	Conductor ("model")
B	Bedrock conductor
D	Narrow bedrock conductor ("thin dike")
S	Conductive cover ("horizontal thin sheet")
H	Broad conductive rock unit, deep conductive weathering, thick conductive cover ("half space")
E	Edge of broad conductor ("edge of half space")
L	Culture, e.g. power line, metal building or fence

FLIGHT LINES WITH EM ANOMALIES

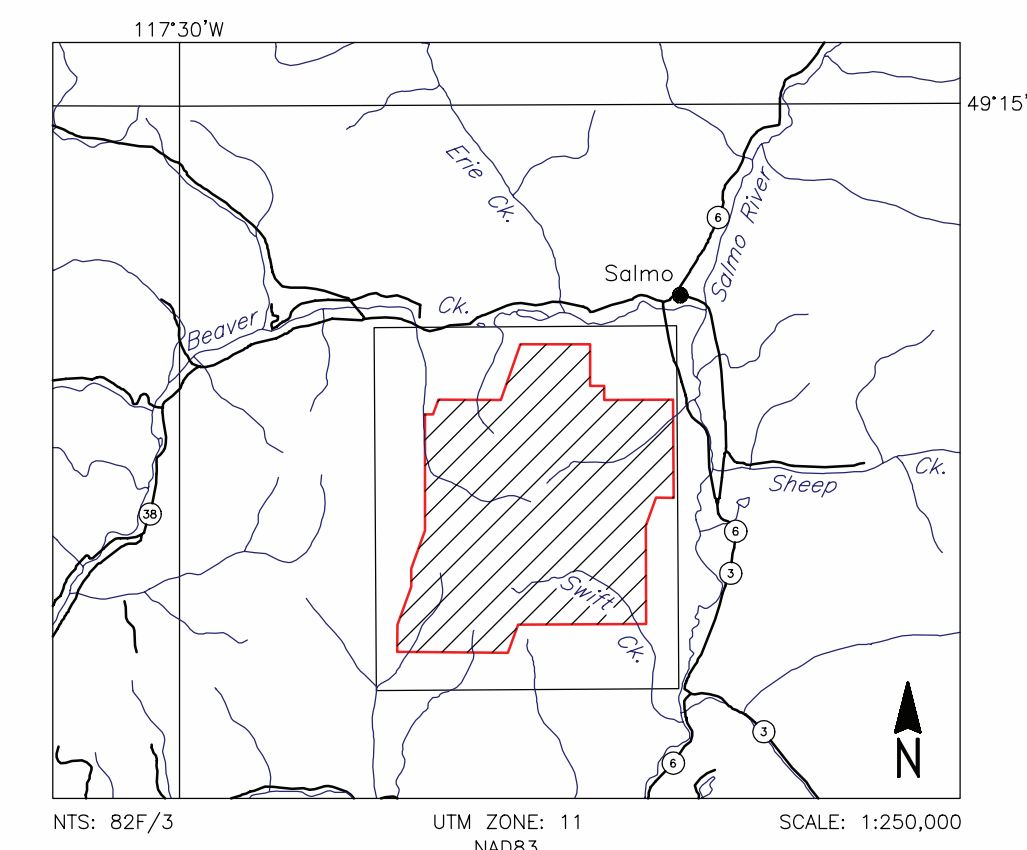


TOTAL MAGNETIC FIELD CONTOURS



Magnetic inclination within the survey area: 71 degrees N
Magnetic declination within the survey area: 17 degrees E

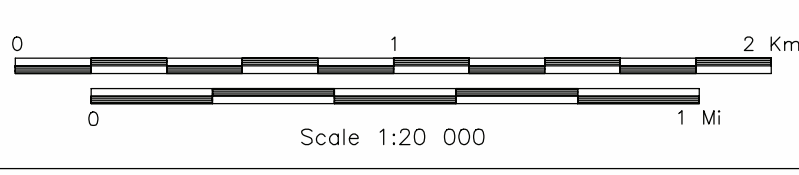
LOCATION MAP



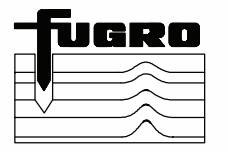
VALTERRA RESOURCE CORPORATION
SWIFT KATIE PROJECT, B.C.

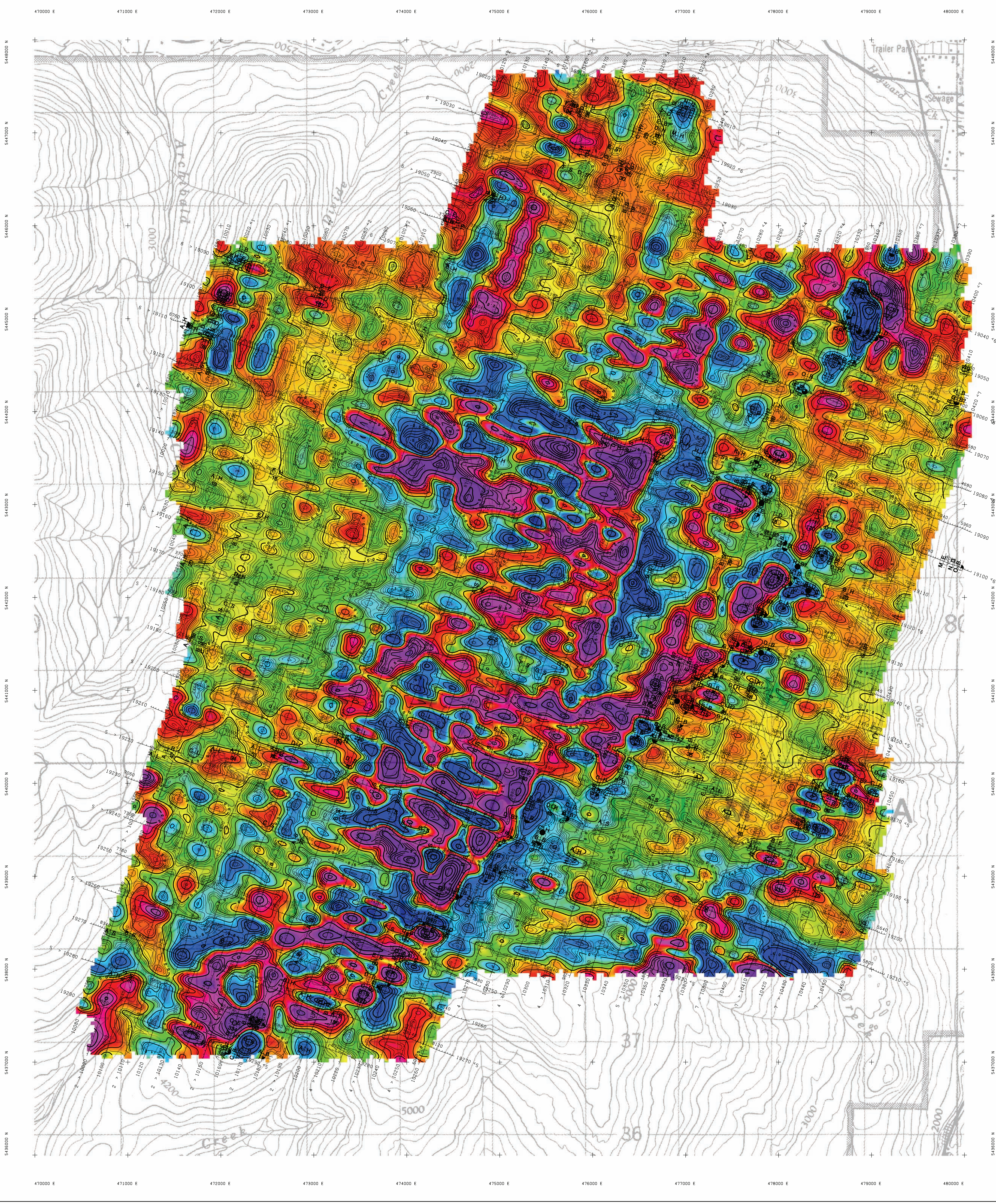
TOTAL MAGNETIC FIELD

FUGRO DIGHEM* SURVEY	NTS: 82F/3	GEOPHYSICIST:
DATE: MARCH, 2008	JOB: 07114	SHEET: 1
Fugro Airborne Surveys		



FUGRO AIRBORNE SURVEYS





TECHNICAL SUMMARY

Navigation Differentially-corrected GPS
Data reduction grid interval 40 metres
Terrain clearance Helicopter 57 m
Electromagnetic sensor 30 m
Magnetometer 30 m
Data sampling interval 0.1 second
Magnetometer / sensitivity Cesium / 0.01 nT
Electromagnetic system DIGHEM

Frequency	Sensitivity	Coil Orientation
1000 Hz	.06 ppm	Vertical coaxial
5500 Hz	.12 ppm	Vertical coaxial
900 Hz	.12 ppm	Horizontal coplanar
7200 Hz	.24 ppm	Horizontal coplanar
56000 Hz	.60 ppm	Horizontal coplanar

ELECTROMAGNETIC ANOMALIES

Grade	Anomaly	Conductance
7	●	>100 siemens
6	●	50-100 siemens
5	●	20-50 siemens
4	●	10-20 siemens
3	●	5-10 siemens
2	●	1-5 siemens
1	●	<1 siemens
	*	Questionable anomaly

Interpretive symbol: B Bedrock conductor, D Narrow bedrock conductor ("thin dike"), S Conductive cover ("horizontal thin sheet"), H Broad conductive rock unit, deep conductive weathering, thick conductive cover ("half space"), E Edge of broad conductor ("edge of half space"), L Culture, e.g. power line, metal building or fence.

Anomaly identifier: Depth is greater than 15 m, 30 m, 45 m, 60 m. Inphase and Quadrature of coaxial coil is greater than 5 ppm, 10 ppm, 15 ppm, 20 ppm.

FLIGHT LINES WITH EM ANOMALIES

Flight number, Flight direction, Flight line number, Reflight Number, Line Number, Area Number, Fiducials identified on profiles, Dip direction, EM anomaly (see EM legend), Conductor axis (on EM maps only), Arcs indicate the conductor has a thickness > 10m, Magnetic correlation in nT (gammas).

CALCULATED VERTICAL GRADIENT CONTOURS

2.5 nT/metre, 0.5 nT/metre, 0.1 nT/metre, 0.05 nT/metre

LOCATION MAP

Map showing the project area in the context of the surrounding region, including the Salmo River, Beaver Ck, and Sheep Ck. Coordinates: NTS: 82F/3, UTM ZONE: 11 NAD83, SCALE: 1:250,000.

VALTERRA RESOURCE CORPORATION

SWIFT KATIE PROJECT, B.C.

CALCULATED VERTICAL MAGNETIC GRADIENT

FUGRO DIGHEM [®] SURVEY	NTS: 82F/3	GEOPHYSICIST:
DATE: MARCH, 2008	JOB: 07114	SHEET: 1

Fugro Airborne Surveys

0 1 2 Km
0 1 Mi
Scale 1:20 000

FUGRO AIRBORNE SURVEYS